Università degli Studi di Palermo

AREA RICERCA E TRASFERIMENTO TECNOLOGICO
SETTORE DOTTORATI E CONTRATTI PER LA RICERCA
U. O. DOTTORATI DI RICERCA

Dottorato di ricerca in Biomedicina, Neuroscienze e Diagnostica avanzata
Dipartimento di Biomedicina, Neuroscienze e Diagnostica avanzata (BiND).
Settore Scientifico Disciplinare: BIOS/12A

A Novel Approach to Investigating the TARDBP p.G376D Mutation in an Italian Familial ALS Case: Molecular Analysis in Fibroblasts and iPSC-Derived Motor Neuron Models.

IL DOTTORE
Martina Pecoraro

IL COORDINATORE
Prof.re Fabio Bucchieri

IL TUTOR
Prof.re Fabio Bucchieri

CICLO XXVI
ANNO CONSEGUIMENTO TITOLO 2025

“There are no secrets to success. It is the result of preparation,

hard work and learning from failure.”

Colin Powel

TABLE OF CONTENTS

TABLE OF FIGURES

TABLE OF TABLES

ABBREVIATIONS

5-FDU	Floxuridine
a.G376D	asymptomatic G376D carrier
AA	Amino acid
ADP	Adenosine diphosphate
ALS	Amyotrophic lateral sclerosis
ALS2	Alsin
AMPA	α-Amino-3-hydroxy-5-methyl-4-isoxazoleproprionic acid
ANG	Angiogenin
ANXA11	Annexin A11
APP	Amyloid precursor protein
ARPP21	CAMP regulated phosphoprotein 21
ATG7	Autophagy related 7
ATXN1	Ataxin 1
ATXN2	Ataxin 2
BBB	Blood-brain barrier
BDNF	Brain-derived neurotrophic factor
bFGF	basic Fibroblast Growth Factor
BIBR1532	2-[(E)-3-naphthalen-2-yl-but-2-enoylamino]-benzoic acid
BIO	6-Bromoindirubin-3'-oxime
BMAA	β-Methylamino-L-alanine
BMP	Bone morphogenetic protein
BSA	Bovine Serum Albumin
BsdR	Blasticidin Resistance
bvFTD	Behavioural variant frontotemporal dementia
C	Carbonium/ Carboxyl
C21ORF2	Chromosome 21 open reading frame 2
C9ORF72	Guanine nucleotide exchange C9ORF72
C-AMP	Cyclic adenosine monophosphate
Cas9	CRISPR-associated protein 9
CAV1	Caveolin 1
CCNF	Cyclin F

CDNF	Cerebral dopamine neurotrophic factor
CFAP410	Cilia and flagella associated protein 410
CFTR	Cystic fibrosis transmembrane regulator
CHAT	Choline acetyltransferase
CHCHD10	Coiled-coil-helix-coiled-coil-helix domain-containing 10
CHIR-99021	Glycogen synthase kinase 3β inhibitor
CHMP2B	Charged multivesicular body protein 2B
C-MYC	Cellular myelocytomatosis oncogene
CNS	Central nervous system
CNTF	Ciliary neurotrophic factor
CO_2	Carbon dioxide
CRISPR	Clustered regularly interspaced short palindromic repeats
CS	Calf serum
CSF	Cerebral spinal fluid
CTD	C-terminal domain
CTF	C-terminal fragment
Cy3	Cyanine 3
DAPI	4',6-Diamidino-2-phenylindole
DAPT	Tert-butyl (S)-{(2S)-2-[2-(3,5-difluorophenyl) acetamido] propanamido} phenylacetate
DCTN1	Dynactin subunit 1
DMH-1	Dorsomorphin homolog 1
DMEM	Dulbecco's modified Eagle medium
DNA	Deoxyribonucleic acid
DNAJC7	DnaJ heat shock protein family (Hsp40) member C7
DOX	Doxycycline
DPR	Dipeptide repeat proteins
DTT	Dithiothreitol
E. coli	Escherichia coli
EB	Embryoid body
EDTA	Ethylenediaminetetraacetic acid
eIF2α	Eukaryotic translation initiation factor 2 alpha
ELP3	Elongator subunit 3

EMG	Electromyography
EnoG	Electroneurography
EPHA4	Ephrin type-A receptor 4
ER	Endoplasmic reticulum
ERBB4	Erb-B2 Receptor Tyrosine Kinase 4
ESCs	Embryonic stem cells
fALS	Familial amyotrophic lateral sclerosis
FDA	Food and Drugs Administration
FGF	Fibroblast growth factors
FIG4	Polyphosphoinositide phosphatase
FITC	Fluorescein isiothiocynate
FTD	Frontotemporal dementia
FOXP1	Forkhead Box P1
FUS	Fused in sarcoma
G3BP	rasGAP SH3 domain binding protein 1
GDNF	Glial cell-line derived neurotrophic factor
GLT8D1	Glycosyltransferase 8 domain containing 1
gRNA	Guide RNA
GSK3	Glycogen synthase kinase-3
HB9	Homeobox gene Hb9
HC	Healthy control
HCl	Hydrochloric acid
HES	Hairy/enhancer of split
hESCs	Human embryonic stem cells
HFE	Homeostatic iron regulator
hiPSCs	Human induced pluritpotent stem cells
HIV-1	Human immunodeficiency virus type 1
HMC	Hypaxial motor column
hnRBP	Human retinol-binding protein
HNRNPA1	Heterogeneous nuclear ribonucleoprotein A1
HNRNPA2B	Heterogeneous nuclear ribonucleoproteins A2/B1
HOX	Homeobox genes
HRE	Exanucleotide repeat expansion

HRP	Horseradish peroxidase
HSP	Heat shock proteins
HTT	Huntingtin
IF	Immunofluorescence
IGF-1	Insulin-like growth factor 1
iPSCs	Induced pluritpotent stem cells
IQR	Interquartile range
ISL-1	Insulin gene enhancer protein ISL-1
ISR	Integrated stress response
IWR1e	4-[(1*R*,2*S*,6*R*,7*S*)-3,5-dioxo-4-azatricyclo [5.2.1.02,6] dec-8-en-4-yl]-*N*-quinolin-8-ylbenzamide
K	Lysine
kDa	Kilodalton
KIF5A	Kinesin family member 5A
KLF4	Kruppel-like factor 4
L-myc	L-myelocytomatosis oncogene
LCD	Low complexity domain
LDN	4-[6-[4-(1-Piperazinyl) phenyl] pyrazolo[1,5-a] pyrimidin-3-yl] quinoline dihydrochloride
LHX3	LIM homeobox 3
LLPS	Liquid-liquid phase separation
LMC	Lateral motor column
LMN	Lower motor neurons
lncRNA	Long non-coding RNA
lvPPA	Logopenic variant of primary progressive aphasia
MALAT1	Metastasis associated in lung adenocarcinoma transcript 1
MATR3	Matrin 3
$MgCl_2$	Magnesium chloride
MMC	Median motor column
MMTV	Mouse mammary tumor virus
MN	Motor neuron
MND	Motor neuron disease
mRNA	Messenger RNA
miRNA	Micro RNA

$NaAsO_2$	Sodium Arsenite
NaCl	Sodium Chloride
naPPA	Non-fluent/agrammatic variant of primary progressive aphasia
NEAA	Non essential amino acid
NEAT1	Nuclear enriched abundant transcript 1
NEFH	Neurofilament heavy chain
NEK1	Serine/threonine-protein kinase Nek1
NES	Nuclear export signal
NKX6.1	Homeobox transcription factor NK6 homeobox 1
NGN2	Neurogenin2
NIL	Neurogenin2-Isl1-Lhx3
NIP	Neurogenin2-Isl1-Phox2a
NIPA1	Non-imprinted in Prader-Willi/Angelman syndrome region protein 1
NLS	Nuclear localization signal
NMR	Nuclear magnetic resonance
NRSF	Neuron-restrictive silencer factor
NT-3	Neurotrophin-3
NTD	N-terminal domain
OCT3/4	Octamer-binding transcription factor 3/4
OLIG2	Oligodendrocyte transcription factor
OPTN	Optineurin
pA	poly Adenine
PABP	PolyAbinding protein
PARylation	Poly (ADP-ribosyl) ation
PAX	Paired box
PB	PiggyBac
PBMC	Peripheral blood mononuclear cell
PBP	Progressive bulbar paralysis
PBS	Phosphate buffered saline
PBS-T	Phosphate buffered saline – Tween20
pDNA	plasmid DNA
PenStrep	penicillin + streptomicin
PET	Positron emission tomography

PFN1	Profilin 1
PGC	Preganglionic column
PHOX2A	Paired like homeobox 2A
PICs	48S preinitiation complexes
PLS	Primary lateral sclerosis
PMA	Progressive muscular atrophy
PMSF	Phenylmethylsulfonyl fluoride
PPA	Primary progressive aphasia
Pre-miRNA	miRNA precursor
Pri-miRNA	Primary-microRNA
PubC	Plasmid Ubiquitin C promoter
Q/N	Glutamine/asparagine-rich domain
RA	Retinoic acid
RAN	Repeat-associated non-ATG translation
RANBP17	Ran-binding protein 17
RBP	RNA-binding protein
REST	RE1-silencing transcription factor
ROS	Reactive oxygen species
RRM	RNA recognition motif
RNA	Ribonucleic acid
RT	Room Temperature
RT-PCR	Reverse transcription – polymerase chain reaction
rtTA	Reverse tetracycline-controlled transactivator
s.G376D	symptomatic G376D carrier
SAG	S-antigen
sALS	Sporadic amyotrophic lateral sclerosis
SB	N-(benzo[d][1,3] dioxin-5-yl)-2-(6-methyl) pyridin-2-yl) imidazoles
SCDF1	Sec-1 family domain-containing 1
SDS	Sodium dodecyl sulfate
SDS-PAGE	Sodium Dodecyl Sulfate – Polyacrylamide Gel Electrophoresis
SETX	Probable helicase senataxin
SeV	Sendai virus
SGs	Stress granules
Sh-p53	Short hairpin RNA targeting p53

SHH	Sonic hedgehog morphogen
SIGMAR1	Sigma non-opioid intracellular receptor 1
siRNA	Small interfering RNA
SMAD	Suppressor of mothers against decapentaplegic
SNCA	α-Synuclein
SOD1	Superoxide dismutase 1
SOX2	Sex determining region Y-box 2
SPG11	Spastic paraplegia 11
SPTLC1	Serine palmitoyltransferase long chain base subunit 1
SQSTM1	p62/Sequestosome 1
STR	Short tanderm repeat
STX	Senataxin
SU- 5402	synthetic small-molecule inhibitor
svPPA	Sematic dementia variant of primary progressive aphasia
T2A	T2A peptide
TALENs	Transcription activator-like effector nucleases
TAR	Trans activation response region
TARDBP	TAR DNA-binding protein 43
TAT	Trans-activator of transcription
TBK1	Serine/threonine-protein kinase 1
TBS-T	Tris-buffered saline – Tween20
TET	Transactivator protein gene
TGF- β	Transforming growth factor beta
TIA-1	T-cell intracellular antigen 1
TIA-R	TIA- receptor
TMS	Transcranial magnetic stimulation
TRA-1-60	Tumor-related antigens 1-60
TRE	Tetracycline response element
TUBA4A	Tubulin α4A
UBQLN2	Ubiquilin-2
UMNs	Upper motor neurons
UNC13A	Protein unc-13 homolog A
UPS	Ubiquitin-proteasome system

UTR	Untranslated region
VAPB	Vesicle-associated membrane protein-associated protein B/C
VCP	Valosin-containing protein
WDR7	WD repeat-containing protein 7
WNT	Wingless-type MMTV integration site family members
WT	Wild type
ZFN	Zinc-finger nucleases

ABSTRACT

Background. Amyotrophic Lateral Sclerosis (ALS) is a neurodegenerative disease that affects motor neurons and leads patients to progressive paralysis and death. ALS can be sporadic ALS (sALS), which affects approximately 90% of cases, or familial (fALS), which affects approximately 10% of cases. To date, more than 40 ALS-related genes have been identified, including TARDBP (Transactive DNA-Binding Protein), which encodes for TDP-43 protein, involved in RNA metabolism. Recently, a novel TARDBP mutation, pG376D, was described in a large Italian family, causing an aggressive and rapid ALS. To date, this mutation is unique among Caucasians.

Aim of the study. To better understand the molecular pathological mechanisms underlying ALS in subjects carrying the G376D TDP-43 mutation, 4 objectives were set:

1) Study of the expression and sub-cellular localization of TDP-43 in patient-derived fibroblasts under both basal and chronic stress conditions
2) Generation of induced pluripotent stem cells (iPSCs) from patient fibroblasts and transfection with NIL and NIP transposons using the PiggyBac system
3) Differentiation and characterization of MNs
4) Study of the expression and sub-cellular localization of TDP-43 in the MNs under both basal and stress conditions (acute and chronic).

Results. Patient-derived fibroblasts from symptomatic TDP-43 G376D mutation carrier (s.G376D), an asymptomatic TDP-43 G376D mutation carrier (a.G376D), and a healthy control (WT) were analysed under basal and chronic stress conditions. Under basal conditions, TDP-43 exhibited its expected nuclear localization, consistent with its physiological role. However, upon chronic stress induction with Sodium Arsenite, the s.G376D fibroblasts showed a reduced ability to form stress granules and a more rapid disassembly of these granules during recovery.

iPSCs were successfully generated from fibroblasts and transfected with NIL constructs using the PiggyBac system. The iPSCs differentiated in MNs – using an established protocol with transcription factors –showed the typical morphology of MNs and expressed canonical markers – ChAT, Hb9, βIII- tubulin and others – validating the robustness of the differentiation protocol. Few challenges were encountered while establishing this human-based ALS model – particularly due to the presence of differentiated cells – therefore, protocols refinements were carried out to enhance the culture quality and viability of MNs population, including improved passaging methods (use of ReLeSR), a selection of post-transfected colonies, and the use of Floxuridine to suppress proliferation of the differentiated cells.

TDP-43 remained mostly nuclear in MNs, with some diffusion in the neurites, under basal conditions, which aligns with aligns with its physiological roles and suggests that pathological mislocalization may occur at later stages of disease progression, highlighting the need for further investigations in mature MNs.

Conclusions. This study provides important insights into the inefficient cellular responses of TDP-43 in symptomatic G376D carriers and offers valuable improvements to iPSC culture and differentiation protocols for ALS modelling. While further refinements are needed to improve the quality of differentiated MNs and reduce the presence of "flat cells", the results presented here lay the groundwork for using iPSC-derived models to investigate ALS pathogenesis and potential therapeutic interventions targeting G376D TDP-43.

CHAPTER I: INTRODUCTION

1. Amyotrophic Lateral Sclerosis

Amyotrophic Lateral Sclerosis (ALS), also known as Motor Neuron Disease (MND) or Lou Gerig's disease (mostly used in United States, from the name of a famous baseball player who died from this disease in 1941) is a neurodegenerative disorder that affects motor neurons, discovered for the first time in the 1869 by the neurologist Jean-Martin Charcot. It is characterized by the progressive degeneration of the upper motor neurons (UMNs, which project from the cortex to the brainstem and the spinal cord) and lower motor neurons (LMNs, which project from the brainstem or spinal cord to muscles) causing a progressive denervation of voluntary muscles [1,2].

1.1. Epidemiology

The ALS has an incidence of approximately 0.2-2.5 per 100000 individuals per year, the range is large because the incidence ratio changes depending on different geographic areas: for example, the European incidence is 3 times higher than the Asian one. Numerous population studies have highlighted the importance of ancestral origin in disease risk [1,4,6]. In the past there was a difference in incidence gender-related with a proportion of 1:2 in male/female, but more recent research has shown that there is no longer difference between the gender, with the ratio now 1:1.2. Even the global incidence is changing and increasing each year, this could be due to the globalization that leads to a change of demographic population and a better knowledge, and therefore diagnosis of the disease [4]. Globally the prevalence is of 6-9 per 100000 individuals [2,4-5].

ALS is mainly a sporadic disease (sALS), but there are cases where a mutation in an ALS-related gene is inherited in a family, mostly with an autosomal dominant pattern; in these cases, we refer to it as familial ALS (fALS). Onset is mainly in adults (58-63 years for sALS and 40-60 years for fALS), but there are cases of juvenile onset (under 25 years of age) [7].

1.2. Clinical features

The neurodegeneration of motor neurons leads to progressive weakness of the muscles (upper and lower limbs, bulbar and respiratory). Most commonly the onset is spinal (weakness of the limbs), but in about 25-30% of cases there is a bulbar onset (characterised by dysarthria and dysphagia). The progression is variable and depends on different factors (sporadic or familial case, gene and mutation involved, onset type, age, risk factor, environmental factors), but generally the survival is around 3 years, and death occurs mostly due to respiratory system failure [1-3]. Negative prognostic factors include an advanced age at onset, bulbar onset and early impairment of respiratory function [8,9].

ALS is a far more complex disease and has different phenotypic subtypes. They can be classified by the regional onset, or by the type of motor neuron involved or even by the frontotemporal involvement (*Fig.1*).

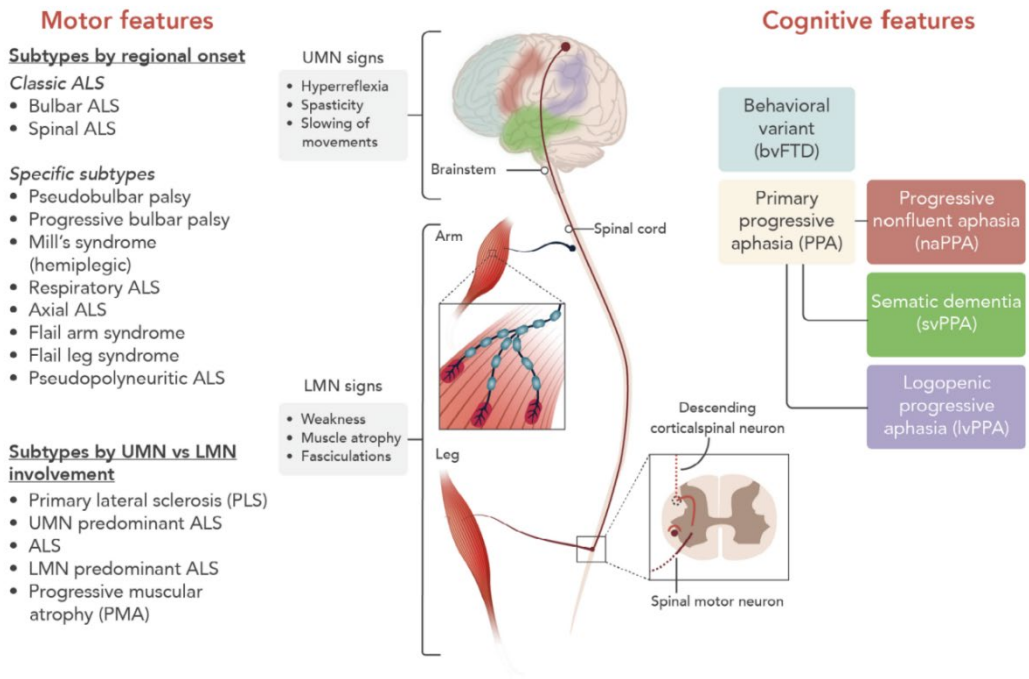

Figure 1. Motor and cognitive features of ALS [3].

The most common classification of ALS is by the region of onset.

Spinal onset, which affects two-thirds of ALS patients, presents with weakness and atrophy in upper or lower limb muscles. Upper limb onset is characterised by the split-hand syndrome, while the lower limb onset affects firstly the anterior tibial and hamstring muscles and after the gastrocnemius and quadriceps muscles.

Bulbar onset, which affects the other one-third of ALS patients, most commonly presents with dysarthria and dysphagia and in the later stages of the disease axial muscle weakness with head drop and posture problems.

Depending on the type of motor neurons affected, UMNs or LMNs, symptoms may vary as listed in Table 1.

Motor Neurons Involved	ALS Symptoms
Upper motor neuron	• Spastic hypertonicity • pathological reflexes (Hoffmann's and Babinski's reflexes) • hyperreflexia; spastic dysarthria
Spinal lower motor neuron	• Hypotonia with weakness and muscular hypotrophy, fasciculations and cramps • flaccid dysarthria • split hand sign (asymmetry of the trophism of the muscle masses in the hands) • increasing dyspnoea (due to the involvement of the respiratory muscles)
Bulbar lower motor neuron	• Dysphagia, dysarthria, dysphonia, hypotrophy e lingual fasciculations • sialorrhea and symmetrical muscle asthenia • possible ab ingestis pneumonia

Table 1. Symptoms related to the involvement of the upper and lower motor neurons [8-12].

Although most patients can be classified in the "Classic ALS" phenotype (spinal or bulbar ALS), the disease is clinically heterogeneous and presents a variety of subtypes:

- PLS (Primary Lateral Sclerosis) involves exclusively the UMNs. Patients with PLS can have a family member affected with ALS [13].
- PBP (Progressive Bulbar Paralysis) involves IX, X and XII cranial nerves and is possibly associates with pseudobulbar hallmarks; this subtype has a more rapid and worse progression with a life expectancy of 24 months [14].
- PMA (Progressive Muscular Atrophy) involves only the LMNs and is considered the less severe ALS subtype. Some patients with PMA have mutations in ALS-related genes [3].
- Pseudobulbar palsy is characterized by "expressionless face" [1], dysarthria and chewing difficulty, and dysphagia. While the PBP involves the LMN, in pseudobulbar palsy the UMN is involved [16].
- Flail arm and Flail leg ALS are two syndromes with LMN involvement, with Flail arm onset in the upper limbs and Flail leg in the lower limbs [3,14,17].

[1] Frontal lobe damage leads to corticobulbar tract damage that makes the face sag and impairs expression [15]

In addition, ALS can be classified by cognitive impairment. Cognitive and behavioural changes, which can occur early in the disease course, are now recognised to occur in 35–50% of patients with ALS, with loss of normal language and executive function (i.e., poor working memory, inhibition, and fluency). Typically, more long-term memory and spatial domains remain intact. Other behavioural changes include apathy, irritability, disregard for hygiene, and eating habit changes.

In about 10-15% of ALS patients, the degenerative process can lead to Frontotemporal dementia (FTD) [18]. FTD is characterized by the degeneration of frontal and anterior temporal lobes and leads to behavioural changes, impairment of executive functioning and/or language impairment [19].

ALS diagnosis consists of clinical investigation through various examinations (electromyography (EMG), electroneurography (ENoG), Nuclear Magnetic Resonance (NMR), Transcranial Magnetic Stimulation (TMS), tomography and Positron Emission Tomography (PET) [8-11]) to exclude other diseases.

The clinical investigation is then based on the revised El Escorial criteria [20], which requires:

a) Evidence of LMNs degeneration by clinical, electrophysiological or neuropathological examinations
b) Evidence of UMNs degeneration by clinical examinations
c) Progression of the motor syndrome within a region or to other regions, as determined by history or examination

in association with the absence of:

a) Electrophysiological and pathological evidence of other disease processes that might explain the signs of LMNs and UMNs degeneration
b) Neuroimaging evidence of other disease processes that might explain the observed clinical and electrophysiological signs.

Up to date, only 2 compounds have been approved for ALS therapy by the Food and Drug Administration (FDA): Riluzole and Edavarone [21]. Riluzole, the first approved drug, blocks the voltage-gated sodium channel in the presynaptic neurons, reducing the glutamate release into the synaptic cleft and consequently the excitotoxicity. Population studies have documented an increase in survival from 6 to 19 months [22].

Edavarone is an antioxidant agent that seems to slow the progression in selected patients, but it is not yet known whether there is an effect on survival.

Aside from these 2 compounds, the standard therapy for ALS is treatment of the symptoms (muscle relaxants, anticholinergic drugs, drugs for neuropathic and nociceptive pain, dietary changes and exercise, and antidepressants).

1.3. Multifactorial disease: genetic and environmental factors.

ALS is a multifactorial disease in which both genetic and environmental factors take part in neurodegeneration.

Environmental risk factors for ALS are:

- Smoking, which seems to be the only probable risk factor [23]
- Dietary factors, especially a higher intake of antioxidants (like Vitamin E) seem to be correlated with a lower risk of ALS [24]
- Mass index and physical activity, since there is a higher frequency of ALS among athletes [25] or individuals who engage in vigorous physical activity
- Exposure to metals or pesticides [24]
- β-methylamino-L-alanine (BMAA), in the western Pacific
- Head injury, especially repeated ones (nevertheless, the association with ALS is not thoroughly certain)
- Viral infections, like enteroviral infections, herpes viruses or retroviruses.

The first ALS-associated gene discovered was SOD1 (Superoxide Dismutase 1) in 1993 [26] and since then more than 120 potential genes have been identified as definitively causative, ALS risk increasing or clinical modifiers (https://alsod.ac.uk/).

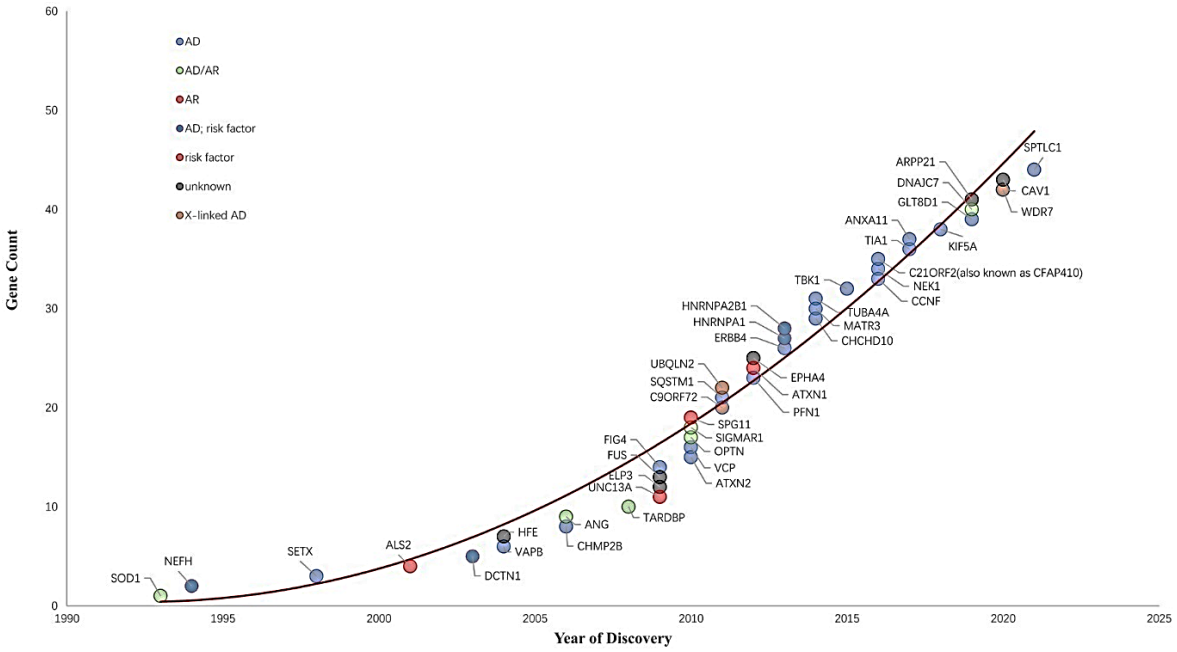

Figure 2. ALS gene discovery from 1990 to 2022. *Representative discovery of genes implicated with strong and moderate evidence in ALS.[27]*

To date (*Fig. 2*), 17 genes are definitively implicated in ALS pathogenesis, and 27 genes have strong or moderate evidence for their roles in causing ALS (*Tab.2*).

Year	Gene (Protein)	Role in ALS	Implicated mechanism
1993	SOD1 (superoxide dismutase 1)	Causative	Oxidative stress
1994	NEFH (Neurofilament Heavy Chain)	Risk factor	Axonal transport
1998	SETX (probable helicase senataxin)	Tenuous	RNA metabolism
2001	ALS2 (alsin)	Tenuous	Endosomal trafficking
2003	DCTN1(dynactin Subunit 1)	Risk factor	Axonal transport, Autophagy
2004	VAPB (vesicle-associated membrane protein-associated protein B/C)	Causative	Endoplasmic reticulum stress, Protein homeostasis
2004	HFE (Homeostatic Iron Regulator)	Risk factor (Strong)	Iron homeostasis
2006	ANG (angiogenin)	Risk factor (Moderate)	RNA metabolism
2006	CHMP2B (charged multivesicular body protein 2B)	Risk factor (Moderate)	Endosomal trafficking, Autophagy, Protein homeostasis
2008	TARDBP (TAR DNA-Binding Protein 43)	Causative	RNA metabolism
2009	FUS (Fused in Sarcoma)	Causative	RNA metabolism
2009	ELP3 (Elongator acetyltransferase complex subunit 3)	Tenuous	RNA metabolism, Cytoskeletal integrity
2009	FIG4 (polyphosphoinositide phosphatase)	Risk factor (Moderate)	Endosomal trafficking
2009	UNC13A (protein unc-13 homolog A)	Causative	Neurite outgrowth, Synaptic neurotransmission
2010	VCP (Valosin Containing Protein)	Causative	Mitochondrial dysfunction, Defective UPS degradation, Autophagy
2010	SPG11 (Spatacsin)	Tenuous	DNA damage
2010	ATXN2 (ataxin 2)	Clinical modifier	RNA metabolism
2010	OPTN (optineurin)	Causative	Autophagy, Neuroinflammation
2010	SIGMAR1 (sigma non-opioid intracellular receptor 1)	Tenuous	UPS and autophagy
2011	C9ORF72 (guanine nucleotide exchange C9ORF72)	Causative	Autophagy, RNA metabolism, Endosomal trafficking
2011	UBQLN2 (ubiquilin-2)	Causative	Autophagy, Protein homeostasis
2011	SQSTM1 (p62/sequestosome 1)	Risk factor (Moderate)	Autophagy, Neuroinflammation

Year	Gene (Protein)	Role in ALS	Implicated mechanism
2011	PFN1(profilin 1)	Causative	Cytoskeleton organization, Axonal growth and transport
2012	EPHA4 (Ephrin type-A receptor 4)	Causative	Cytoskeletal function, Axonal degeneration
2012	ATXN1 (ataxin 1)	Risk factor (Strong)	Nucleocytoplasmic transport
2013	ERBB4 (Erb-B2 Receptor Tyrosine Kinase 4)	Risk factor (Moderate)	Neuronal development
2013	HNRNPA1 (heterogeneous nuclear ribonucleoprotein A1)	Causative	RNA metabolism
2013	HNTNPA2B1 (heterogeneous nuclear ribonucleoprotein A2/B1)	Tenuous	RNA metabolism
2014	MATR3 (matrin 3)	Tenuous	RNA metabolism
2014	TUBA4A (tubulin α4A)	Risk factor (Strong)	Cytoskeletal dynamics, Axonal transport
2014	CHCHD10 (coiled-coil-helix-coiled-coil-helix domain-containing 10)	Causative	Mitochondrial dysfunction, Synaptic integrity
2015	TBK1 (serine/threonine-protein kinase 1)	Causative	Autophagy, Neuroinflammation
2016	C21ORF72/CFAP410 (Cilia and Flagella Associated Protein 410)	Risk factor (Strong)	Cilia formation, DNA damage repair, Mitochondrial function
2016	NEK1(serine/threonine-protein kinase Nek1)	Causative	DNA damage and repair, Cell cycles, Cilia formation
2016	CCNF (Cyclin F)	Risk factor (Strong)	Autophagy, Axonal defects, Protein aggregation
2017	ANXA11 (annexin A11)	Causative	Protein homeostasis
2017	TIA1 (TIA1 cytotoxic granule associated RNA binding protein)	Tenuous	TDP-43 accumulation, RNA metabolism
2018	KIF5A (Kinesin heavy chain isoform 5A)	Causative	Axonal transport
2019	DNAJC7 (DnaJ heat shock protein family (Hsp40) member C7)	Risk factor (Moderate)	Protein homeostasis
2019	ARPP21 (cAMP Regulated Phosphoprotein 21)	Tenuous	Toxic factor acts synergistically with GLT8D1 mutation
2019	GLT8D1 (glycosyltransferase 8 domain containing 1)	Tenuous	Ganglioside synthesis
2020	CAV1 (Caveolin 1)	Unassigned	Intracellular calcium homeostasis
2020	WDR7 (WD Repeat Domain 7)	Unassigned	Calcium flux, Neurotransmitter release

Year	Gene (Protein)	Role in ALS	Implicated mechanism
2021	SPTLC1 (Serine palmitoyl transferase long-chain base subunit 1)	Unassigned	Sphingolipid synthesis

Table 2. ALS-associated genes and the implicated disease mechanism are listed by year of discovery in ALS [27]**.** *Causative: variants in these genes have been shown to increase the risk of ALS based on statistical tests. Risk factor (Strong): variants in these genes have been shown to increase the risk of ALS in well-conducted recent studies. Risk factor (Moderate): variants in these genes have been shown to increase risk of ALS in smaller studies. Tenuous: Genetic variants in these genes have been associated with ALS in smaller studies published some time ago that have not stood up to replication. Clinical modifier: Genetic variants in these genes have been linked to a difference in the clinical phenotype of ALS, often disease duration. Unassigned: Variants in these genes have been linked to the ALS phenotype, but the category has not yet been assigned. (https://alsod.ac.uk/).*

A meta-analysis of the genetic epidemiology of ALS confirmed the most prevalent genetic causes of ALS are SOD1, C9ORF72 (chromosome 9 open reading frame 72), TARDBP (TAR DNA binding protein) and FUS (fused in sarcoma) [28].

SOD1 (Superoxide Dismutase 1). SOD1 gene encodes for a homodimeric metalloenzyme that catalyses the reaction that changes toxic O_2^- into O_2 and H_2O_2, which is part of the defence mechanism against oxidative stress. SOD1 is altered in 20% of fALS and 2-7% of sALS and more than 200 mutations have been described, mainly missense mutations (https://alsod.ac.uk/). The pathological mechanism proposed for ALS-associated mutations is a gain-of-function due to the improper folding of the SOD1 protein, leading to its aggregation.

C9ORF72 (Chromosome 9 Open Reading Frame 72). The pathogenic hexanucleotide repeat expansion (HRE) (GGGGCC)n found in C9ORF72 is the most common genetic cause of ALS. It is present in up to 50% of fALS cases and around 10% of sALS cases. This mutation in C9ORF72 is associated with neuronal inclusions. Three pathological mechanisms have been proposed: a loss of function due to the decreased expression of the protein, and two gain-of-function due to the production of toxic GGGGCC repeat-containing RNAs or to the accumulation of dipeptide repeat proteins (DPR) produced by noncanonical translation (repeat-associated non-ATG translation, RAN).

TARDBP (TAR DNA Binding Protein). The TARDBP (trans-activation element DNA-binding protein) gene is mutated in 5% of fALS cases and 1% in sALS cases. More than 60 different mutations have been identified. The pathological mechanisms proposed are linked to its cytoplasmic mislocalization and its aggregation, due to an increase of the phosphorylated TDP-43 in the cytoplasm or to a depletion of the nuclear TDP-43 (further explored in **paragraph 2**).

FUS (Fused in Sarcoma). Mutant FUS is observed in 4% of fALS patients and 1% of sALS patients. More than 120 mutations have been described at present, predominantly in the 3′ region encoding an arginine/glycine-rich region and a NLS domain (nuclear localization signal). FUS, which is essentially in the nucleus, regulates RNA processing, splicing, and mRNA trafficking. More than 60% of cases with FUS mutations show disease onset before 45 years of age, with many juvenile ALS cases. Two plausible pathological mechanisms have been proposed: a gain of function due to the mutant FUS protein aggregates that accumulate in neurons, disrupting their normal function and leading to cell death, and a loss of function due to the lack of the normal function of FUS, which can lead to defects in RNA processing, potentially contributing to cell dysfunction or death.

1.4. Physiopathological mechanisms involved in ALS

Most of the ALS-related genes are involved in the protein homeostasis and RNA metabolism of the cells, leading in most cases to protein aggregation, mainly ubiquitinated (in fact, post-mortem studies have shown protein aggregates in upper and lower motor neurons [28]). Different

mechanisms are involved in ALS, and their interaction leads to a disruption of the cellular network (*Fig.3*).

Oxidative stress. Excess levels of reactive oxygen species (ROS) and the cell's inability to neutralize them contribute to neuronal injury that leads to other pathophysiological processes. Oxidative stress in cellular models promotes alteration in TDP-43 (acetylation, phosphorylation, mislocalization and/or cytoplasmic aggregation), which leads to dysregulation of mitochondrial functions and RNA metabolism [2].

Mitochondrial dysfunction. Different ALS models show that mitochondrial function is impaired: altered energy production, excess generation of ROS, disruption of mitochondrial axonal transport, altered mitochondrial morphology and dynamics, perturbation of mitophagy and calcium buffering, and triggering of apoptosis. For example, TDP-43 physiologically binds mitochondria-transcribed mRNA, but mutations in *TARDBP* increase the mitochondrial localization of TDP-43[29].

Exitotoxicity. Excessive stimulation of postsynaptic glutamate receptors induces toxicity induced by calcium entry in motor neurons, which are very sensitive due to a lower calcium buffering capacity and higher presence of AMPA receptors [30].

Impaired protein homeostasis. The balance between the biogenesis and degradation of protein is very important for the cells. Mutations in some ALS-related genes disrupt this balance due to translation of misfolded proteins that accumulate or with aberrant localization or that can impair the degradation system (autophagy and Ubiquitin-proteasome system (UPS)) [31]. In addition, multiple ALS-associated genes encode proteins (like TDP-43 and FUS) which interfere with stress granules (SGs) dynamics. Stress granules are membraneless compartments constituted by mRNA and RNA-binding proteins (RBPs) that temporarily assemble in response to stress by stopping all the mRNA translation aside from the cytoprotective ones (further explored in **Paragraph 5**).

Aberrant RNA metabolism. Many RNA-binding proteins are involved in the pathogenesis of ALS. The RNA-binding proteins are a group of proteins that interact with RNA molecules to regulate various aspects of RNA metabolism, including RNA processing, stability, splicing, transport, localization, translation, and degradation. These proteins play essential roles in maintaining cellular function by controlling the life cycle of RNA and ensuring proper gene expression. Therefore, mutations in genes encoding these proteins can have widespread effects on gene expression and cellular homeostasis. The two major RBPs involved in ALS are TDP-43 and FUS, which predominantly localize in the nucleus but, when mutated, mislocalize to the cytoplasm. The mislocalization to the cytoplasm causes the depletion inside the nucleus (thus not exploiting their physiological functions) and aggregation in the cytoplasm, where they may cause toxicity [32-34]. Mutations in other RBPs such as angiogenin (ANG), senataxin (STX), matrin-3 (MATR3), heterogeneous nuclear ribonucleoproteins A1 (hnRNPA1) and A2B1 (hnRNPA2B1),

and ataxin-2 (ATXN2) further support the notion that disrupted RNA metabolism probably plays an important role in ALS [35].

Neuroinflammation. The central nervous system (CSN) of ALS patients can show signs of neuroinflammation either histologically (post-mortem samples or in the cerebrospinal fluid (CSF) and blood) and in imaging studies [36]. Astrocytes and microglial cells modulate inflammatory signalling by releasing neuroprotective or neurotoxic factors.

DNA damage and repair. Several ALS-associated genes have a role in the DNA repair mechanism (NEK1 and C21ORF2) or can lead to elevated DNA damage (TARDBP).

Impaired axonal transport. Axonopathy is a hallmark in ALS studied in patients and models and is characterized by pathological accumulations of organelles and phosphorylated neurofilaments in motor neuron axons. Some ALS-associated mutations have been found in genes involved in cytoskeletal and axonal transport [37]. Increasing evidence suggests that ALS axonopathy progresses through a "dying-back" mechanism (where axon degeneration begins at the distal end of the axon and gradually progresses backwards toward the cell body), starting from an energy depletion in the distal axon due to mitochondrial dysfunction and defective anterograde axonal transport [38].

Dysregulated endosomal and vesicle transport. ALS-associated gene variants that affect the endosomal transport are: TARDBP (its loss alter dendritic endosomes and thus reduce neuronal health), ALS2 (associated with a form of autosomal recessive juvenile onset), UNC13A (involved in priming synaptic vesicles and neurotransmitter release), VAPB, OPTN, CHMP2B, FIG4 (mediates retrograde trafficking of endosomal vesicles to the Golgi apparatus) [39].

2. TAR DNA binding protein-43 (TDP-43)

TAR (TransActivation Response region) DNA binding protein-43 (TDP-43) is a protein, codified by TARDBP gene (locus 1p36.22), of 414 amino acids and a molecular weight of 43 kDa, discovered for the first time in 1995 by Ou et al [42]. Ou et al. studied this protein for the first time in the HIV-1 (Human Immunodeficiency Virus type 1), where plays a critical role in Tat (Trans-Activator of Transcription) activation and thus the regulation of gene expression.

TDP-43 is a highly conserved and ubiquitously expressed RNA-binding protein [43], belonging to the heterogeneous nuclear ribonucleoprotein (hnRNP) family, which acts as key protein in the cellular nucleic acid metabolism due to its sequence-specificity ability to bind RNA [44].

The structure of TDP-43 (*Fig.3*) consists of [45]:

- N-terminal domain (NTD, aa 1-102), which comprises the Nuclear Localization Signal (NLS, aa 82-98). The first 10 residues of the NTD are crucial for the formation of the functional homodimers and TDP-43 physiological functions, RNA splicing, but it is also involved in the aggregation of the full-length TDP-43 [46]. The NTD is also involved in liquid-liquid phase separation (LLPS).
- two RNA recognition motifs: RRM1 (aa 104–176) and RRM2 (aa 192–262), which comprehend the Nuclear Export Signal (NES, aa 239–250). The RRM domains have high specificity towards short UG/TG-rich sequences of the RNA/DNA molecules [47].
- C-terminal domain (CTD, aa 274–414) which encompasses a prion-like glutamine/asparagine-rich (Q/N) domain (aa 345–366) and a glycine-rich region (aa 366–414). The CTD is highly disordered, and its structure resembles the prion-like domain of yeast proteins and thus is aggregation-prone. Through this domain, TDP-43, not only binds to 3' Untranslated Regions (UTRs) of several thousand mRNAs, but also its mRNA (an autoregulation mechanism to control its cellular concentration) [48]. This domain is physiologically involved in LLPS. Most of ALS-associated TDP-43 mutations and phosphorylation sites reside in this region.

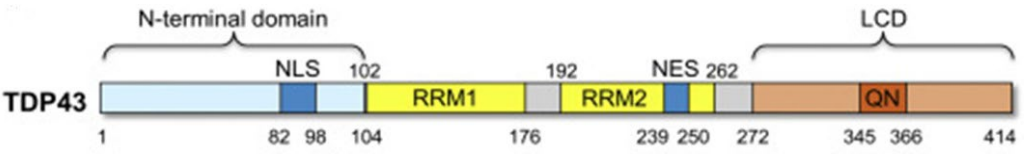

Figure 3. Structural organization of TDP-43*. NLS: Nuclear Localization Signal, RRM1 (RNA Recognition Motif 1), RRM2 (RNA Recognition Motif 2), NES: Nuclear Export Signal, LCD: Low Complexity Domain), QN: glutamine/asparagine-rich domain.* [49]

TDP-43 is mostly localized in the nucleus but, since its RNA-binding activity, shuttles to the cytoplasm where executes its functions. Physiologically, TDP-43 is natively dimeric or exists in a monomer-dimer equilibrium [50].

TDP-43 physiologically is involved in various aspect of RNA metabolism [45] (*Fig. 4*):

1. *Transcription*: it can act as a transcriptional repressor and is associated with proteins implicated in transcription.
2. *Splicing*: it regulates the splicing patterns of transcripts of several important genes, such as Cystic fibrosis transmembrane conductance regulator (CFTR), FUS, SNCA (a-synuclein), HTT (Huntingtin), and APP (Amyloid precursor protein) and itself.
3. *mRNA maturation and stability*: it interacts with regulatory 3′ UTR sequences of various mRNAs and affects their half-life positively and/or negatively.
4. *Transport*: it associates with RNA and forms granules that transport along the axons to deliver them in the dendrites.
5. *Translation*: it has several protein partners of the translation machinery, it can even form complexes with some of them.
6. *microRNA (miRNA) and long non-coding RNA (lncRNA) processing*: It is involved in the miRNA[2] biogenesis, since it is a component of the nuclear Drosha complex, which facilitates the binding with pri-miRNAs[3], resulting in their cleavage into pre-miRNAs[4] [52]. TDP-43 also binds several lncRNAs[5], such as nuclear enriched abundant transcript 1 (NEAT1) and metastasis-associated in lung adenocarcinoma transcript 1 (MALAT1).
7. *Stress granules (SGs) formation*: it is involved in the assembly and maintenance of SGs[6], and it also regulates the expression of key SG nucleating proteins, rasGAP SH3 domain binding protein 1 (G3BP) and T cell-restricted intracellular antigen-1 (TIA-1).

[2] miRNA are short endogenous sequences (20–22 nucleotides) of single-stranded non-coding RNA involved in finely controlling gene expression.
[3] Pri-miRNAs are long primary transcripts which consist of a short double strand RNA (dsRNA) region and a loop.
4 Pre-miRNAs are intermediate precursors that are formed after the cleavage of the pri-miRNAs by the nuclear Drosha complex.
[5] lncRNA are non-coding transcripts of more than 200 nucleotides that have a broad role but generally involve transcriptional regulation of other genes.
[6] Further explored in **Paragraph 5**.

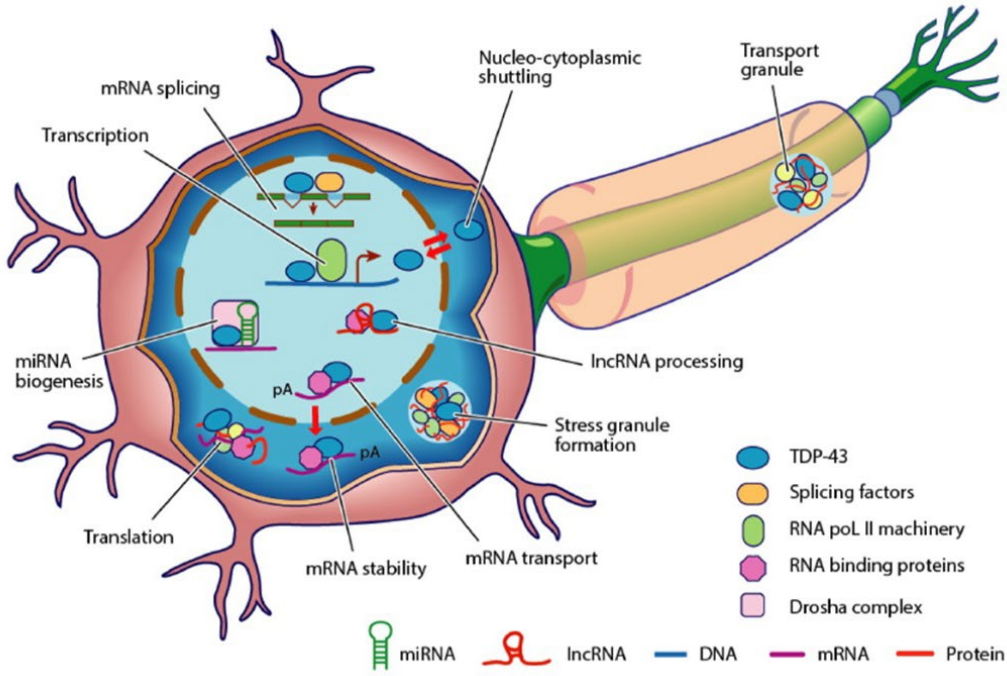

Figure 4. Schematic representation of TDP-43 physiological function [51]***.*** *TDP-43 is crucial for RNA metabolism, such as transcription and splicing, mRNA maturation, miRNA biogenesis, mRNA transport and more. More than 6000 of mRNA target are associated with TDP-43 (around 30% of the entire transcriptome).*

2.1. Pathological role of TDP-43 in ALS

The pathological inclusion of TDP-43 in the brain is one of the defining features of ALS, and its presence has become a hallmark of the disease. TDP-43 undergoes a series of pathological alterations that culminate in its mislocalization from the nucleus to the cytoplasm, where it aggregates and forms insoluble inclusions. These inclusions are a key pathological feature of ALS and are found in motor neurons, glial cells, and other brain regions associated with the disease.

The effects of the ALS-associated mutations on the TDP-43 protein include increased propensity to aggregate, enhanced cytoplasmic mislocalization, altered protein stability,

resistance to proteases or modified binding interactions with other proteins and more (*Fig.5*). Most of the mutation are in the exon 6 of TARDBP which encodes for the CTD, enhancing its aggregation propensity or its mislocalization to the cytoplasm or increased susceptibility to the protease-mediate degradation. Some mutations are found in both familial and sporadic cases.

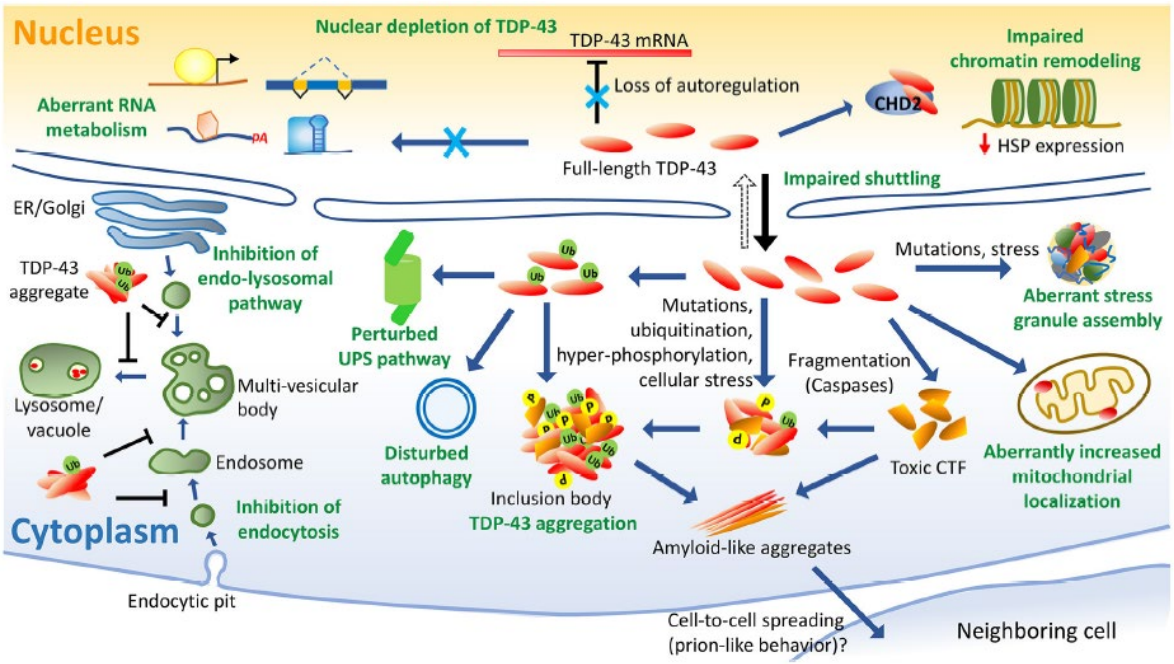

Figure 5. Schematic representation of TDP-43 pathological mechanisms in ALS [45]***.*** *In ALS, TDP-43 undergoes abnormal changes, such as hyperphosphorylation, mislocalization from the nucleus to the cytoplasm, and aggregation into insoluble inclusions within motor neurons and other brain cells.*

2.1.1. Mislocalization: loss and gain of function

One of the principal alterations of TDP-43 in ALS is its mislocalization from the nucleus to the cytoplasm and thus its inclusion in cytoplasmic bodies in the brain [43,53].

TDP-43 is mostly nuclear but its presence in the cytoplasm is physiological since it shuttles between the two compartments to carry out its functions. However, when TDP-43 is mutated, its cytoplasmic concentration increases, leading to its depletion in the nucleus and to a tendency to aggregation. The mechanism underlying the mislocalization it's still unclear, but the effects alter the normal cellular function, leading to neurons degeneration, due to both a loss of function and a gain of function of TDP-43. The loss of function mechanism results from TDP-43 nuclear depletion where it cannot carry out its normal functions (impaired RNA splicing, disruption of mRNA stability and transport, aberrant chromatin remodelling), while the gain of function mechanism results from its accumulation and toxic aggregation into the cytoplasm (post-translation modifications of TDP-43 lead to toxic aggregates formation, sequestration of RNA and proteins, cellular toxicity) [54,55].

2.1.2. Post-translational modifications

The alterations that TDP-43 goes through are mostly post-translational modifications, such as phosphorylation, acetylation, proteolytic cleavage and ubiquitination.

Phosphorylation. TDP-43 has 41 serine, 15 threonine and 8 tyrosine residues,

which may act as potential phosphorylation sites. Some of the most well-known phosphorylation sites reside in CTD and include Ser-379, Ser-403, Ser-404, especially Ser-

409 and Ser-410, which are considered crucial for cytoplasmic aggregation [43]. The phosphorylated TDP-43 in the cytoplasm is often found in ubiquitin-positive and tau-negative inclusions in the brain cortex and spinal cord of ALS and FTD patients [56]. The aggregates formed by phosphorylated TDP-43 are thought to exacerbate the loss of function mechanism and contribute to cell stress, mitochondrial dysfunction, and thus neuronal death.

Ubiquitination. In 2006, TDP-43 was identified as a key component of the insoluble and ubiquitinated inclusions in the brains of ALS and FTD patients [43,53]. The most well-known ubiquitination sites are the lysines K-48 and K-63. Scotter et al. have also found that when K-48 is poly-ubiquitinated, TDP-43 is degraded through the UPS, instead, when K-63 is polyubiquitinated TDP-43 is removed through the autophagic system [57]. Despite being ubiquitinated, TDP-43 aggregates are not efficiently degraded. This suggests that there is a failure of the UPS in ALS, which is unable to clear the ubiquitinated TDP-43 aggregates effectively, leading to their accumulation in the cytoplasm and disruption of cellular processes.

Acetylation. TDP-43 has 20 lysine residues, but not all of them can be acetylated. The most well-known acetylation sites are K-145 and K-192. In ALS, TDP-43 acetylation can impair its ability to bind RNA, regulate gene expression, and participate in RNA processing [58].

Proteolytic cleavage. TDP-43 presents 8 asparagines that could be sites for proteolytic cleavage, such as Asp89, Asp174 and Asp391. This cleavage generates C-terminally truncated fragments (CTF), such as CTF25 and CTF35, leading to the formation of the corresponding truncated protein, TDP-25 and TDP-35. CTF35 is generated by caspase-3/7-mediated cleavage after Asp89; CTF25 could be generated by caspase-4-mediated cleavage after Asp174 and by the cleavage after Asp169 [59]. Li et al. discovered that TDP-43 is cleaved initially after Asp174, generating CTF25, and this activates the downstream caspase-3/7 pathway, generating CTF35. This proteolytic cleavage of TDP-43 impairs its RNA binding capability and increases its propensity to aggregate in the cytoplasm.

Poly ADP-Ribosylation. TDP-43 glutamate or aspartate can be poly ADP-ribosylated (or PARylated) under DNA damage or cellular stress conditions. This modification can alter TDP-43's ability to bind RNA and other proteins, causing its mislocalization to the cytoplasm and its aggregation. In addition, PARylation seems to promote TDP-43's accumulation in stress granules [60].

Cysteine oxidation. TDP-43 has 6 cysteines, mostly localized in the RRM. Under oxidative stress conditions, TDP-43's cysteines can undergo oxidation, which could affect its RNA-binding functions and lead to TDP-43 misfolding and aggregation [61].

2.1.3. Cytoplasmic aggregations and cytotoxicity

The pathological alterations that TDP-43 undergoes, lead to impairment of its physiological functions which lead to cytoplasmic aggregation and thus causes a cascade of detrimental effects (*Fig.5*). The nuclear depletion of TDP-43, due to its mislocalization, lead to aberrant

RNA metabolism, accumulation to the cytoplasm and alteration of the ability to autoregulate its levels, promoting cytoplasmic aggregations.

Furthermore, the pathological changes in TDP-43 influence the protein turnover due the disruption of the UPS and autophagy. In ALS, the UPS is perturbed probably due to age-dependent malfunctions or ALS-associated mutations in proteins involved in the UPS, impairing TDP-43 clearance [57].

The accumulation of TDP-43 in the cytoplasm also influences autophagy. In addition, ALS-associated mutation in TDP-43 can lose the ability to bind the mRNA of protein ATG7 (Autophagy related 7), a key protein of the autophagy [62].

Pathological TDP-43 aggregates can have an impact on the mitochondrial functions: microtubule-mediated transport, membrane integrity, increased oxidative stress, dynamics, interactions with ER, calcium dysregulation and microglial activation [63].

In ALS and FTD, TDP-43 aggregates show prion[7]-like behaviour, such as self-propagation and intercellular spread. Misfolded TDP-43 aggregates can recruit normally folded TDP-43 inside, causing it to misfold and thus propagate within the cell. Furthermore, some studies suggest that TDP-43 can spread outside the cell through either exosome-mediated transfer or direct cellular connections [64].

2.2. The concept of TDP-43 proteinopathy

TDP-43 inclusions are a hallmark of ALS and FTD disease. However, numerous studies have found inclusions of non-mutated TDP-43 in other neurodegenerative diseases: dementia with Lewy bodies [65], corticobasal degeneration [66], progressive supranuclear palsy [67], Guam parkinsonism-dementia [68], Pick's disease [69], hippocampal sclerosis [67], Alzheimer's, Huntington's and Parkinson's disease [65]. Despite the differences in etiology, clinical symptoms and hallmarks between these diseases, TDP-43 shows the same pathological patterns (nuclear depletion, aggregation, ubiquitination and phosphorylation) in neurons and glia as ALS and FTD. These common TDP-43 pathomechanisms allow this group of neurodegenerative disease to be described as TDP-43 proteinopathies [51,70].

2.3. ALS-associated TDP-43 mutations

Since TDP-43 discovery, more than 60 mutations have been found and associated with ALS (5% in fALS cases and 1% in sALS cases). Most of the mutations are missense[8] and falls in the exon 6 which codify for CTD, aside from G40G, D65E, A66A in the NTD, A90V in NLS, S104S and D169G in RRM1, P225P in RRM2 and N267S (*Fig. 6*). Since the CTD is highly disordered and

[7] "Proteinaceous infectious particle" is a misfolded protein that induces misfolding in normal variant of the same protein.

[8] Missense mutations occur when a single nucleotide base in a DNA sequence is substitute with another, resulting in a different codon and a different amino acid.

encompass the Q/N-rich domain, the mutations in this region heighten TDP-43 aggregation-proneness. The possible reason behind the local prevalence of the mutations could be due to a better compatibility with normal development during early life stages [71].

The first mutations associated with ALS were discovered in 2008:

- D169G, G287S, A315T, G348C, R361S, A382T, N390D, N390S [72]
- G290A, G298S [73]
- G294A, Q331K, M337V [74]
- Q343R [75].

Since then, more mutations have been found each year (*Table 3*) and their functional consequences in ALS have been understood.

ALS-associated TDP-43 mutations					
G40G	D65E	A66A	A90V	S104S	D169G
P225P	N267S	G287S	G290A	S292N	G294A
G294V	G295C	G295R	G295S	G298S	Q303H
M311V	A315A	A315E	A315T	S317T	A321G
A321V	Q331K	S332N	G335D	M337V	Q343R
N345K	G348C	G348R	G348V	N352N	N352S
N352T	G357R	G357S	M359V	R361S	R361T
P363A	A366A	G368S	Y374X	S375G	G376D
N378D	N378S	N378_A382del	S379C	S379P	A382P
A382T	I383T	I383V	G384R	W385G	S387del/insTNP
N390D	N390S	S393L	c.-12-54G>A	c.-66G>T	c.-69C>T
c.403-80G>A	c.411A>G	c.543+112C>A	c.81G>A		

Table 3. List up to date of ALS-associated TDP-43 mutation *(https://alsod.ac.uk/output/gene.php/TARDBP).*

Most missense mutations exhibit an autosomal dominant pattern of inheritance and a spinal onset in both UMN and LMN of the disease. The most frequent ALS-associated TDP-43 mutation is the A382T, observed both in fALS and sALS, followed by the M337V, the G348C, and the G294V [76]. Many mutations result in substitutions to threonine and serine residues and may thus increase TDP-43 phosphorylation. Other mutations enhance aggregates formation (Q331K, M337V, Q343R, N345K, N390D), others may increase TDP-43 fragmentation with potential aggregation of CTF (A382T, S393L) and others may enhance TDP-43 mislocalization (G294V, A315T, M337V, A382T, and G376D) [77]. Some mutations are involved with the stress granules dynamics: D196G and R361G TDP-43 accumulate in major quantity in the stress granules; G348C TDP-43 forms larger stress granules; A315T and Q343R TDP-43 increase their size but

decrease their distribution density; D169G, G294A, Q343R, N390D, Q331K, and M337V TDP-43 enhance inclusion bodies [45].

However, all the existing data suggest that the effect of TDP-43 mutations may vary from patient to patient even within the same family, because they are heavily influenced by personal genetic background.

2.3.1. G376D TDP-43

In 2011, the novel mutation p.G376D was detected by Conforti et al. in a 67-year-old Italian woman, who developed progressive upper-limb weakness [78]. This woman belonged to a large Apulian family with several members affected by a rapidly progressive form of ALS. The construction of the family tree of this Apulian family (*Fig.7*), thanks even to the non-profit 2HE Association (https://www.ioposso.eu/2he), revealed an autosomal dominant inheritance pattern with high yet incomplete penetrance [79]. According to 2HE Association, since 2014 to date, among the 39 individuals diagnosed with this mutation, 25 cases have developed symptoms manifesting ALS, resulting in about 1 new case each year. To date, this family tree has expanded to include 8 generations, tracking back to 1890, with a total of 890 individuals and it is still evolving (personal communication).

The only other description of this mutation is an Asian fALS case [80] and a Swiss case [81], which was later revealed to be a member of the same Apulian family living in Switzerland (2HE Association, personal communication). Therefore, this mutation remains unique in Caucasians.

The pathological mechanism behind this mutation is still unknown, and therefore, the 2HE Association has started a program and collected biological samples (DNA, plasma and fibroblasts of asymptomatic, symptomatic carriers and healthy controls) from members of this family, which has the advantage of sharing a similar genetic background. Various research groups in Italy, including the one led by the late Professor Vincenzo La Bella, under whom I completed my PhD, are part of this program dedicated to studying, understanding and ultimately developing treatments for this mutation.

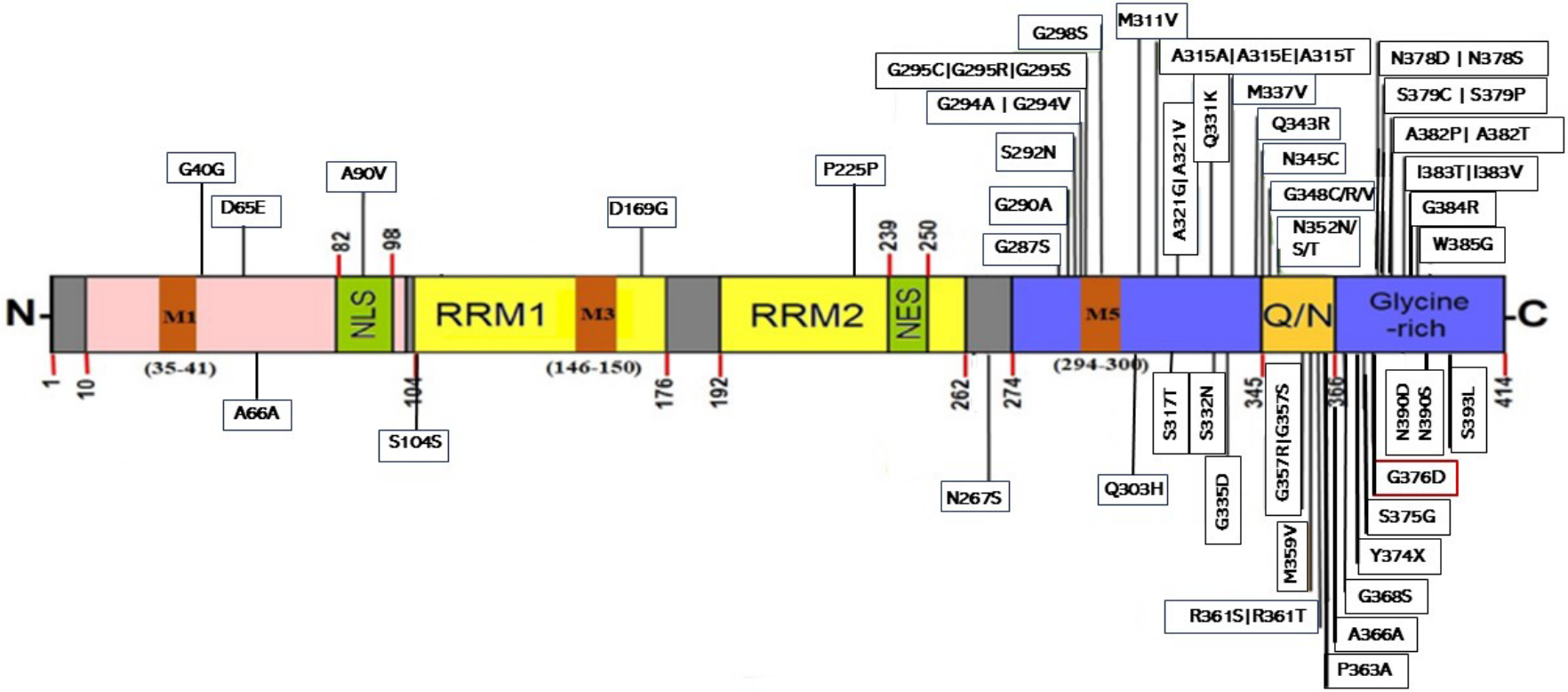

Figure 6. Representation of TDP-43 structure and the localization of its ALS-associated mutations. *Most of the mutations are localized in exon 6 that codify for the CTD.*

This is a revisited and updated image from Prasad et al,2019 [45].

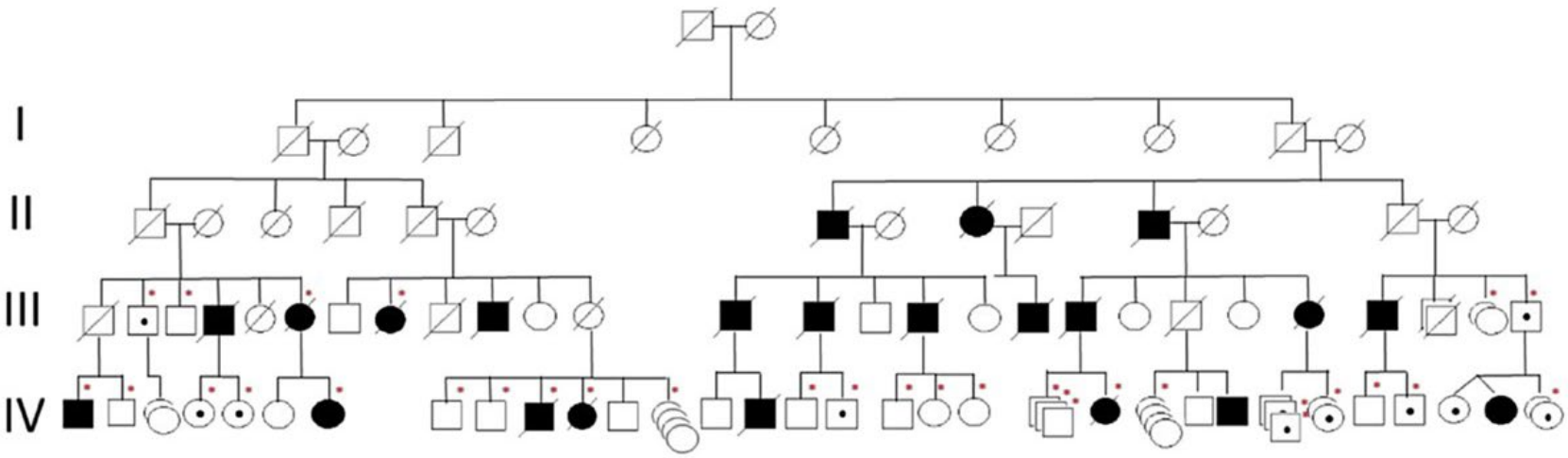

Figure 7. G376D TDP-43 family tree of Apulian family [79]***.*** *Square indicates male; circle female; slash deceased; black symbols patients affected by ALS; empty symbols with black dot are asymptomatic carriers. Red dot indicates DNA available for the study. To date, this family tree has expanded to include 8 generations, tracking back to 1890, with a total of 890 individuals and it is still evolving.*

3. Induced Pluripotent Stem Cells

In 2006, a revolutionary technological discovery was made by Yamanaka and Takahashi, which generated embryonic stem cells (ESCs)-like cells from mouse somatic cells [82]. These cells were termed induced pluripotent stem cells (iPSCs) and possess the ability to self-renew and differentiate into almost any cell type. In 2007, Yamanaka and Takahashi generated iPSCs from human fibroblasts [83], using the same 4 transcription factors: Oct3/4 (Octamer-binding transcription factor 3/4), Sox2 (Sex determining region Y-box 2), Klf4 (Kruppel-like factor 4) and c-Myc.

This new technology marked a turning point in the study of disease-related cell types (especially for diseases lacking suitable animal models), which are essential to study the disease pathogenesis, to screen new therapeutics and to develop cell replacement therapy, ultimately leading to patient-specific therapy.

In recognition of this revolutionary work, in 2012, Yamanaka was awarded the Nobel Prize in Physiology or Medicine.

3.1. iPSC generations: reprogramming and characterization

To generate iPSCs, Yamanaka et al. used the so-called "Yamanaka factors" in the fibroblasts of mouse. These four transcription factors were Oct3/4, Sox2, Klf4 and Myc.

Oct3/4. Oct3/4 is a pluripotency regulator during embryonic development, and its repression induces loss of pluripotency and differentiation, therefore, it plays a fundamental role in activating pluripotency-associated genes, maintaining the undifferentiated state of the stem cells and inhibiting differentiation genes [82-85, 88].

Sox2. Sox2 is a transcriptional factor that regulates pluripotency and neural differentiation. Together with Oct3/4, it maintains the self-renewal ability of iPSCs and is essential for their reprogramming. In addition, Sox2 interacts with other neural transcription factors and activates the expression of neural progenitor genes [82-86, 88].

c-Myc. C-Myc, together with its binding protein Max, is involved in cell proliferation, growth, differentiation and apoptosis and its repression stops self-renewal in ESCs and promotes differentiation. C-Myc may allow Oct3/4 and Sox2 to bind to their specific target DNA loci [82,87,88].

Klf4. Klf4 is a zinc finger-type transcription factor that regulates proliferation, apoptosis, differentiation and development. Nanog activate Klf4, which in turn, activates the expression of Nanog, Sox2 and Oct3/4. Together with c-Myc, its role is not essential for iPSCs reprogramming but enhances the effects of Oct3/4 and Sox2 [82,88,89].

The first somatic cells used to generate iPSCs were fibroblasts (of mouse first, and human after) [82,83]. To date, the fibroblasts are the most used somatic cell type since they have a lot of advantages:

- can grow from a skin punch biopsy, which is an easy and not too much invasive procedure
- are easily cultured, requiring a minimum of serum and medium
- have a high proliferative rate.

Aside from fibroblasts, theoretically every type of somatic cells can be used as starting material, however in the practice, the other cell types used today to generate iPSCs are: 1) PBMCs (peripheral blood mononuclear cells), 2) exfoliated renal cells (from urine), 3) keratinocytes (from plucked hair). These cells are more accessible than fibroblasts, since they can be collected through non-invasive methods (blood, urine, hair) [90-92].

3.1.1. Delivery methods for reprogramming

iPSCs can be generated through viral or non-viral delivery methods of the transcription factors.

Viral delivery methods. The first reprogramming methods were viral transduction, specifically retroviral and lentiviral transduction [82,93], and to date, they are still widely used. However, retrovirus and lentivirus can integrate into the iPSCs genome, leading to improper activation of proto-oncogenes and insertional mutagenesis.

Therefore, non-integrative methods have been developed, such as Adenovirus[9] and Sendai virus[10], although they are less effective than integrative ones [94]. Adenovirus do not integrate into the iPSCs genome, but it results in transient delivery; therefore, several transductions are required for reprogramming. In addition, it is a DNA virus, so it leaves a DNA footprint in the iPSCs. F-deficient Sendai virus, instead, is an RNA virus that does not have a DNA phase and does not enter the nucleus, therefore, it will not leave a DNA footprint, and it will be cleared from the cells after around 10 passages. In addition, Sendai virus has a high efficiency (more than 80%), compared to the previous methods and even the non-viral methods [94,97].

Non-viral methods. Several non-viral methods have been successfully developed [98] such as (*Fig. 8*):

- Episomal vectors are now an established method to reprogram human fibroblasts into human iPSCs (hiPSCs) with a good efficiency [99].

[9] Adenovirus is a non-enveloped, double-stranded DNA with icosahedral capsid virus belonging to the Adenoviridae family [95].

[10] Sendai virus (mouse parainfluenza virus type 1 or hemagglutinating virus of Japan (HVJ)) is a non-segmented negative-strand RNA virus belonging to the Paramyxovirus family with a large spherical shape. A SeV virion consists of the nucleocapsid (genomic RNA complexed with proteins), an envelope (a lipid bilayer) and a matrix connecting the nucleocapsid and envelope [95].

- PiggyBac system[11] is promising for mouse iPSCs but has a very low efficiency for reprogramming human mesenchymal stem cells (50-fold less than retroviral delivery) [100].
- Minicircle DNA[12] has low efficiency of reprogramming in neonatal fibroblasts and there are no reports in other somatic cell types [101].
- Direct protein delivery has a lower efficiency of mRNA delivery [102].
- Synthetized mRNA has the advantage of having high efficiency and being commercially available but is labour intensive [103].

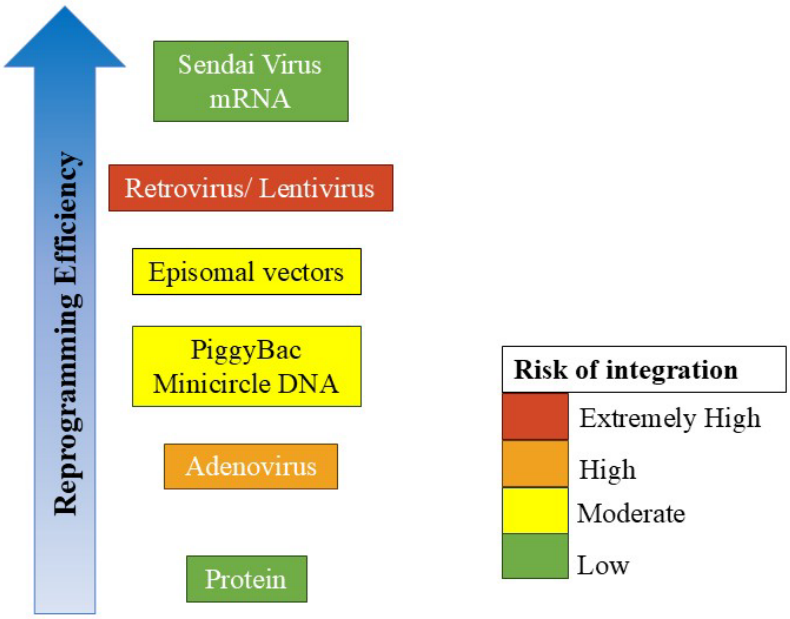

Figure 8. Viral and non-viral delivery methods. *Reprogramming delivery methods, viral and non-viral, ordered by reprogramming efficiency and distinguished (by colour) based on their risk of integration in the iPSCs genome.*

3.1.2. Isogenic iPSCs

Patient-derived primary cells are valuable tools for disease modelling, aiding in the study of the disease and the development of therapeutic strategies. However, their use is limited due to the restricted growth potential and to difficulty in accessing certain cell types. The development of human iPSC technology overcomes limitations of primary cells by offering the possibility of using hiPSCs derived from easily available patient-derived cells as a model. Obtaining the necessary starting material from patients remains a challenge, as it's not always feasible due to patient refusal or the lack of patients with very rare mutations. Furthermore, when using an iPSCs-based disease model (particularly those with defined genetic causes), most of the time, the adequate controls are iPSCs derived from a healthy family member, but

[11] PiggyBac is transposon that in the presence of a transposase can be integrated into chromosomal TTAA sites and subsequently excised from the genome footprint-free upon re-expression of the transposase [98].
[12] Minicircle DNA are minimal vectors containing only the eukaryotic promoter and cDNA(s) that will be expressed [98].

this condition can lead to confounded data interpretation due to cell heterogeneity and different genetic backgrounds. For this reason, isogenic iPSCs are increasingly being used as disease model.

Isogenic iPSCs are iPSCs that have been gene-edited: 1) correction of disease-causing gene mutations in patient-derived iPSCs; 2) introduction of specific mutation in wild-type (WT) iPSCs. This allows the generation of iPSCs lines genetically identical to the donor somatic cells, which can ensure the identification of the physiopathological mechanisms underlying the disease with the sole variable of the introduced/corrected mutation and without the genetic background variable and line-to-line variations (further explored in **sub-paragraph 3.2**) [104].

The most used gene-editing technologies are:

- CRISPR/Cas9 (Clustered Regularly Interspaced Short Palindromic Repeats/ CRISPR-associated protein 9). CRISPR/Cas9 involves a guide RNA (gRNA) that matches the desired target gene and Cas9, an endonuclease, which breaks a double-stranded DNA, allowing the cell's repair mechanism system to knock out the gene or enable the insertion of new genetic material [105].
- ZFNs (zinc-finger nucleases). ZFNs consist of a customized array of zinc-fingers engineered to bind to a specific DNA sequence and a non-specific DNA endonuclease domain. When the ZFN binds the targeted sequence, the nucleases domain dimerizes and makes a double-strand break on DNA, allowing then the cell's repair mechanism system to intervene [106].
- TALENs (transcription activator-like effector nucleases). TALENs consist of a non-specific DNA nuclease fused to a DNA-binding domain, engineered to target specific DNA sequences. Like the ZFN, the nuclease induces double-strand breaks, which are then repaired by the repair mechanism system [107].

3.1.3. Characterization of iPSCs

To ensure that the reprogramming process is successful, it is very important to characterize the iPSCs before differentiating them, through different assays [83,108].

Morphology. iPSCs present typical stem cell morphology: compact and well-defined borders – colonies should have smooth and "round" edges with clear boundaries, a high nucleus-to-cytoplasm ratio – cells should appear dense with large nuclei and minimal cytoplasm, uniform cell morphology – cells within the colony should look similar in size, tightly packed, prominent nucleoli – the nuclei often show one or more nucleoli, flat colony structure – colonies should grow in a flat monolayer, high refractivity under phase-contrast microscopy, absence of differentiated cells.

Pluripotency markers. To ensure that the reprogramming process was successful, the iPSCs must express pluripotency markers. Therefore, the pluripotency markers to be studied must certainly be Oct3/4, Sox2 and Nanog, but it would be recommended to study other markers in

combination with the first ones, such as c-Myc, KlF4 and Tra-1-60 (Tumor-related antigens 1-60) to better determine the pluripotency of the iPSCs.

Embryoid body and teratoma formation. iPSCs should be able to differentiate into cells of the three germ layers (ectoderm, endoderm and mesoderm), therefore embryoid body and teratoma formation assays are carried out. In the embryoid body (EB) formation assay the iPSCs are grown in suspension so that they can spontaneously aggregate to form the EB, while in the teratoma formation assay, they are injected into an immunodeficient mouse to become a teratoma. Then the expression of markers belonging to the three germ layers is tested on EBs and teratoma.

STR. STR[13] (Short Tandem Repeat) assay, along with gene sequencing (in case of iPSCs with a specific mutation) is carried out to authenticate the iPSCs identity.

Karyotype. During reprogramming, the iPSCs could acquire genetic abnormalities (aneuploidies and structural changes), therefore, the karyotype is required after reprogramming to ensure that the iPSCs obtained are stable and without any abnormalities.

Silencing of transgenes. The transgenes used for reprogramming should not be expressed anymore after some passage; therefore, is important to study their silencing.

3.2. Challenge of using iPSCs as disease models: the impact of cellular heterogeneity

The use of iPSCs as a disease model is a powerful tool in the research field and gene therapy. Despite their numerous advantages, iPSCs-based disease model presents some challenges that are still to be overcome, such as cellular heterogeneity, lack of maturity of the iPSCs-derived phenotypic cells and incomplete disease representation.

Cellular heterogeneity refers to the variability shown within iPSCs cultures derived from the same donor [109]. This heterogeneity can complicate the interpretation of the results and could be due to: 1) clonal variation, i.e. subtle genetic differences during the reprogramming process can lead to variations between iPSCs clones from the same donor; 2) incomplete reprogramming process, some cells may remain partially differentiated; 3) epigenetic variations between cells during the reprogramming process; 4) variability due to passage number and culture conditions of the somatic cells.

Especially in the case of polygenic or sporadic disease, the use of iPSCs as a disease model is even more challenging since the phenotypic cells obtained from the differentiation of the iPSCs often exhibit an immature, embryonic-like phenotype, lacking the functional and molecular characteristics of a fully developed adult. Moreover, conventional iPSC-derived cell cultures (2D-cuture systems) do not reflect the complex interactions between different cell types or the influence of the in vivo environment. As a result, disease mechanisms, especially those associated with late-onset or multifactorial conditions such as amyotrophic lateral sclerosis (ALS), cannot

[13] STR (short tandem repeats) are short sequences of DNA of 2-6 bp that are repeated in tandem [110], used as molecular marker of loci for DNA profiling, forensic genetic and authentication of cells.

be fully elucidated using single-cell-type models alone [109]. Co-culture of two-different types of phenotypic cells and organ-on-a-chip (3D-culture systems) promises to overcome these limitations by enabling the study of cellular interactions and more accurately simulating the physiological microenvironment.

4. IPSCs-derived Motor Neurons

ALS is characterized by the progressive degeneration of the UMNs and LMNs. The UMNs reside in the cerebral cortex, specifically within the primary motor cortex, and their axons descend to the brainstem and establish a pathway that connects with the spinal cord. The LMNs - which include the branchial, visceral and spinal MNs - reside in the brainstem and the spinal cord and innervate skeletal muscle in the periphery [111].

Until recently, the study of MNs affected by ALS relied on post-mortem brain tissue, animal models or neuron-like cell lines. However, each of these models presents significant limitations; for example, findings from animal models cannot always be extrapolated directly to humans. The advent of iPSCs technology has opened new avenues for studying ALS.

Insights into motor neuron development in vivo enabled Wichterle et al. to successfully differentiate embryonic stem cells (ESCs) into MNS in 2002 [112], a breakthrough that was later extended by Dimos et al., who derived MNs from iPSCs in 2008 [113]. Since then, many researchers have contributed to the development of differentiation protocols, which can be categorized into: 1) differentiation through the use of small molecules which mimic morphogen signals in embryo development; 2) differentiation through the expression of lineage-specific transcription factors; 3) differentiation through use of 3D cultures.

4.1. Methods for differentiating iPSCs into MNs

Several factors must be considered when selecting a method for differentiating iPSCs into MNs. In 2D-culture systems, in particular, the fundamental aspects to consider are the differentiation yield and the homogeneity of the resulting MNs population. Consequently, many laboratories are developing increasingly sophisticated differentiation protocols to optimize these outcomes. The 2D culture system is useful for studying the development of MNs and the disease pathology driven by intrinsic cellular factors, but it cannot mimic the effect of a more complex microenvironment. Therefore, it is useful to use the co-culture or 3D-culture system with heterogeneous cells, such as MNs and skeletal muscle or microglia, to better understand multifactorial disease and the interaction with the microenvironment [114].

Given that ALS primarily affects LMNs located in the spinal cord, the present thesis focuses specifically on the generation of spinal MNs from iPSCs. The following sections provide an overview of current differentiation protocols aimed at producing sMNs in vitro (*Fig. 9*).

4.1.1. In vivo MNs development: the basis for in vitro differentiation

The differentiation process of iPSCs is based on in vivo embryonic development, in which the iPSCs are guided through the neural progenitor stages towards a motor neuronal fate. The signalling pathways during embryonic motor neuron development have been extensively studied [115]. In vivo, the ectoderm undergoes a process called neurulation, which leads to the formation of three ectodermal masses:

- the neural tube, which gives rise to the CNS (Central Nervous System), composed of the brain and the spinal cord
- the neural crest cells, which form the peripheral ganglion, the pigments of the skin and the dorsal root ganglia
- the external ectoderm, which generates the epidermis.

After the neurulation, the neural tube undergoes by several stimulations of inductive signalling for the subsequent differentiation process. The ectodermal cells acquire neural identity through the activation of FGFs (Fibroblast growth factors) and Wnt (Wingless-type MMTV integration site family members) signalling, and at the same time, the mesodermal and endodermal cells are inhibited through the dual-SMAD, i.e. inhibition of BMPs (Bone Morphogenetic Proteins) and TGF- β (Transforming Growth Factor Beta) signalling [111, 116].

FGFs, Retinoic Acid (RA), and Wnt signalling are fundamental for establishing caudal (spinal) neural identity. RA promotes the expression of rostral Hox genes[14] (e.g., Hox1 – Hox5), while FGF signalling induces more caudal Hox genes (e.g., Hox6 – Hox9), thereby defining motor neuron columnar identities. These factors are expressed in a decreasing dorsal to ventral gradient, while simultaneously co-operate with an increasing ventral to dorsal gradient of SHH (sonic hedgehog morphogen). SHH are critical for the induction of spinal MN progenitors through the sequential activation of transcription factors such as PAX6, NKX6.1 and OLIG2. OLIG2 represses HES expression, which induces Neurogenin2 (Ngn2). Ngn2 is required for cell cycle exit and induction of MN transcription factors such as HB9, Isl-1 and LHX3, which further specify and stabilize the MN identity. As $HB9^+$ MNs exit the cell cycle and mature, they start to express CHAT (Choline Acetyltransferase), which is responsible for synthesizing acetylcholine at the neuromuscular junction [111, 118].

After the formation of the general MN progenitor, inductive signals along the rostro-caudal axis ulteriorly develop MNs to adjust to specific local needs, leading to the formation of anatomically defined motor columns. There are four main columns: the median motor column (MMC, which innervate axial muscles[15]), the lateral motor column (LMC, which innervate limb muscles), the hypaxial motor column (HMC, which innervate muscles derived from the ventral mesenchyme[16]), and the preganglionic column (PGC, which connect to the sympathetic ganglia) [111].

The spatial expression of Hox genes, along with transcription factors such as FOXP1 and LHX3, determines the subtype identity of spinal MNs. For example, LMC neurons are characterized by a $FOXP1^+/LHX3^-$ profile, whereas MMC neurons express $FOXP1^-/LHX3^+$.

[14] Hox genes (or homeobox sequences) are a conserved 180 bp region of DNA that encodes a DNA-binding homeodomain. Homeobox-containing genes often encode transcription factors that play crucial roles in development and patterning [117].
[15] Axial muscles are mainly involved in the maintenance of the body posture and are found all along the body axis [111].
[16] The ventral mesenchyme gives rise to the body wall musculature composed of the intercostal and abdominal muscles present only at thoracic level [111].

These molecular signatures are critical for classifying MN subtypes both in vivo and in vitro [111].

4.1.2. In Vitro differentiation: Small Molecules

Inspired by the MNs in vivo development, several approaches have been proposed to successfully differentiate iPSCs into spinal MNs.

Wichterle et al. were the first to develop a protocol to successfully differentiate mouse ESCs into spinal MNs by culturing them in suspension to form EBs. The EBs were exposed to RA and SHH signalling to generate MN progenitors, which became MNs using neurotrophic factors. This protocol was successful but time-consuming [112].

To enhance differentiation efficiency, different strategies have been applied in the years (*Tab. 4*). Following are some of the most relevant modifications to improve the differentiation in MNs:

- Chambers et al. introduced the dual-SMAD inhibition to promote the formation of neural stem cells (NSCs) [119]
- Amoroso et al. increased the yield of MNs through the increase of RA concentration and the addition of SHH agonists, and later Qu et al. increased even more the yield by advancing the timing of RA treatment [120, 121].
- Maury et al. and Du et al. demonstrated that inhibiting GSK3 with CHIR-99021, a Wnt pathway agonist, during neural induction promoted neural differentiation and enhanced generation of MN progenitors [122, 123]
- Ben-Shushan et al. inhibited the Notch signalling with γ-secretase inhibitors (e.g. DAPT) to accelerate MN differentiation [124].

Other optimisation efforts have also demonstrated the impact of timing, plating, and media composition on the yield and purity of MN populations. These efforts highlight the complexity of developing efficient MN differentiation protocols, where small changes in protocol can affect outcomes.

Year	Small molecules	Duration (days)	MN efficiency (%)	References
2008	RA, SHH, BDNF, GDNF, CTNF	30	20	Dimos et al. (2008)
2009	RA, SHH, BDNF, GDNF, IGF-1	35	>40	Hu & Zhang, (2009)
2009	RA, PMA, GDNF, BDNF, CTNF	48–62	>35	Karumbayaram et al. (2009)
2012	SB, Dorsomorphin, RA, PMA, BDNF, GDNF, forskolin	71	>10	Bilican et al. (2012)
2013	LDN, SB, RA, SHH, BDNF, GDNF, CNTF	31	30	Amoroso et al. (2013)
2013	RA, PMA, GDNF, BDNF	31	40	Sareen et al. (2013)
2014	LDN, SB, RA, SAG, PMA, BDNF, GDNF, CNTF	31	>30	Grunseich et al. (2014)
2013	Dorsomorphin, RA, SHH, BDNF, GDNF, IGF-1	20	70	Qu et al. (2014)
2015	Dorsomorphin, SB, BIO (GSK inhibitor), RA, PMA, c-AMP, BDNF, GDNF, IGF-1	28–42	>60	Shimojo et al. (2015)
2015	SB, LDN, RA, SAG, CHIR, DAPT	25	70	Maury et al. (2015)
2015	CHIR, DMH-1, SB, RA, PMA, BDNF, GDNF, CNTF, IGF-1, Compound E	30	95	Du et al. (2015)
2016	RA, SHH, c-AMP, BDNF, GDNF, IGF-1	21–30	40	Dafinca et al. (2016)
2016	LDN, SB, RA, PMA, CHIR, c-AMP, BDNF, GDNF, IGF-1	28	80	Hu et al. (2016)
2018	CHIR, DMH-1, SB, RA, PMA, BDNF, GDNF, CNTF, IGF-1, Compound E	18–53	60	Sances et al. (2018)
2018	CHIR, Dorsomorphin, Compound E, SHH, SAG, PMA, RA, CTNF, BDNF, GNDF, NT-3	21	73	Bianchi et al. (2018)
2018	SB, CHIR, Dosomorphin, RA, PMA, DAPT, db-cAMP, BDNF, GDNF, IGF-1	40	70	Fujimori et al. (2018)
2018	LDN, SB, RA, SHH, BDNF, GDNF, CNTF	27	20	Bossolasco et al. (2018)
2019	SB, Dorsomorphin, RA, PMA, BDNF, GDNF, forskolin	28–42	>90	Bax et al. (2019)
2020	CHIR, DMH-1, SB, RA, PMA, BDNF, GDNF, CNTF, IGF-1, Compound E	28	67	Thiry et al. (2020)
2020	Dorsomorphin, FGF2, Noggin, SB, RA, SHH, BDNF, GDNF, IGF-1	20	80	Faye et al. (2020)
2020	SB, LDN, RA, SAG, CHIR, DAPT	29	>90	Garcia-Diaz et al. (2020)
2021	LDN, SB, IWR1e, CHIR, RA, PMA, DAPT	28–42	16	Sato et al. (2021)
2021	RA, PMA, BDNF, GDNF, IGF-1, c-AMP	28–52	>90	Cutarelli et al. (2021)

Table 4. List of protocols using small molecules to differentiate hiPSCs into MNs [115]. *In the Table the protocols are ordered by year of publication and highlight the small molecules used, the duration and the yield of differentiation. For each protocol, the references cited can be found in Castillo-Bautista et al. paper (2023).*

4.1.3. In vitro differentiation: Transcription factors

Despite the significant progress achieved using small molecules to mimic developmental mechanisms for high-yield and faster MN differentiation, several challenges remain. Notably, applying the same differentiation protocol to various iPSC lines often results in inconsistent efficiencies. Even within the same iPSC line, different passages or subclones can produce variable yields of MNs, further complicating reproducibility. These limitations have led researchers to delve into new approaches, such as the expression of transcription factors.

Mazzoni et al. generated MNs forcing the expression of the transcription factors NGN2, ISL1, and LHX3 (collectively referred to as NIL) and NGN2, ISL1 and PHOX2A (collectively referred as NIP) in mouse ESCs, which are known to define post-mitotic MN identity, respectively spinal and cranial. NIL expression in mouse ESCs resulted in nearly 80% efficiency of spinal MN differentiation in just 6 days [125]. Similar approaches, Adenovirus or Sendai virus have yielded promising results in hESCs and iPSCs, though with variable efficiency and technical challenges related to virus handling and transduction variability [126, 127]. To address these limitations, alternative non-viral methods have been developed. Goparaju et al. have demonstrated that synthetic mRNAs encoding neurogenic transcription factors can differentiate with a high MN purity, although technically demanding [128]. Another approach was developed by De Santis et al which used a PiggyBac transposon-based system (from epB-Bsd-TT[17]) for a rapid and efficient spinal and cranial MN generation, with over 90% of cells expressing MN markers by day 5 [130].

Despite these advances, one persistent challenge remains: the functional immaturity of the derived MNs. While transcription factor-based protocols accelerate differentiation and increase yield, the resulting MNs often lack full physiological maturity, indicating that additional transcriptional programs or environmental cues may be required to recapitulate in vivo MN functionality.

4.1.4. In vitro differentiation: 3D- culture systems

During development, MNs interact with many other cell types, such as glial cells and skeletal muscle cells. These interactions may contribute to key aspects of MN function and their development and are often spatially organized in vivo: MN somas and dendrites primarily engage with central glial cells, while axons form connections with Schwann cells and muscle fibers in the periphery. To better mimic this complex and dynamic environment in vitro, researchers have developed co-culture approaches and 3D systems, such as organoids.

Among these, microfluidic devices are powerful tools which typically consist of two or more chambers connected by microchannels. Basic motor circuits can be reconstituted by culturing

[17] A transposon is a DNA segment, which can change its relative position within the entire genome of a cell. The piggyBac (PB) transposon is a highly efficient movable genetic element that recognizes transposon-specific inverted terminal repeats (ITRs) sequences on both ends of the transposon and through a “cut and paste” mechanism moves the contents from its original positions and efficiently integrates them into TTAA chromosomal sites [129].

iPSC-derived MNs in one compartment, allowing axons to extend through the microchannels to innervate skeletal muscle cells in the opposing compartment between 28 to 36 days [131,132]. Such systems enable the isolation of subcellular compartments, allowing researchers to distinguish between local and retrograde signalling events and to conduct highly controlled, localized manipulations.

Another approach is organ-on-a-chip systems, which should mimic intricate intercellular interactions, including those of the blood-brain barrier (BBB). Some platforms have successfully integrated MNs into these systems, forming motor units in the presence of skeletal muscle fibers [133]. These systems offer a high level of physiological relevance in comparison to the microfluidic chambers, but are technically demanding, costly, and often challenging to standardize.

In contrast to 2D-cultures approaches, iPSC-derived organoids are self-organizing 3D-cultures that more closely mimic early developmental processes. Since the first report of cerebral organoids in 2013, developed by Lancaster et al. [134], several types, such as spinal cord and sensorimotor organoids, have been developed to model different regions of the nervous system. An upgraded and promising approach involves the generation of assembloid**s**, in which multiple organoids are combined to mimic interregional neural circuits. Andersen et al. have developed one of the most complete models of MN signalling, a cortico-spinal assembloids which integrates cortical and spinal MN with skeletal muscle organoids [135].

Despite their promise, both organ-on-a-chip and organoids have several limitations: reproducibility challenges, batch-to-batch variability, and heterogeneity in cellular composition and spatial organization (particularly for organoids). Moreover, their complex setup and long maturation timelines restrict their scalability and utility in high-throughput applications [114].

4.1.5. In vitro differentiation: "aged" MNs

Aging represents a significant risk factor for the onset and progression of numerous neurodegenerative diseases, including ALS. For better understanding, it is important to distinguish between mature MNs (obtained by most of the differentiation methods discussed in the above sub-paragraphs) and "aged" MNs. Mature MNs are exhibit intrinsic excitability, can generate and propagating action potentials, form functional synaptic connections and express synaptic proteins, voltage-gated ion channels, and neurotransmitter receptors. Instead, "aged" MNs show dendritic retraction, synaptic loss, reduced electrophysiological performance, telomere shortening, compromised mitochondrial dynamics and function, increased accumulation of DNA damage, global heterochromatin loss, nuclear lamina disorganization, protein aggregation, and cellular senescence [114].

This discrepancy presents a major limitation in the study of late-onset neurodegenerative diseases, as these pathologies are characterized by age-related cellular decline.

To overcome this limitation, several strategies have been proposed to induce aging-like phenotypes in iPSC-derived MNs. One approach involves the expression of progerin, a truncated form of Lamin A associated, which induces several age-associated cellular alterations, including nuclear abnormalities and DNA damage [136].

Another approach involves the inhibition of telomerase, using BIBR1532 to accelerate telomere shortening and induce premature aging phenotypes [137].

The manipulation of age-associated regulatory proteins, such as RANBP17 [138] and the transcriptional repressor NRSF/REST [140], induces transcriptional and epigenetic profiles more closely resembling those of aged neurons, offering an additional route to induce aging in vitro.

Collectively, these approaches underscore the importance of incorporating aging features into iPSC-based models for neurodegenerative disease research.

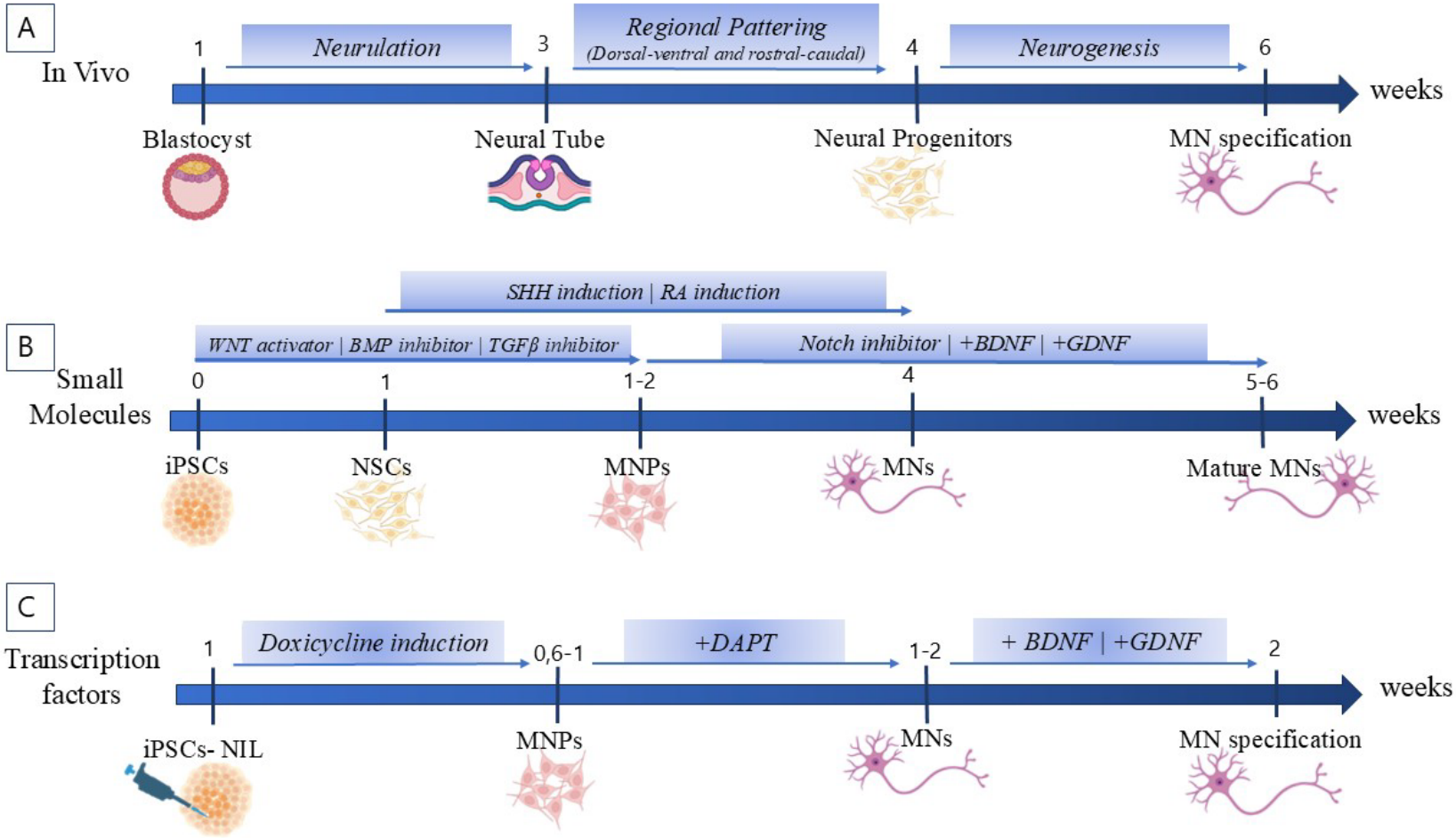

Figure 9. Comparison of motor neurons differentiations: in vivo VS in vitro. *A) Timeline of in vivo differentiation from blastocyst to MN, showing the most relevant steps; B) Timeline of in vitro differentiation using small molecules from iPSCs to MNs, showing the most important activation/inhibition pathways; C) Timeline of in vitro differentiation using transcription factors from transfected (NIL) – iPSCs to MNs, showing the crucial steps.*

5. Stress Granules

Stress granules (SGs) are membraneless cytoplasmic organelles of the size of 100-2000 nm, containing RBPs and RNAs, that form in response to cellular stress, such as oxidative stress, heat shock, viral infection or nutrient deprivation. SGs include PICs (stalled 48S preinitiation complexes) consisting of translationally arrested mRNAs (mostly housekeeping), small ribosomal subunits, translation initiation factors and RBPs. Over the last 20 years, numerous SG- related RBPs, involved in the SGs formation and stability, have been discovered, such as PABP (PolyA-binding protein), G3BP (RasGAPSH3-binding protein) and TIA-1 (T-cell intracellular antigen-1) [140]. More in-depth analyses have shown that SGs are constituted of two layers: a "core", that is a stable centre substructure, and a "shell" that surrounds the core and whose composition is more dynamic.

SGs are transient granules that form in response to cellular stress, inhibiting the translation machinery by sequestering mRNA. When the cells receive a stress-induced insult, the translation initiation is inhibited, primarily by the activation of the integrated stress response (ISR). ISR activation relies on the phosphorylation of eIF2α (eukaryotic translation initiation factor 2 alpha) by one or more of four eIF2α kinases [141]. The IRS pathway term in accumulating of stalled mRNAs which, together with their associated proteins, condense into SGs. Once the stress-inducing insult is resolved, the SGs disassemble, and the translation is resumed [140-142]. The cytoskeletal proteins, such as microtubules, take part in the assembly and disassembly of SGs.

SGs play a protective role during cellular stress: by halting general translation, the cell redirects cellular energy toward the expression of stress-response genes and sequesters pro-apoptotic signalling molecules, promoting cell survival [140-142]. However, under particular conditions, SGs dynamics can be altered, contributing to the disease process.

As previously described in **sub-paragraphs 1.4**, SGs dynamic is impaired in ALS due to different pathological mechanisms, including the alteration of ALS-associated RBPs, such as TDP-43, FUS and hnRNPA1. Chronic stress or genetic mutations may impair the normal dynamics of SGs assembly and disassembly, leading to the formation of persistent or aberrant granules, which may facilitate the cytoplasmic aggregation [143].

5.1. Role of SGs in TDP-43 aggregation in ALS

Cytoplasmic mislocalization and aberrant post-translational modifications of TDP-43 occur in ALS. Once it is accumulated in the cytoplasm, TDP-43 could be recruited to SGs, compromising the normal function of SGs, thus impairing stress response.

TDP-43 RRM1 domain and amino acid residues 216-315 (C-term) are required for TDP-43 recruitment to the SGs [144].

TDP-43 can localize to SGs under selected stress conditions, though findings are not always consistent: TDP-43 aggregation can occur both in association with and independently of SGs formation [145]. Fernandes et al. studied the co-localization of TDP-43 to SGs in yeast, where SGs

facilitate TDP-43 aggregation in the early-phase, but then, TDP-43 aggregates persist even when SGs disassemble (SGs marker absence) [143].

These inconsistencies may be attributed to differences in the choice of antibodies or cell lines, or specific TDP-43 mutations. Nevertheless, doubts remain regarding the interaction between TDP-43 and SGs: is TDP-43 actively involved in the formation of SGs? Do SGs facilitate TDP-43 aggregation? Or is TDP-43 aggregation independent of SGs dynamics, with their co-localization being merely coincidental?

Consequently, targeting the mechanisms that regulate SGs dynamics and TDP-42 aggregation represents a critical step toward understanding ALS and other TDP-43 proteinopathies, and may contribute to the development of effective therapeutic strategies.

CHAPTER II: AIM OF THE PROJECT

Amyotrophic lateral sclerosis (ALS) is a multifactorial neurodegenerative disorder. Since its first identification, increasing studies have been conducted to classifying the disease, identify early diagnostic biomarkers, understand the molecular mechanisms underlying its progression, and develop therapeutic strategies.

One of the most relevant ALS-associated genes is TARDBP, which encodes for TDP-43 protein, a key regulator of RNA metabolism in motor neurons (MNs).

In 2011, a novel mutation in TARDBP, G376D, was identified by Conforti et al. in an Italian family (from the Apulia region). This mutation was associated with a particularly rapid and aggressive disease course.

The aim of this project – as part of the national initiative "*ScintilLA*" promoted by the 2HE Association – is to investigate for the first time the pathogenetic mechanism of G376D mutation in TDP-43 with the goals to: 1) elucidate the molecular events associated with the pheno-conversion – i.e. the transition from an asymptomatic mutation carrier to a symptomatic carrier – for a tempestive diagnosis and intervention; 2) lay the groundwork for personalized therapeutic approaches, such as siRNA or ASO (Anti-sense oligonucleotide).

Specifically, the objectives of this project are:

1. Study the expression and sub-cellular localization of TDP-43 in patient-derived fibroblasts under both basal and chronic stress conditions
2. Generate induced pluripotent stem cells (iPSCs) from patient fibroblasts and transfect them with NIL and NIP transposons using PiggyBac system (focusing primarily on NIL-MNs)
3. Differentiate iPSCs into MNs and characterize them through immunocytochemistry
4. Study the expression and sub-cellular localization of TDP-43 in the MNs under both basal and stress conditions (acute and chronic).

This thesis aims to provide the first insights into the molecular pathophysiology of the p.G376D TARDBP, with a long-term goal of contributing to the development of personalized therapy.

CHAPTER III: MATERIAL AND METHODS

1. Primary Fibroblasts: source, culture conditions and experimental procedure

1.1. Patient- and control-derived fibroblasts

For this study, the fibroblasts were obtained from 3 study subjects belonging to the Apulian family carrying the pG376D TARDBP mutation:

- ***WT***, a female healthy subject of 34 years old
- ***a.G376D***, a female asymptomatic G376D carrier of 34 years old (still asymptomatic to date)
- ***s.G376D***, a male symptomatic G376D carrier of 42 years old (deceased in 2020)

The age refers to the moment of fibroblasts collection.

Informed consent for genetic testing and skin biopsy was obtained from each study subject or a close relative if the subject was too severely disabled to give written consent. The experiments were carried out following the World Medical Association Declaration of Helsinki and the protocols were approved by the Palermo 1 Ethics Committee (Protocols 7/2017 and 4/2019).

1.2. Skin biopsy and fibroblast culture conditions

Fibroblasts were obtained through skin biopsy in the volar region of the left arm. The obtained skin fragment was immediately placed in PBS 1X (phosphate-buffered saline). Each biopsy was coded to ensure the subject's anonymity. The skin fragment was sliced and placed in 4-wells plate and cultured in complete medium (DMEM (Dulbecco's modified Eagle's medium) supplemented with 10% CS (calf serum), 2mM L -glutamine, 1mM sodium pyruvate, 100U/mL penicillin and 100U/mL streptomycin) in a 5% CO_2 incubator at 37°C. The medium was changed every 3–4 days until the released fibroblasts were grown to 80% confluence (about 20 days). Fibroblasts were then maintained in culture on T75 flask and passaged every 5-7 days by Trypsin 0,25X. All experiments were performed with cells at the 3^{rd}/4^{th} passage on flask.

For long-term storage, the fibroblasts in a T75 flask with ~80% confluence were frozen in freezing solution (50% DMEM, 40% FBS (Fetal Bovine Serum) and 10% DMSO (Dimethylsulfoxid), Sigma-Aldrich (St. Louis, MO, USA)). Then the cells were placed in a Mr. Frosty and kept at -80°C overnight with a slow freezing rate of -1°C/min and transferred into liquid nitrogen for cryopreservation on the day after.

To restore the frozen fibroblasts, the frozen vial containing fibroblasts was thawed rapidly in a 37°C water bath until only a small piece of frozen material remained. The cells were transferred to a 15 ml tube and centrifuged at 300g for 8 min. Then, the pellet was resuspended in complete medium and seeded in a T75 flask with 10 ml of complete medium.

All the reagents used were from Euroclone (Pero, MI, Italy) unless specified otherwise.

1.3. Chronic stress paradigm

Chronic stress induction was carried out following the protocol proposed by Ratti et al., 2020 [146]. In short, the fibroblasts were exposed for 30 hours to DMEM with 15µM Sodium Arsenite ($NaASO_2$) while the controls were incubated for the same amount of time but with complete medium. After stress exposure, the cells were rescued by substituting the medium with a complete one. The analyses were carried out a selected times: T0 (i.e. immediately after 30h exposure, no recovery time), T24 (i.e. 24h of recovery after stress), T48 (i.e. 48h of recovery after stress) and T72 (i.e. 72h of recovery after stress) (*Fig. 10*).

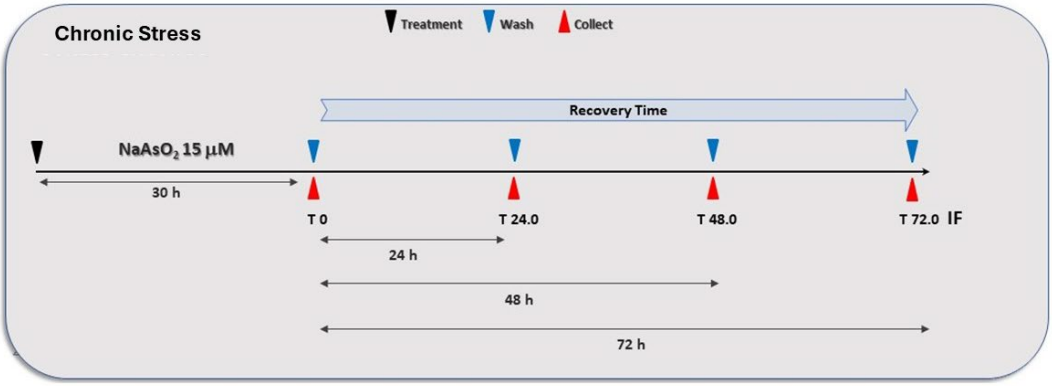

***Figure 10. Chronic Stress Paradigm**. Timeline of stress exposure with recovery and collection time. Black triangles indicate the start of treatment with $NaAsO_2$; Blue triangles indicate the time of interruption of stress and of washes during recovery time; Red triangles indicate the time of collection of the cells for the immunocytochemistry.*

1.4. Immunocytochemistry assay

Fibroblasts were cultured on glass coverslips in a 4-well plate and plated at a concentration of 10000 cells/ml in duplicate for each subject. The following protocol is an adapted version of La Bella et al., 1998 [147]. Cells were fixed with 4% paraformaldehyde for 30 min at room temperature (RT), permeabilized with PBS-TritonX100 0,5% for 10 min and then blocked with 2% BSA (bovine serum albumin) for 1 hour. The cells were incubated overnight at 4°C with primary antibody solution (PBS-TritonX100 0,1%, 0,2% BSA and primary antibodies). The following day the cells were rinsed with PBS-TRitonX100 0,1% to remove primary antibody and incubated for 1 hour at RT in the dark with secondary antibody solution (PBS-TritonX100 0,1%, 0,2% BSA and secondary antibodies).

Polyclonal TDP-43 (N-term) antibody at 1:1000 dilution (Proteintech Group Inc., Chicago, IL, USA) was used in both basal expression and chronic stress experiments.

To detect stress granule after stress induction, co-staining was carried out, adding a monoclonal anti-TIA-R antibody[18] (BD Transduction Laboratories TM, San Jose, CA, USA) at 1:500 dilution to the polyclonal TDP-43 antibody.

[18] TIA-R, together with TIA-1 and G3BP1, are used as SGs markers.

Secondary Cy3-conjugated donkey anti-rabbit antibody and secondary FITC-conjugated donkey anti-mouse antibody at 1:1500 dilution (Chemicon International Inc., Temecula, CA, USA) were used for TDP-43 and TIA-R detections, respectively.

Microscopy analyses were carried out with an Olympus IX70 fluorescence microscope and a Nikon A1 confocal microscope.

1.5. Nuclear and cytoplasmic fractionation

Subcellular fractions (nuclei and cytoplasm) were prepared from cultured fibroblasts at approximately 80% confluence, as previously described [148]. Briefly, cells were resuspended in RBS 100 buffer (10mM Tris-HCl, pH 7.4, 100mM NaCl, 2.5mM $MgCl_2$, 1mM EDTA, cocktail of protease inhibitors and 1mM PMSF) containing 40µg/ml digitonin and incubated for 10 min at 4°C. The cells were then disrupted by passaging them through a syringe. The suspension was centrifuged at 900 *g* for 10 min at 4°C to obtain a pellet (nuclei) and a supernatant (cytoplasmic fraction). The cytoplasmic fraction was taken and put in corresponding labelled tubes, while the nuclei fraction was resuspended with the same RSB 100 buffer but without digitonin and sonicated at 40Hz for a few seconds.

Both nuclei and cytoplasmic fractions were stored at –80°C until use.

All the reagent used were from Sigma-Aldrich (St. Louis, MO, USA).

1.6. Western Blot

Subcellular fractions were thawed on ice, mixed with SDS-PAGE sample buffer, and placed at 95°C for 4 min. A 10% SDS-PAGE electrophoresis and Western blotting were performed. Low-range pre-stained molecular weight markers Sharpmass VI (Euroclone – Pero, MI, Italy) were used in all experiments. Blots were incubated with 1:2000 dilution of polyclonal TDP-43 antibody (Proteintech Group Inc. – Chicago, IL, USA) overnight at 4 ° C.

Secondary HRP-conjugated donkey anti-rabbit antibody (Chemicon, Darmstadt, Germany) was used at a dilution of 1:5000 in 1% milk/PBS-T. Protein bands were visualized using ECL star (Euroclone – Pero, MI, Italy) and the chemiluminescence detection was performed by ChemiDoc-It Imaging Systems (UVP, Cambridge, UK).

In some experiments, filters were washed and stripped out of the bound antibodies for 30 min at 65°C with a stripping solution (62,5 mM Tris-HCl ph 6,8, 2% SDS, 100 mM DTT). The filters were washed with TBS-t and re-blocked with 10% milk/PBS-T. After blocking, membranes were reused for detection of the cytosol marker α-tubulin with 1:1250 dilution of the respective monoclonal antibody (Sigma-Aldrich – St. Louis, MO, USA). Polyclonal anti-Lamin A antibody (Millipore – Burlington, MA, US) at 1:1000 dilution was used as a nuclear fraction marker. Secondary HRP-conjugated donkey anti-mouse antibody (Chemicon – Darmstadt, Germany) was used at a dilution of 1:5000 in 1% milk/PBS-T.

2. Human Induced Pluripotent Stem Cells: generation, culture condition and NIL/NIP transfection

2.1. Generation of hiPSCs and culture conditions

The hiPSCs used for this project were generated from the same fibroblasts (at 3rd/4th passages) by Dr Jessica Rosati (Research Institute "Casa Sollievo della Sofferenza" (IRCSS) – Mendel, Rome, Italy) following the protocol by D'Anzi et al., 2022 [149]. In this protocol, fibroblasts have been reprogrammed using three non-integrative episomal vectors containing the reprogramming factors OCT 3/4, SOX2, L-MYC, KLF4, LIN28, Sh-P53 [99,150]. To ensure that the fibroblasts have been reprogrammed into hiPSCs, they were tested for:

- Typical human stem cell-like morphology in phase contrast microscopy
- Presence of pluripotency markers through immunofluorescence and RT-PCR (OCT 3/4, TRA-1-60 by immunofluorescence and OCT4, KLF4, LIN28, L-MYC and SOX2 by RT-PCR)
- Absence of transgene expression through RT-PCR
- EBs formation and differentiation in three germ layers through quantitative RT-PCR[19]
- Teratoma formation in mouse
- Chromosomal variation in the karyotype
- Authentication of hiPSCs identity through STR assay and gene sequencing.

The hiPSCs were cultured in NutristemXF medium (Sartorius – Gottingen, Germany) in a Matrigel (Corning – NY, USA)-coated 6-well plate and passaged once a week using the "scraping" method. The "scraping method" consist in detaching the colonies by scraping them with a p200 tip. The scraped fragments will be collected with a micropipette and seeded at a desired concentration (from 1:2 to 1:6 dilution) in a new Matrigel-coated 6-well plate. In some cases, the iPSCs are passaged by "manual picking", which consists in cutting the colony with a needle in square of similar size (*Fig. 11*). Each square is collected with a micropipette and seeded at a desired concentration (from 1:2 to 1:6 dilution) in a new Matrigel-coated 6-well plate. For long-term storage, the hiPSCs with ~80% confluence were frozen in Nutrifreez D10 (Sartorius – Gottingen, Germany). Then the cells were placed in a Mr. Frosty and kept at -80°C overnight with a slow freezing rate of -1°C/min and transferred into liquid nitrogen for cryopreservation on the day after.

To restore the frozen hiPSCs, the frozen vial containing hiPSCs was thawed rapidly in a 37°C water bath until only a small piece of frozen material remained. The cells were transferred to a 15ml tube with 9ml of DMEM/F12 supplemented with 10µM Y-27632 and centrifuged at 300g

[19] Ectodermal lineage was confirmed by overexpression of SOX1, NESTIN and PAX6, mesodermal lineage by the expressions of BRACHIURY and EOMES and endodermal lineage by the overexpression of GATA4, FOXA2 and SOX17.

for 5 min. Then, the pellet was resuspended in NutristemXF supplemented with 10µM Y-27632 and seeded in 1 well of a Matrigel-coated 6-well plate with 2ml of NutristemXF with 10µM Y-27632.

Once every two weeks the hiPSCs were tested for the absence of mycoplasma agent with N-GARDE Mycoplasma PCR Reagent set (Euroclone – Pero, MI, Italy) following the manufacturer's instructions.

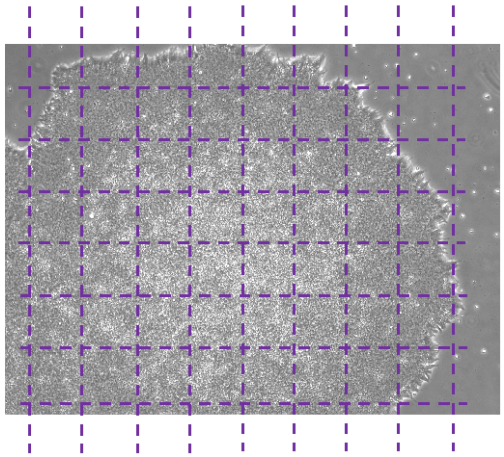

Figure 11. Manual picking. *The iPSCs colony is cut with a needle following the scheme in this figure, forming square of similar size.*

2.1.1. Passaging with ReLeSR

The iPSCs have been initially passaged by "scraping", however this is a laborious and inefficient method. Therefore, later the iPSCs have been passaged using ReLeSR (Stemcells Technologies, Vancouver, Canada), a non-enzymatic dissociation reagent. After removing the medium, 1ml ReLeSR have been added to the well for 1 min at RT. The ReLSR has been removed, and the cells are incubated for 3 min at RT. After the incubation time has passed, only the non-differentiated iPSCs will be detached at first by gently hitting the plate for 30 sec and after adding 2mL of DMEM/F12 to wash the surface. The suspension was put in a 15ml tube and centrifuged at 300g for 5 min. The supernatant was removed, and the pellet resuspended with NutristemXF until the rightful size of cell aggregates[20] is obtained (~50-200 µm). The aggregates are seeded in a Matrigel-coated 6-well plate at the desired density (1:10 or 1:20 dilution).

[20] iPSCs are always passaged in aggregates and never at single-cells, unless for differentiation. Single-cells iPSCs tend to spontaneously differentiate.

2.2. NIL/NIP transfection with PiggyBac in hiPSCs

In this work, the differentiation method used is the PiggyBac System which gives the possibility of generating a stable and inducible iPSCs line integrated with the NIL or NIP construct (*Fig.12*). For this purpose, the hiPSCs have been transfected following the protocol by De Santis et al., 2018 [130].

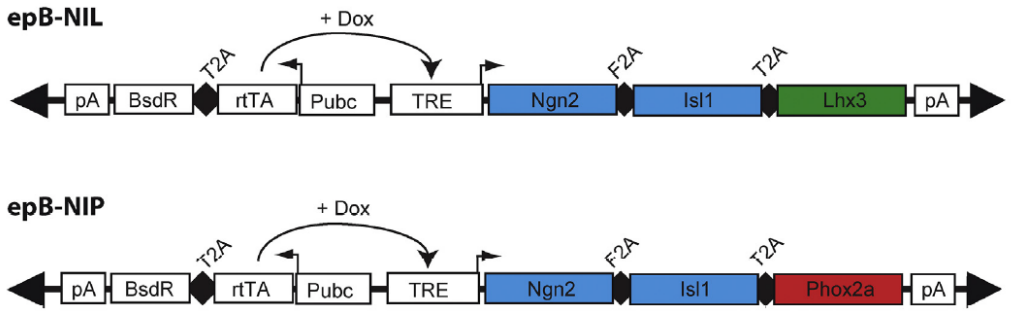

Figure 12. Schematic representation of the epB-NIL and epB-NIP constructs [130]. *pA: polyadenylation signal; BsdR: blasticidin resistance gene; T2A: self-cleavage peptide; rtTA: TET transactivator protein gene; Pubc: human Ubiquitin C constitutive promoter; TRE: TET responsive element; Dox: doxycycline; Ngn2: Neurogenin 2; Isl1: Insulin gene enhancer 1; Lhx3: LIM homeobox 3; Phox2a: Paired Like Homeobox 2A. Black triangles represent terminal repeats of the transposon.*

The PiggyBac System is composed of a transposable vector and a transposase, obtained from Dr. A. Rosa (Sapienza University of Rome, Rome, Italy) and inserted in two butch of Stbl3™ Chemically Competent E. coli (*Escherichia Coli*) (Invitrogen – Waltham, MA, USA). The DNA of the two Stbl3 E. coli butches were purified through NucleoBond Xtra Maxi (Macherey-Nagel – Dueren, Germany), thereby obtaining the corresponding plasmid DNAs (pDNA): ePB – Bsd – TT – NIL/NIP pDNA and HyPB – MDM – IPB7 – CMV pDNA [151].

The iPSCs were co-transfected using Lipofectamine Stem Transfection Reagent (Invitrogen – Waltham, MA, USA) with a ratio of 3:1 for a total of 5µg pDNA (4,5µg ePB – Bsd – TT – NIL/NIP pDNA + 0,5µg HyPB – MDM – IPB7 – CMV pDNA) following the manufacturer's instructions. Selection in 2,5µg/ml blasticidin (Cayman Chemical Company – Ann Arbor, MI, USA) for 10 days gave rise to stable and inducible cell lines.

2.3. iPSCs differentiation in motor neurons

The NIL- or NIP- iPSCs were differentiated into MNs following the protocol by Garone et al., 2019 [152] (*Fig. 13*).

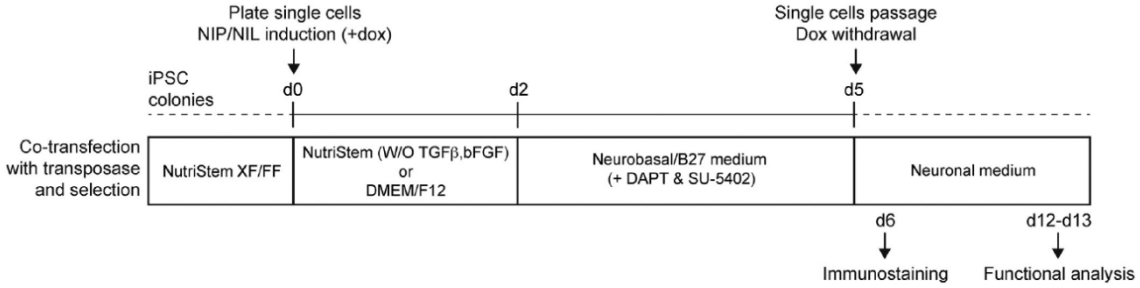

Figure 13. Timeline of differentiation protocol [130]. *Dox: Doxycycline.*

Briefly, the iPSCs are dissociated at single-cells using Accutase (Sigma-Aldrich – St. Louis, MO, USA) and seeded into a Matrigel-coated 6-wells plate at a density of 500000 cells/well in NutristemXF with 10µM Y-27632 (Sigma-Aldrich – St. Louis, MO, USA). The next two days (d1 and d2) media has been daily changed with Induction media (DMEM/F12, Gibco, supplemented with 1% Non-Essential Amino Acids (NEAA), Euroclone, 1% PenStrep/Glutamine, Gibco) with 1µg/ml Doxycycline (Sigma-Aldrich – St. Louis, MO, USA). The following 3 days (d3-d5), media has been daily changed with Differentiation media (Neurobasal, Gibco, supplemented with 1% PenStrep/Glutamine, 1% NEAA, 1% B27 without Vitamin A, Gibco, 5µM DAPT, Sigma, 4µM SU5402, Sigma) with 1µg/ml Doxycycline. At day 6 (d6), the cells have been dissociated using Accutase and re-seeded in a Poly-L-Ornithine/Laminin (Sigma-Aldrich – St. Louis, MO, USA) – coated 96-wells plate at a density of 60000 cells/well in Maturation media (Neurobasal supplemented with 1% PenStrep/Glutamine, 1% B27 without Vitamin A, 20ng/ml Brain-Derived Neurotrophic Factor (BDNF), Proteintech, 10ng/ml Glial Cell Line-Derived Neurotrophic Factor (GDNF), Proteintech, and 0,2mM Ascorbic Acid, Sigma). For 24h, the cells have been treated with 4µM Floxuridine (5-FDU - Cayman Chemical Company – Ann Arbor, MI, USA). From day 7, the maturation media have been changed every 3 days, and the neurons have been kept in culture for at least one week before the immunocytochemistry assay.

2.4. MNs immunocytochemistry

At day 14 (d14) of differentiation, MNs have been fixed with 4% paraformaldehyde for 15 min at RT and thereafter permeabilized for 45 min at RT on gentle shaking with Permeabilization Block Solution (10% FBS, 1% BSA, 0,1% TritonX100 in PBS 1X). The MNs were incubated overnight at 4°C with staining solution (0,1% BSA in PBS 1X) and the primary antibodies under gentle shaking. The following day the cells were rinsed with staining solution to remove primary antibody and incubated for 1 hour at RT in the dark under gentle shaking with staining solution and secondary antibodies.

Polyclonal TDP-43 (N-term) antibody at 1:1000 dilution (Proteintech Group Inc., Chicago, IL, USA), monoclonal Isl1 at 1:500 dilution (Millipore – Burlington, MA, US), monoclonal HB9 at 1:100 dilution (Santa Cruz Biotechnology, Dallas, TX, USA), Polyclonal βIII-tubulin at 1:40 dilution (Sigma-Aldrich – St. Louis, MO, USA), monoclonal CHAT at 1:66 dilution (Millipore – Burlington, MA, US), monoclonal MAP2 at 1:200 dilution (Millipore – Burlington, MA, US) and polyclonal Neurofilament200 at 1:500 dilution (Sigma-Aldrich – St. Louis, MO, USA) were used to characterize the MNs populations. Secondary Cy3-conjugated donkey anti-rabbit antibody and secondary FITC-conjugated donkey anti-mouse antibody at 1:1500 dilution (Chemicon International Inc., Temecula, CA, USA) were used. MNs were stained with DAPI using Fluoroshield with DAPI (Sigma-Aldrich – St. Louis, MO, USA) mounting medium.

Microscopy analyses were carried out with an Olympus IX70 fluorescence microscope and a Nikon A1 confocal microscope.

3. Data analysis and statistics

Data for all the experiments were obtained by 3 separate experiments, each performed in duplicate. Data obtained by counting the cells from each subject showing the pattern of TDP-43 expression and the proportion of cells containing stress granules at different times after stress insult were calculated as a percentage of the total number of counted cells and expressed as the median with interquartile range (IQR) of 3 separate experiments, each performed in duplicate.

SIGMASTAT 3.5 software (Systat Software Inc. – San Jose, CA, USA) was used for statistical analysis. Differences in the proportions of the patterns of TDP-43 staining and the granule-containing cells for each subject group were analysed by 1-way ANOVA (variance on ranks), followed by post hoc analysis with Dunn's method. P values < 0.001 were considered significant.

CHAPTER IV: RESULTS

1. Expression and subcellular localization of TDP-43 in basal and chronic stress conditions

Skin fibroblasts were collected from three groups of donors belonging to the same Apulian family: 1) symptomatic G376D carrier (s.G376D); 2) asymptomatic G376D carrier (a.G376D); 3) healthy control (WT). Fibroblasts were cultured as described in **Chapter III, sub-paragraph 1.2**.

1.1. TDP-43 is mostly localized in the nucleus under basal conditions

Since G376D is a rather novel mutation with no data published on the expression of the protein, the first experiment carried out was to understand if abnormal behaviour was already present in basal condition. Therefore, the expression and localization of TDP-43 in the three groups of fibroblasts have been studied through immunocytochemistry and western blotting assays (*Figs. 14* and *15*), as described in **Chapter III, sub-paragraph 1.4**. Both assays showed that TDP-43 is mostly nuclear, an expected result, previously described in other works [50]. The few cells that showed a presence of TDP-43 even in the cytoplasm have not been considered as a pathological marker, instead as a physiological one, since TDP-43 is a protein that has to shuttle between the nucleus and cytoplasm.

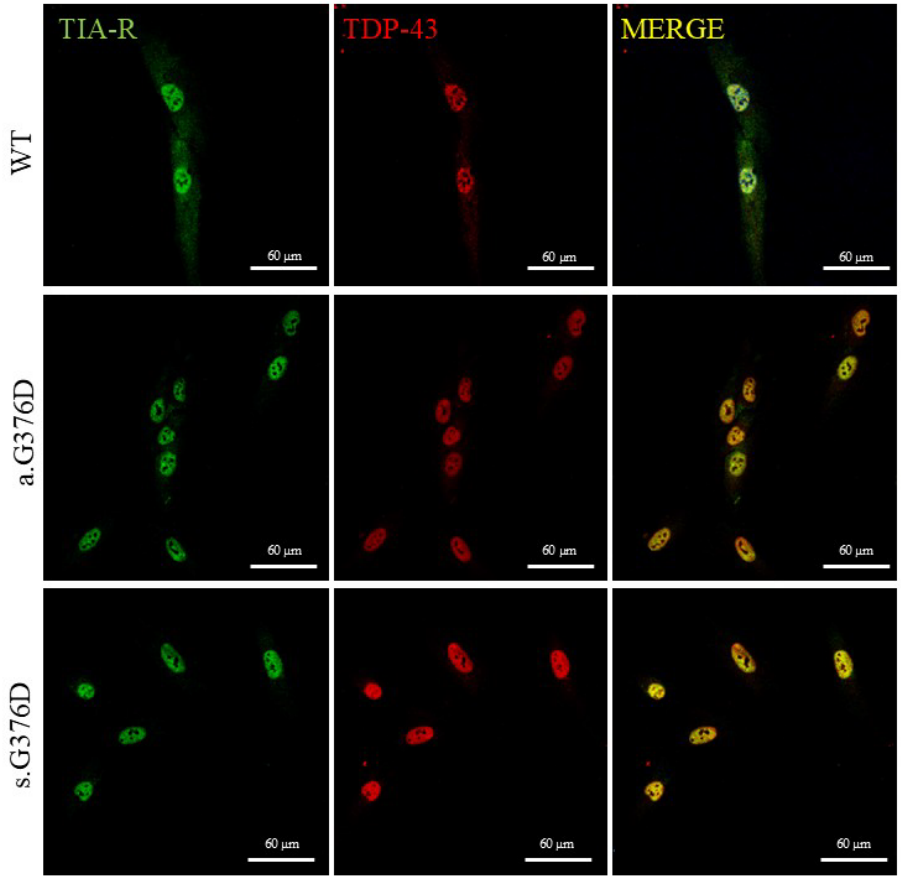

Figure 14. Localization of TDP-43 and TIA-R in basal condition in fibroblasts. *Nuclear localization and expression of TDP-43 (red) and TIA-R (green) in fibroblasts of symptomatic G376D carrier through immunocytochemistry. Scale bar: 60 µm.*

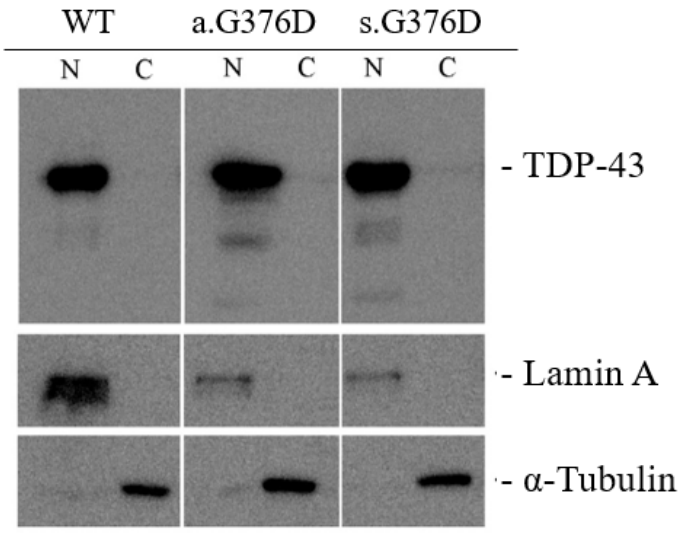

Figure 15. Expression of TDP-43 in basal condition in fibroblasts. *Comparison of the subcellular fractions from fibroblasts, showing a mostly nuclear expression of TDP-43 in all three groups. Lamin A was used as nuclear fraction control, while α-Tubulin as cytoplasmic fraction control. The different expression of Lamin A in a.G376D and s.G376D in comparison to WT is due to technical variability.*

1.2. Symptomatic G376D carrier fibroblasts are more susceptible to chronic stress

As described in **Chapter III, sub-paragraph 1.3**, the three groups of fibroblasts were subjected to chronic stress insult using 15μM $NaAsO_2$ for 30h. The effects of stress were analysed through an immunocytochemistry assay. At rescue – immediately after chronic stress, T0 – the localization remained predominantly nuclear, but with an increase in the number of cells expressing the protein also in the cytoplasm. Specifically, at T0, it was observed (*Fig.16, panel A, and Fig. 17*):

- In WT, most cells show TIA-R positive granules (42%) and TDP-43 cytoplasmic aggregates (10%). Only a few cells showed a co-localization of TIA-R and TDP-43
- In a.G376D, TIA-R positive granules (30%) and TDP-43 cytoplasmic aggregates (8%) were present but none of them co-localized
- In s.G376D, the total number of TIA-R granules (4%) and TDP-43 cytoplasmic aggregates (2%) was lower in comparison to the other two subjects, with no apparent co-localization between the two proteins.

After 30 hours, the fibroblasts start a period of recovery time of 72 hours in which the stressor was removed, and complete medium was given. After 24 hours of recovery, the cells were rescued and analysed through microscopy (*Fig.16, B panel*). In both WT and a.G376D fibroblasts, there was a decrease in the number of cells with TIA-R granules (more than half less), while in the s.G376D all the granules had disassembled. However, the localization of TDP-43 was again nuclear.

At T48 and T72 (time of recovery after stress), there was a total recovery in all groups showing no more stress granules.

The statistical analysis regarding the percentage of stress granules and TDP-43 aggregates in fibroblasts after chronic stress (T0) was performed using the median and interquartile range (IQR), comparing WT with G376D TDP-43 mutation carriers. Among the markers analyzed, only TIA-R showed a statistically significant difference between groups (p.value < 0.001). Although no statistically significant differences were observed in the other groups, s.G376D exhibited a trend toward a lower number of TDP-43 aggregates. This trend may become more pronounced with a larger sample size.

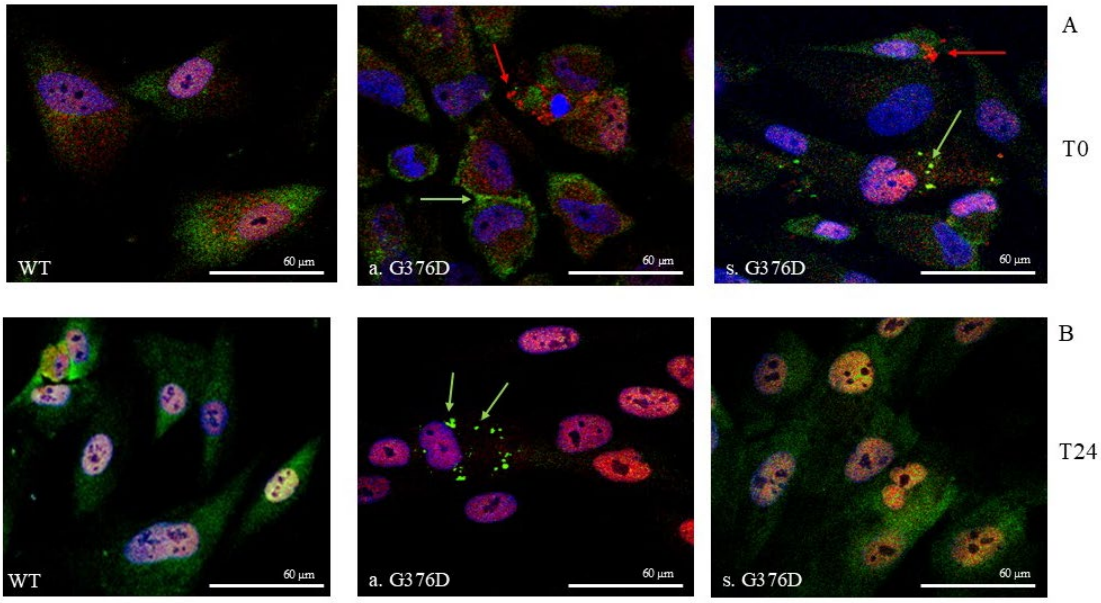

Figure 17. Comparison of chronic stress on fibroblasts at T0 and T24. *Effects of chronic stress after 30 h (T0) and after 24h recovery (T24) on the expression and sub-cellular localization of TDP-43 (red) and SGs formation (TIA-R positive, green) in the three subjects. Green arrows highlight TIAR-positive aggregates (i.e. SGs) while Red arrows the TDP-43 aggregates. DAPI: in blue. Scale bar: 60 µm.*

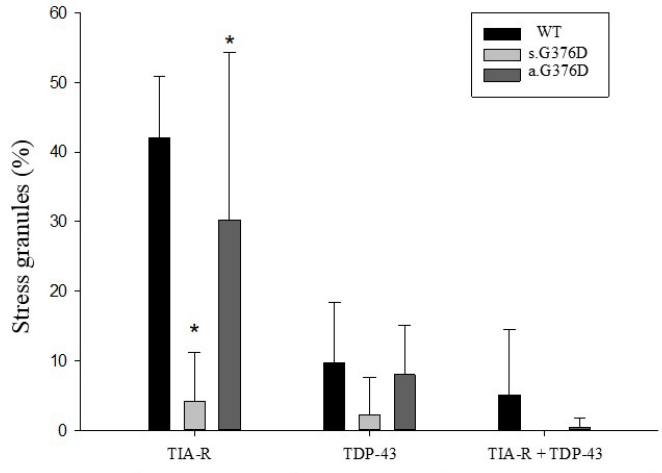

	TIA-R	TDP-43	TIAR+TDP-43
WT	42%	10%	5%
s.G376D	4%	2%	0%
a.G376D	30%	8%	0,4%

Figure 16. Percentage of cells, showing stress granules and TDP-43 cytoplasmic aggregates at T0 after chronic stress (insults). **: p.value <0,0001 (ANOVA on ranks followed by Dunn's method post-hoc analyses.*

To confirm these data, a western blot assay was carried out with the subcellular fraction of fibroblasts at T0 (*Fig. 18*), comparing them with the corresponding non-treated fractions. TDP-43 in all three groups was mostly expressed in the nuclear fraction, even though there was a slight expression in the cytoplasmic fraction.

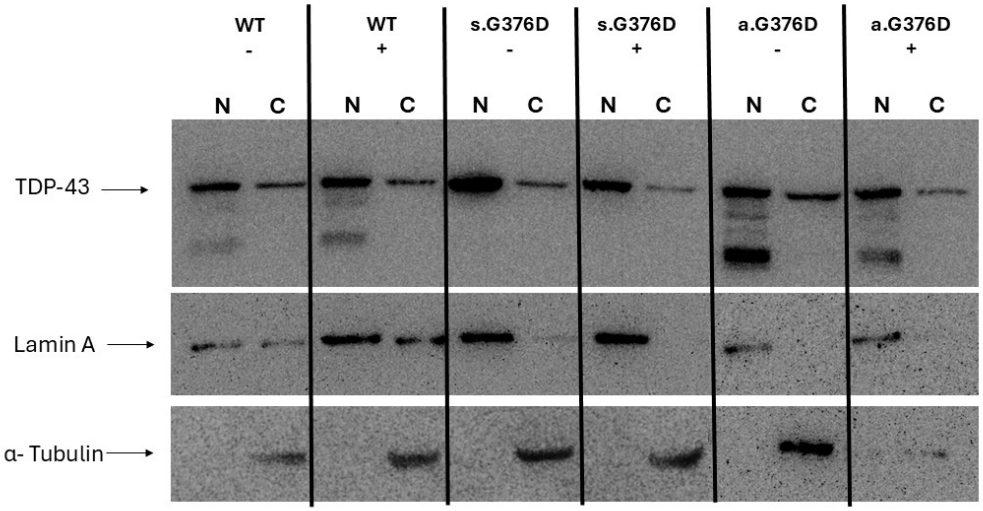

Figure 18. Expression of TDP-43 of subcellular fractions in non-treated and treated (T0) fibroblasts of the three subjects. *Comparison of the expression of TDP-43 before and after stress in fibroblasts: 1) the row with (-) are the non-treated cells, the row with (+) are the treated cells with $NaAsO_2$ at TO. Lamin A and α- Tubulin are used as nuclear and cytoplasmic fractions controls. The presence of Lamin A in the cytoplasmic fraction is due a contamination during the fractionation procedure.*

2. Differentiation and characterization of iPSCs-derived MNs

2.1. From progenitors to MNs

Fibroblasts are mesenchymal cells and do not fully represent the changes that may occur in affected motor neurons. In fact, most of this work is devoted to the characterization of iPSC derived from the collected fibroblasts and their differentiation in MNs.

The iPSCs were generated and transfected with NIL/NIP plasmid by Dr. Rosati's research group [129,148,149].

Initially, the aim was to begin differentiation from the progenitor state (day 5 of the differentiation protocol). According to De Santis et al. (2018), cells can be frozen at day 5 of differentiation, once the induction with Doxycycline is completed, at which point they exhibit markers and characteristics typical of MNs progenitors. Accordingly, Dr. Rosati's research group differentiated the three iPSCs lines – transfected with either NIL or NIP – up to day 5, after which the cells were collected and cryopreserved.

In this study, differentiation was initiated by thawing the progenitors (NIP and NIL) and seeding them in Matrigel-coated 6-well plates, followed by one week of culture in Maturation medium.

Given that ALS predominantly affects spinal MN, this work focused on NIL-MNs, and all the subsequent experiments were conducted using this population.

The spinal MNs were characterized at various time points during differentiation – day 7, day 9, day 12[21] - using markers including Neurofilament200, MAP2, Isl-1, Chat and βIII-tubulin (*Fig. 19 – 21*), as described in **Chapter III, sub-paragraph 2.4**. Additionally, TDP-43 staining was performed at each time point (*Fig. 20*). Since minimal differences were observed between day 7 and day 9, subsequent analyses focused on day 7 and day 12.

MNs derived from all three subjects were positive for the tested markers, confirming that this differentiation protocol reliably generates spinal MNs in 15 days.

TDP-43 was mostly nuclear in all the MNs, as observed in fibroblasts, with slight diffusion in the neurites consistent with its physiological role.

[21] The days are counted considering day 1 the first day of differentiation when the doxycycline was added, day 5 as the day of freezing and thawing the progenitors.

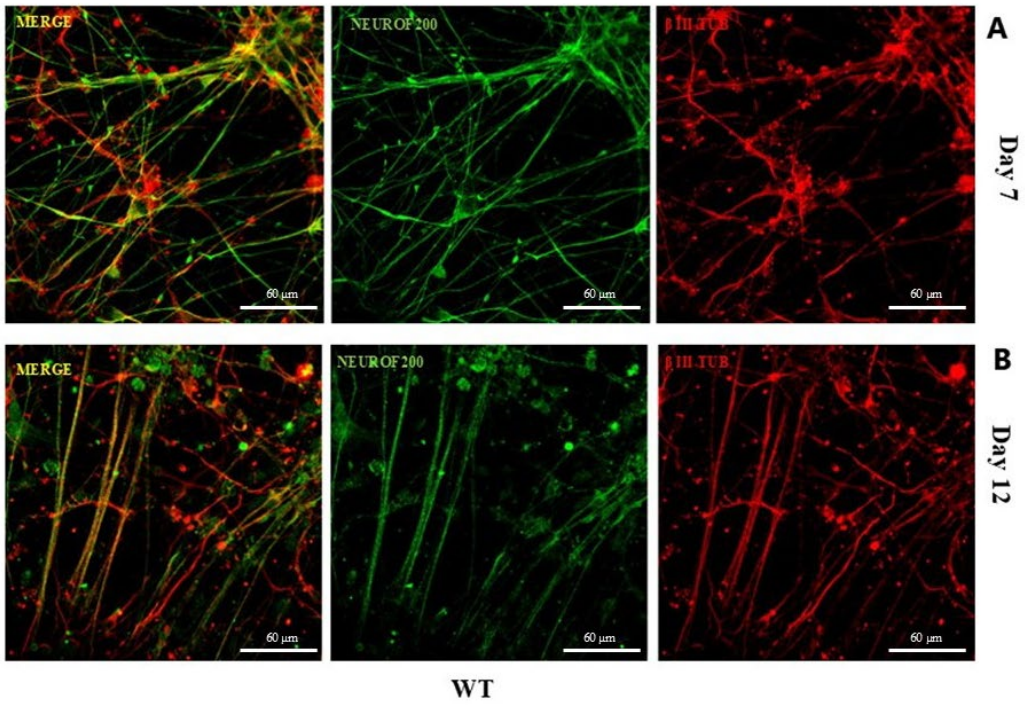

Figure 19. Characterization of WT NIL- MNs. *Developing WT MNs were characterized using several markers. Shown here are representative immunofluorescence images stained for Neurofilament 200 (green) and βIII-tubulin (red). A) Developing MNs at day 7, B) newly matured MNs at day 12. Scale bar: 60 µm.*

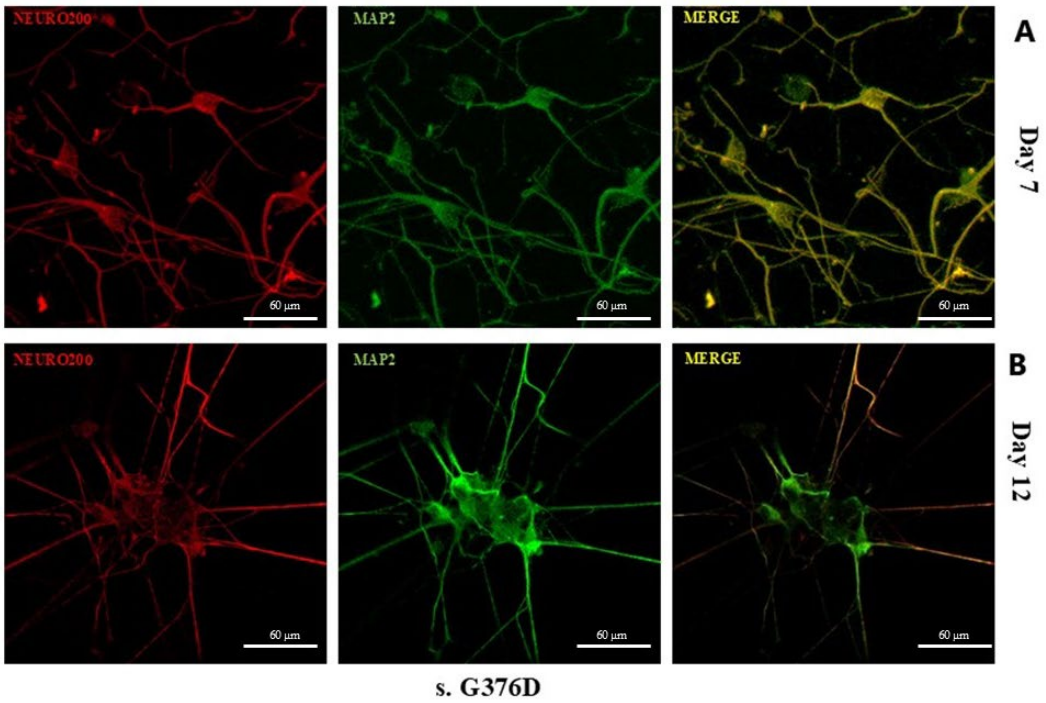

Figure 20. Characterization of s.G376D NIL- MNs. *Developing s.G376D MNs were characterized using several markers. Shown here are representative immunofluorescence images stained for MAP2 (green) and Neurofilament 200 (red). A) Developing MNs at day 7, B) newly matured MNs at day 12. Scale bar: 60 µm.*

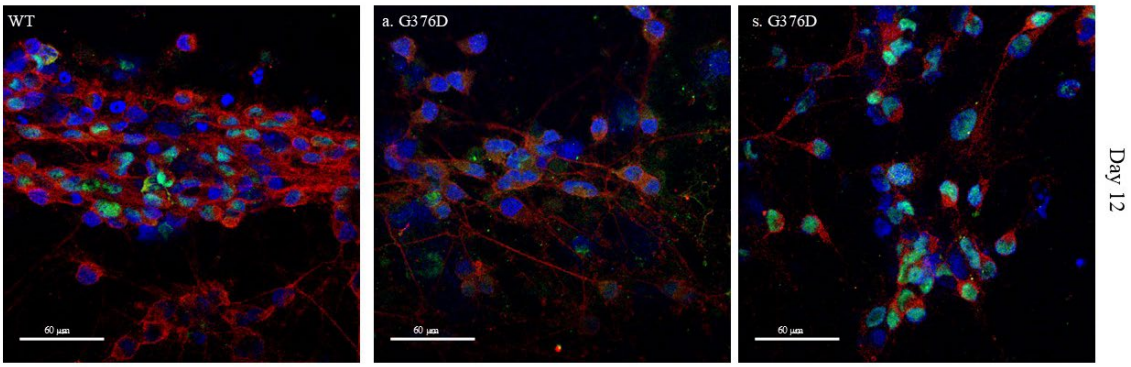

Figure 21. Subcellular localization of TDP-43 in NIL-MNs. *At day 12, MNs are newly matured, as demonstrated by the presence of ChAT (red) in the three groups (left: WT; center: a.G376D; right: s.G376D). TDP-43 (green) remains predominantly nuclear, with slight diffusion into the neurites. DAPI: in blue. Scale bar: 60 µm.*

Alongside the characterization experiments, a subset of MNs was maintained in culture to obtain more mature MNs. According to protocol [129], MNs can be cultured for 30-40 days from the start of the differentiation. This extended culture period revealed two observations: 1) improved spatial organization of the neurites; 2) the emergence of "flat cells", which negatively impact MNs survival.

During the differentiation, neurite linearization was observed, contributing to enhanced spatial organization. This was evident not only morphologically but also through Neurofilament200 staining. At day 7, neurites appeared disorganized (*Fig. 22, A panel*), whereas by day 16, they exhibited a linear structure with direct connections between cells (*Fig. 22, B panel*).

However, prolonged culture of MNs led to an increased presence of "flat cells" – non-neuronal, proliferative cells that persist despite the use of a differentiation medium. These cells eventually reached confluence, competing for nutrients and thereby compromising MNs viability (*Fig.23*).

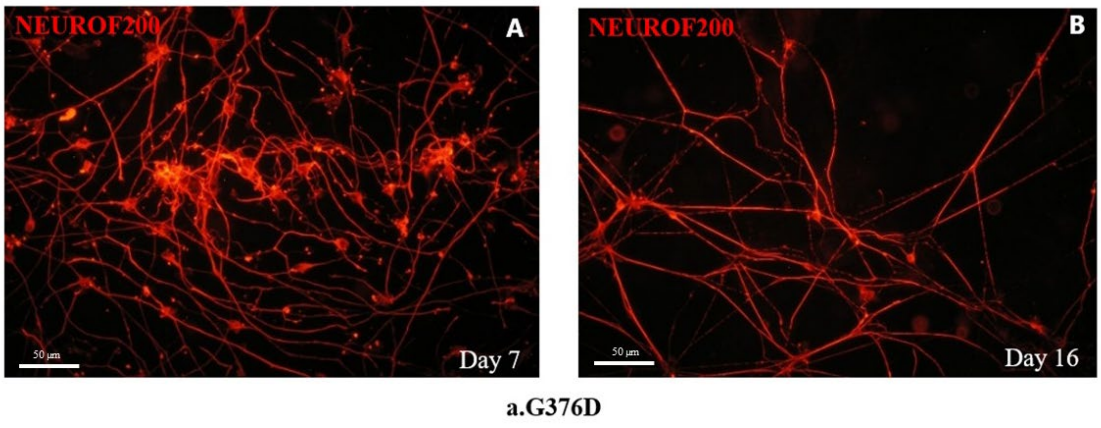

Figure 22. Spatial organization of the neurites in a.G376D. *Stained with Neurofilament 200 (red), the neurites were: A) disorganized at day 7, B) organized with a linear structure at day 16. Scale bar: 50 µm*

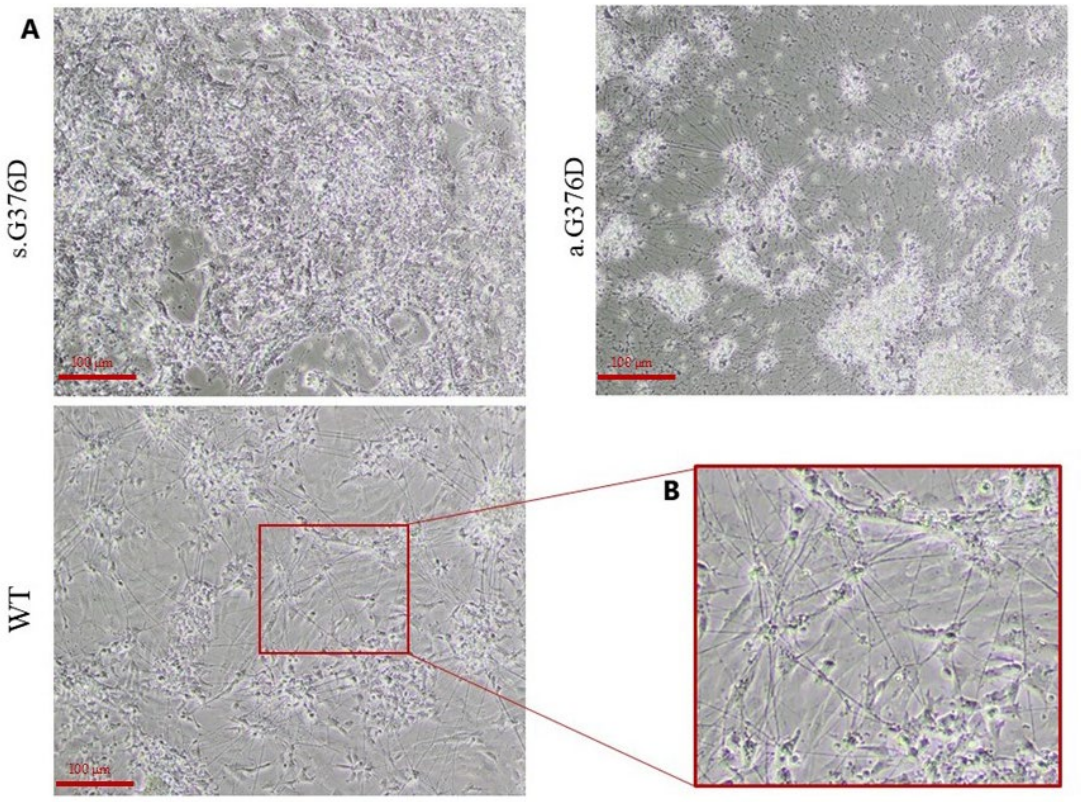

Figure 23. Presence of "flat cells" at day 20. *A) Phase-contrast image (10x) of the three lines of MNs at day 20 showing the abundant presence of "flat cells". Scale bar: 100µm. B) Magnification of the WT image in panel A of the "flat cells".*

2.2. From iPSCs to MNs

The need to initiate differentiation directly from the iPSCs stage, rather than from the progenitors, emerged following consultation with both Dr. Rosati (who generated and transfected the iPSCs) and Dr. Rosa (developer of the NIL and NIP plasmids, and the differentiation protocol used in this study). They suggested that the high rate of MNs mortality and the presence of "flat cells" could be attributed to increased susceptibility of the progenitor cells to the transport on ice, as these cells are already partially differentiated and therefore more vulnerable.

The culture of iPSCs and their differentiation were carried out as described in **Chapter III, paragraph 2**. Briefly, the iPSCs were cultured in NutristemXF medium in a Matrigel-coated 6-well plate and passaged once a week by scraping. The iPSCs were dissociated into single-cells using Accutase and seeded into a Matrigel-coated 6-wells plate at a density of 500000 cells/well in NutristemXF with 10µM Y-27632 to start the differentiation. The next two days (d1 and d2) media has been daily changed with Induction media with 1µg/ml Doxycycline. The following 3 days (d3-d5), media has been daily changed with Differentiation media with 1µg/ml Doxycycline. At day 6 (d6), the cells have been dissociated using Accutase and re-seeded in a Poly-L-Ornithine/Laminin – coated 96-well plate at a density of 60000 cells/well in Maturation media. From day 7, the maturation media have been changed every 3 days and neuron kept in culture for at least one week before the immunocytochemistry assay.

The characterization was carried out through immunocytochemistry, in the same way as previously described in **sub-paragraph 2.1**.

Nevertheless, the results were consistent with the previous observations: spinal MNs specification was confirmed by motor neuronal markers, such as ChAT, and TDP-43 remained predominantly localized in the nucleus. However, high MNs mortality and the presence of proliferative "flat cells" persisted too (*Fig. 24*).

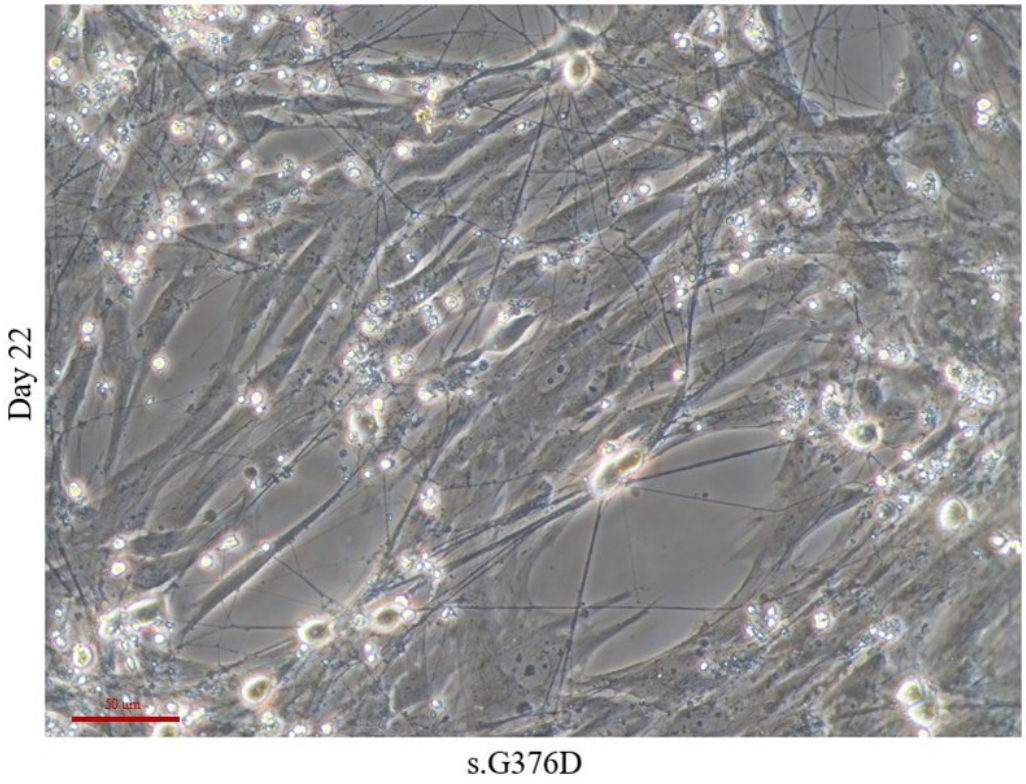

Figure 24. Proliferative non-neuronal cells*. Phase-contrast image of s.G376D MNs at day 22, showing few but long neurites and abundant "flat cells". Scale bar: 50µm.*

3. Protocols improvements: iPSC culture conditions and NIL transfection, MNs differentiation and characterization.

Upon further analysis, it became evident that the colonies did not exhibit the typical morphology of high-quality iPSCs (*Fig. 25, A panel*). High-quality iPSCs should show morphologically the following characteristics [109]:

- Compact and well-defined borders – colonies should have smooth and "round" edges with clear boundaries
- High nucleus-to-cytoplasm ratio – cells should appear dense with large nuclei and minimal cytoplasm
- Uniform cell morphology – cells within the colony should look similar in size, tightly packed
- Prominent nucleoli – the nuclei often show one or more nucleoli
- Flat colony structure – colonies should grow in a flat monolayer
- High refractivity under phase-contrast microscopy
- Absence of differentiated cells – no colony's "outburst"[22] (*Fig. 25, B panel*), elongation or morphology changes.

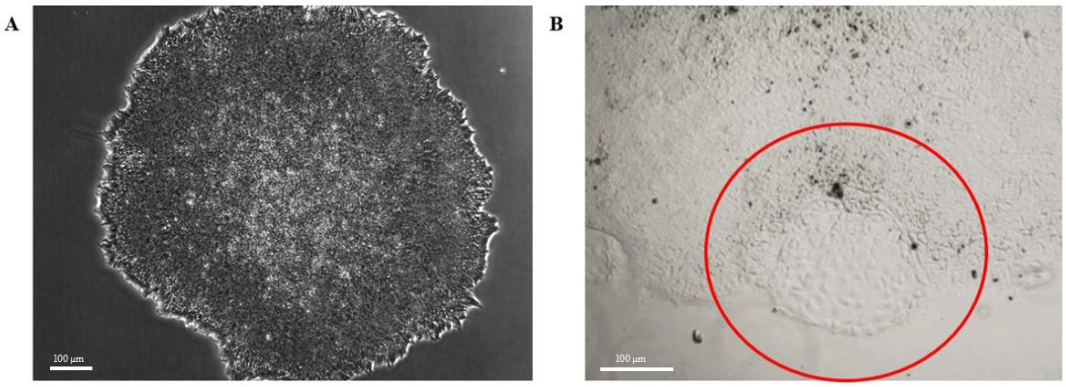

***Figure 25. High-quality iPSCs (WT**). A) Phase-contrast image of a colony of a WT iPSCs. B) "Outburst" of differentiated cells at the colony's border (in the red circle). Scale bar: 100µm.*

Instead, the iPSCs used in this study contained a significant number of differentiated cells ("flat cells"). While a well-established iPSC line should have less than 20% differentiated cells, more than 60% of the cells in this case were already differentiated (*Fig.26*).

Given these findings, it was necessary to restart from the iPSC stage, improving the culture condition protocol, transfecting the cells again with the PiggyBac system, and introducing Floxuridine during the differentiation.

[22] Colony's "outburst" is referred to an area of the colony's border in which the cells spontaneously differentiated and spread outside the borders.

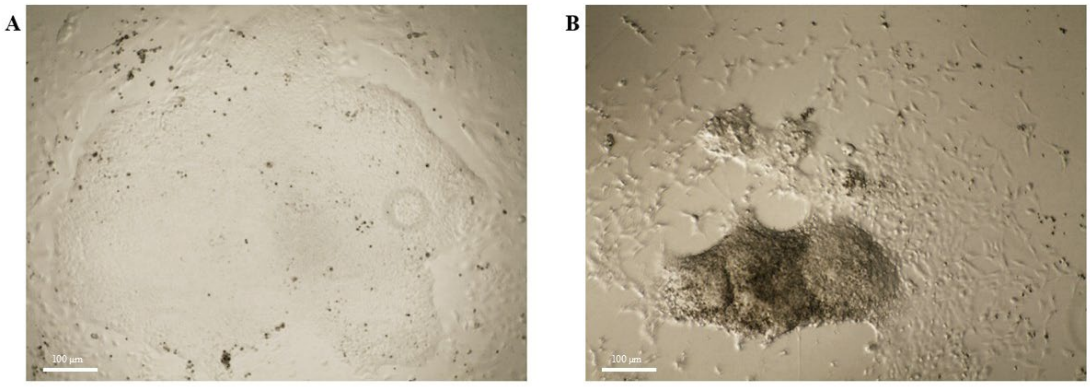

Figure 26. Defective iPSCs*. A) iPSCs colony surrounded by differentiated cells, B) differentiated colony. Scale bar: 100µm.*

This part of the study was carried out with Dr. J. Sterneckert's research group (Center for Regenerative Therapies TU Dresden (CRTD), Germany). Unfortunately, the s.G376D and a.G376D iPSCs didn't survive after thawing. Therefore, the following results only refer to the WT line.

3.1. Improvements on iPSCs culture conditions

The first improvement was related to the culture conditions, especially the passaging method. The "scraping" method is outdated and not standardized, as it causes physical stress to the cells, leading to spontaneous differentiation, and results in low passaging yield – from 1 confluent well it is typically possible to perform a 1:6 dilution. Today, it is standard to use gentle dissociation reagents such as Dispase and ReLeSR, which not only reduce the physical stress but increase the passaging yield (making even a 1:50 dilution possible). Dispase[23] is a proteolytic enzyme that cleaves extracellular matrix proteins without damaging cell surface proteins, detaching intact colonies. ReLeSR[24], on the other hand, is a non-enzymatic, chemical reagent that loosens cell-substrate interactions, allowing a selective detachment of undifferentiated colonies, leaving differentiated cells behind (*Fig. 27*). Therefore, Dispase is more suitable for high-quality iPSCs while ReLeSR is preferable for cultures with a high percentage of differentiated cells.

Given that the iPSCs used in this study had more than 60% of differentiated cells, ReLeSR was chosen as the dissociation reagent for passaging.

[23] https://www.stemcell.com/products/dispase-1-u-ml.html
[24] https://www.stemcell.com/products/relesr.html

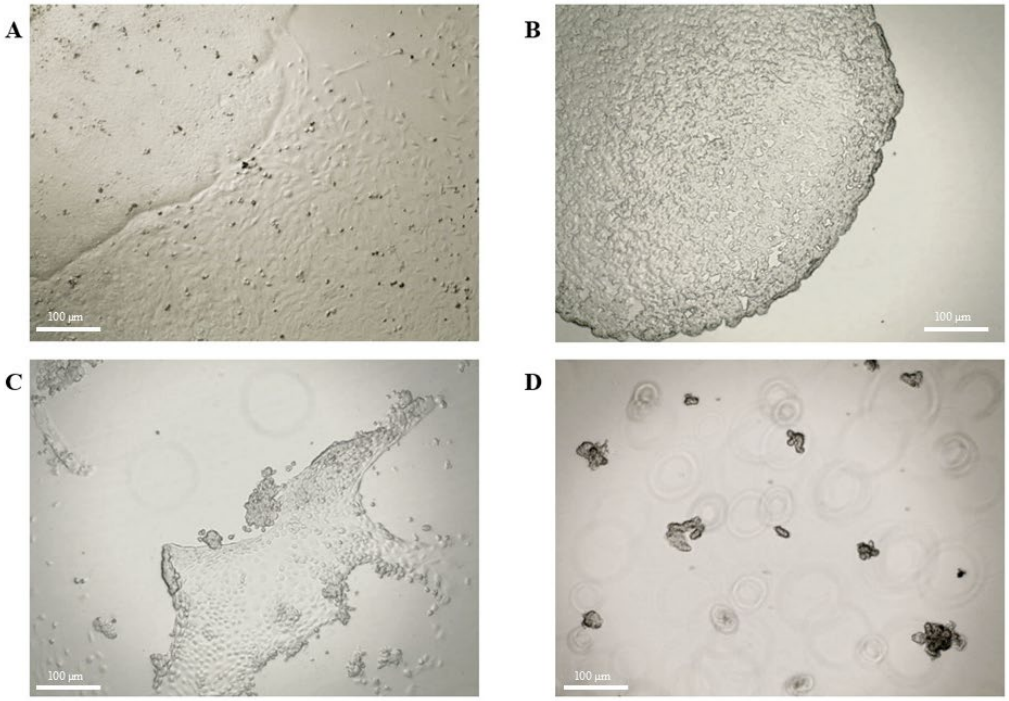

Figure 27. Passaging with ReLeSR. *A) iPSCs colony surrounded by differentiated cells before passage. B) Treatment with ReLeSR, the border of the colony starts to detach. C) Remained differentiated cells after passage with ReLeSR. D) Recommended size of the fragments obtained with ReLeSR. Scale bar: 100µm.*

The iPSCs were thawed and cultured as described in **Chapter III, sub-paragraph 2.1**. During the first two passages, it was necessary to perform "manual picking" due to the abundance of differentiated cells and a low number of colonies (2-4 colonies per cryovial). "Manual picking" is a non-standardised passage method similar to "scraping": while in "scraping" the colonies are scraped using a p200 tip, in "manual picking" the colonies are cut in squares of similar size using a needle, and each square is aspirated using a micropipette. This technique allowed only a select few to form a colony and helped reduce the number of differentiated cells. After the two passages with "manual picking", the iPSCs have been passaged using ReLeSR, as described in **Chapter III, sub-paragraph 2.1.1**. This approach reduced the percentage of differentiated cells to 10-20% after 8 passages (*Fig. 28*), significantly improving the quality of the iPSCs.

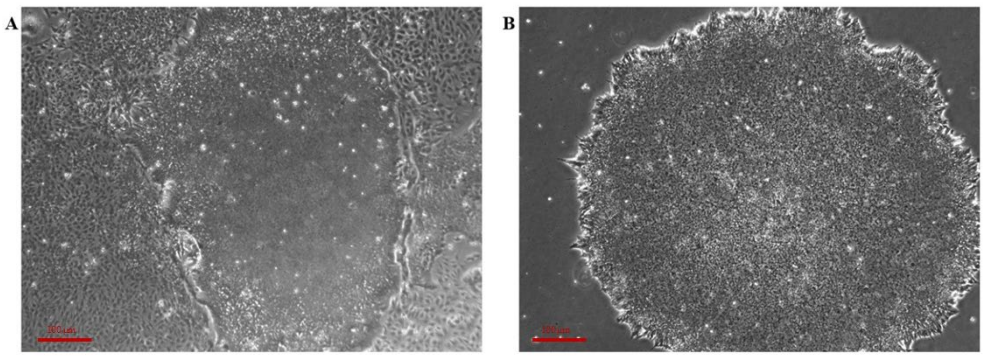

Figure 28. Increased quality of iPSCs after improvements on culture conditions*. A) WT iPSCs at passage 10, B) WT iPSCs at passage 18. Scale bar: 100µm.*

3.2. Transfection with NIL plasmids using the PiggyBac system

Once the iPSCs had a low percentage of differentiated cells, they were transfected with the NIL plasmid as described in **Chapter III, sub-paragraph 2.2**.

After the transfection using Lipofectamine, the cells are selected using 2,5 µg/ml Blasticidin for 10 days. The concentration of blasticidin was chosen after testing the cell viability with CellTiter-Glo Luminescent Cell Viability Assay (Promega – Madison, WI, USA) following the manufacturer's instructions (*Fig. 29*).

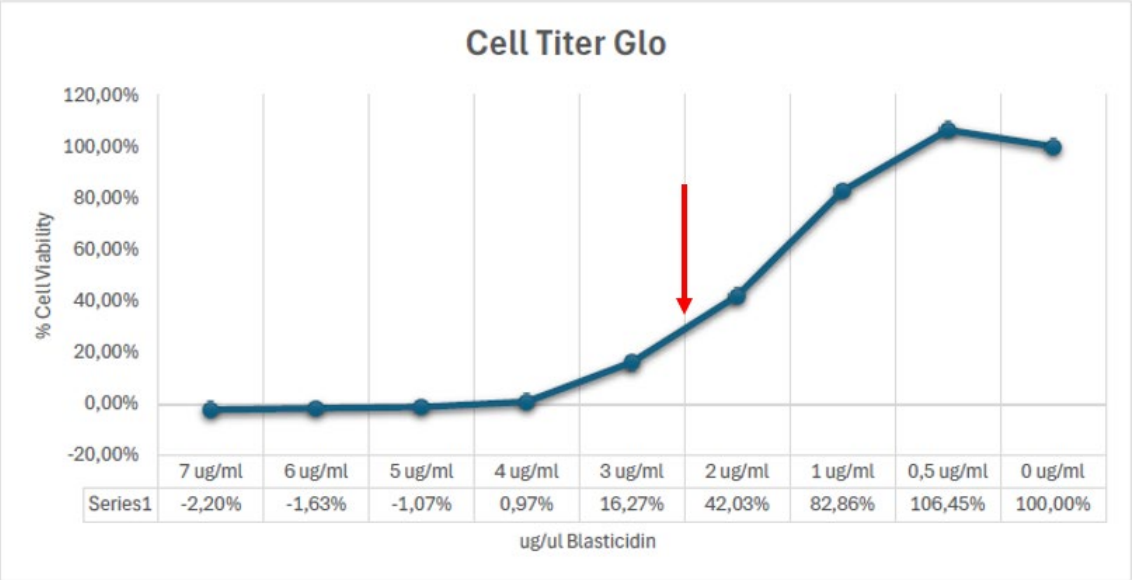

Figure 29. Cell viability assay. *Blasticidin was tested at different concentration – 7, 6, 5, 4, 3, 2, 1, 0.5 and 0 µg/ml – on iPSCs. The range of Blasticidin was between 2 and 3 µg/ml: 2 µg/ml let survive almost half the cells, while 3 µg/ml let survive less than 20%. Therefore, it was chosen to use 2,5 µg/ml.*

Immediately after the blasticidin selection, the transfected iPSCs that survived showed an imperfect iPSCs morphology (*Fig. 30, A panel*). This morphology was not surprising and in fact it is expected, since the iPSCs have gone through diverse stress stimuli – the transfection itself and the antibiotic selection. But after some passages, the NIL-iPSCs started showing the normal iPSCs morphology (*Fig. 30, B panel*).

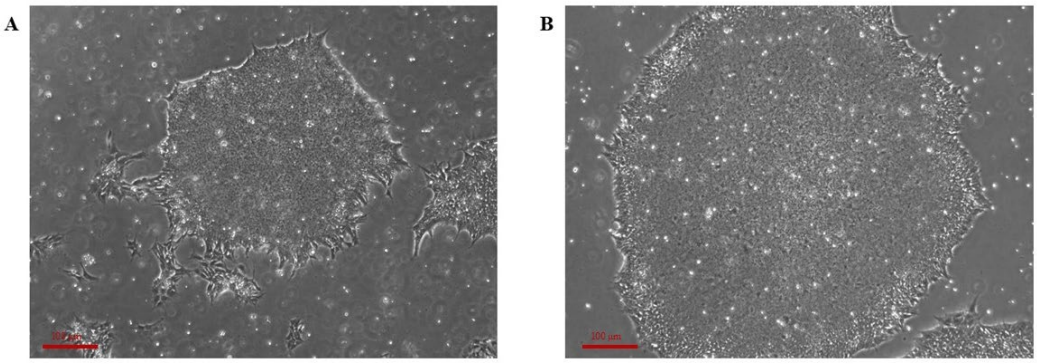

Figure 30. Established NIL- iPSCs line. *A) NIL- iPSCs after blasticidin selection, B) established NIL- iPSCs colony after 3 passages. Scale bar: 100µm.*

3.3. Differentiation and MNs characterization

While the differentiation protocol itself required no modifications, the presence of "flat cells" posed a significant issue for the execution of the subsequent experiments.

Since "flat cells" are non-neuronal cells that proliferate, it was necessary to find a solution to stop their proliferation if not possible to remove them completely.

Floxuridine is an antimetabolite and pyrimidine analogue that suppresses the proliferation of cells by inhibiting the thymidylate synthase and therefore the DNA synthesis. It is commonly used to selectively inhibit the proliferation of the feeder cells in stem cell culture. Because iPSCs divide more slowly, they are not significantly affected by low concentrations of Floxuridine.

Since the appearance of "flat cells" typically occurred after the completion of doxycycline induction, 4μM Floxuridine was added for 24 hours on day 6. If necessary, the treatment was extended for an additional 24 hours.

Following Floxuridine treatment, the "flat cells" remained present, but their proliferation was halted, which made it possible to complete differentiation and maintain MNs in culture for prolonged periods (*Fig. 31*). The cells did differentiate into MNs, showing not only motor neuronal morphology but also motor neuronal markers.

Once MNs were mature, they were characterized through an immunocytochemistry assay, as previously described. Stained with DAPI, two types of nuclei were observed: small nuclei belonging to MNs and large nuclei belonging to non-neuronal cells. The staining of the motor neuronal markers was consistent with the previously obtained, but with a notable reduction of the "flat cells" (*Fig. 32*).

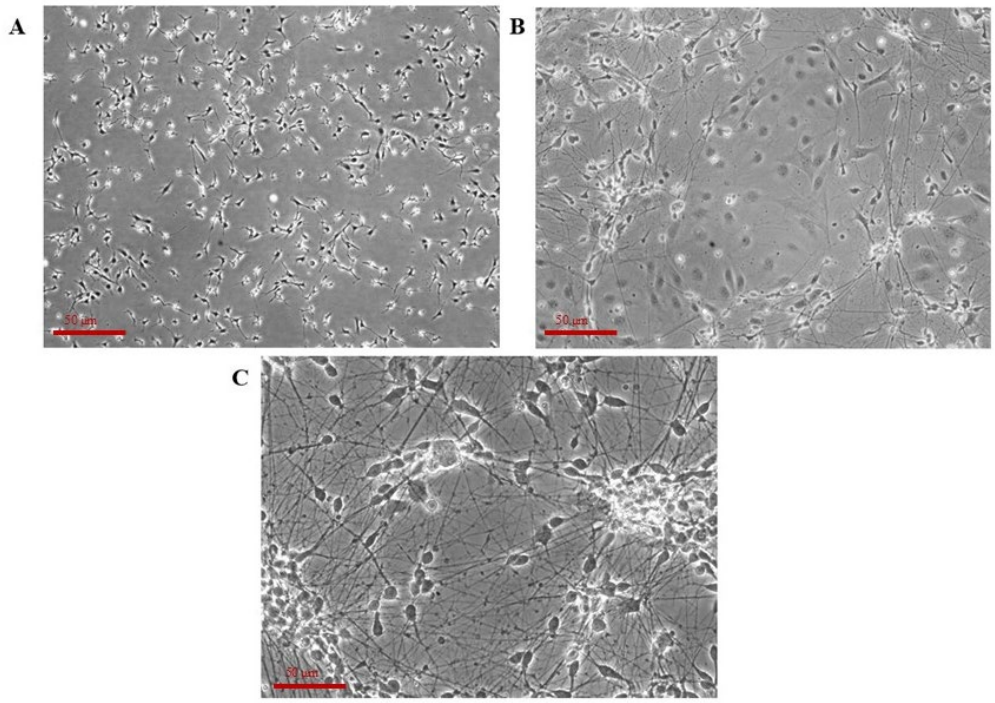

Figure 31. Differentiation of NIL- iPSCs into MNs. *A) Day1. Start of the induction with Doxycycline. B) Day 5, last day of dox induction and a day before Floxuridine treatment. Visible presence of "flat cells". C) Day 15, mature MNs. Reduced presence of "flat cells". Scale bar: 50µm.*

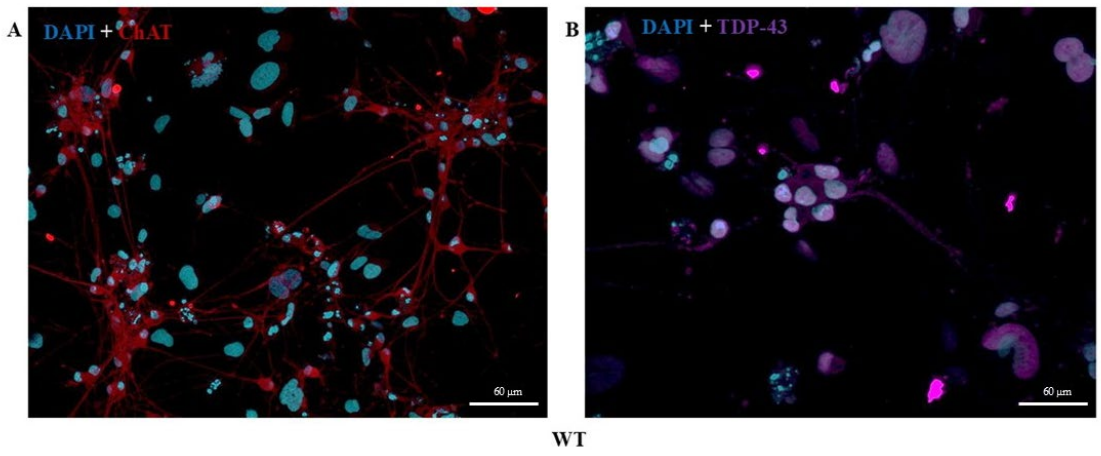

Figure 32. Characterization of WT MNs*. A) ChAT (red)-positive MNs with small nuclei stained with DAPI (blue). Large nuclei are from undifferentiated cells. B) TDP-43 (Violet) is mostly nuclear, but physiologically present even in the neurites. Scale bar: 60µm.*

CHAPTER V: DISCUSSION

Amyotrophic lateral sclerosis is a neurodegenerative disorder characterized by the progressive degeneration of motor neurons. While ALS is predominantly sporadic, approximately 10% of cases exhibit a familial history, with several genes identified as being associated with the disease (*Tab. 2*). One of the most significant ALS-associated gene is TARDBP, which encodes for TDP-43 – a RBP involved in RNA metabolism and in transport of RNA granules along the axon. To date, more than 50 mutations in the TARDBP gene have been identified (*Tab. 3*), among which the G376D mutation is particularly notable as it gives rise to a more rapid and aggressive form of ALS. While this mutation is relatively novel (identified for the first time in 2011 by Conforti et al.), studies have begun to shed light on its role in ALS pathogenesis: abnormal protein aggregation, cellular stress and neurodegeneration. However, much remains to be understood regarding the cellular mechanisms underlying disease onset and progression, particularly in asymptomatic carriers who may later develop symptoms.

This study aimed to investigate the expression, localization and functional implications of TDP-43 in fibroblasts derived from both asymptomatic and symptomatic G376D carriers and healthy controls, belonging to the same Apulian family (*Fig. 7*). Additionally, iPSCs were generated from these fibroblasts to differentiate into motor neurons. The work focused on understanding the cellular behaviour of TDP-43 under both basal and chronic stress conditions and aimed to develop a human-based ALS model using iPSCs-derived MNs to explore disease-specific phenotypic changes in G376D mutation carriers.

1. Does the G376D mutation have an impact on stress response?

Under basal conditions, it was observed that TDP-43 was predominantly localized to the nucleus in fibroblasts from all three groups (s.G376D, a.G376D and WT), consistent with previous studies showing the physiological role of TDP-43 as a nuclear protein (*Fig. 14*). The presence of TDP-43 in the cytoplasm was minimal and not considered pathological, as it aligns with the well-known shuttling behaviour of this protein between the nucleus and the cytoplasm.
This finding suggests that under basal conditions, the expression and sub-cellular localization of TDP-43 in fibroblasts from G376D carriers does not exhibit a clear pathological alteration. This is important for understanding the baseline molecular status of these cells.

Since patients affected by ALS have elevated levels of cortisol, a steroid hormone that increase in response to stress, the behaviour of TDP-43 under chronic stress conditions was investigated. The decision to focus on chronic stress rather than acute stress was made to replicate more accurately the long-term stress response that may contribute to the gradual progression of ALS pathology.

In response to chronic stress, induced by Sodium Arsenite, a distinct change occurred in TDP-43 subcellular localization and stress granules formation. The fibroblasts from all three groups showed a diffusion of TDP-43 in the cytoplasm and formation of TIAR-positive stress granules immediately after stress exposure (T0). However, s.G376D cells showed a less pronounced response compared to the a.G376D and WT (30% and 40% of TIAR-positive granules, respectively), with lower levels of stress granules (4% of TIAR-positive granules) and TDP-43 aggregates (*Fig. 16, A panel and Fig, 17*).

This result suggests that s.G376D carriers may exhibit a reduced ability to respond to stress, as evidenced by the lower number of SGs. Interestingly, this altered stress response may reflect an underlying susceptibility to stress insult in these cells, which could contribute to the pathogenesis of G376D ALS.

After 24 hours of recovery from the stress, both WT and a.G376D showed the presence of some SGs, indicating that the stress response was still active (Fig. 16, B panel). The persistence of SGs, even after the stressor had been removed from the environment for 24 hours, suggests that the cellular effects of stress continue to linger within the cells. In contrast, s.G376D cells showed a complete disassembly of SGs, which strengthens the reduced ability to respond to stress.

In the scientific community, there is still a debate regarding whether TDP-43 is actively involved in the SGs formation. Some studies suggest that TDP-43 works together with SGs, as evidenced by their co-localization, while others propose that the co-localization is merely incidental due to the increased abundance and prolonged presence of TDP-43 in the cytoplasm. In this study, co-localization was observed only in the WT, while in the G376D carriers, it seems that SGs and TDP-43 do not co-localize. This result aligns more closely with the hypothesis of incidental co-localization.

2. iPSCs-derived MNs can be obtained in 15 days using the PiggyBac System

iPSCs-derived MNs have become a powerful ALS model for studying its pathophysiology, as they can provide insight into the specific neuronal vulnerabilities that occur in ALS patients. Historically, the study of ALS-affected MNs has depended on post-mortem brain tissue, animal models or neuron-like cell lines. However, each approach had notable limitations, such as the inability to directly translate findings from animal models to human conditions. The development of iPSCs technology has revolutionized the study of ALS by providing a more relevant and human-specific model.

For this study, iPSCs from all three groups (s.G376D, a.G376D, and WT) were successfully generated by Dr. J. Rosati's research group and transfected with both NIL and NIP plasmids, kindly given by Dr. A. Rosa.

The established iPSCs lines were successfully differentiated into MNs – spinal and cranial – following the protocol by Garone et al. (2018), initially starting from the progenitor stage. The MNs were characterized using motor neuronal markers, such as ChAT, Neurofilament 200, MAP2, βIII-tubulin, Isl-1, HB9, at multiple time points (day 7, 9 and 12) (*Fig. 19 – 21*).
This result indicates that the differentiation protocol used in this study is robust and successfully generates MNs from iPSCs in 15 days.
The localization of TDP-43 in MNs was predominantly nuclear, with slight diffusion into neurites. Given that the cytoplasmic diffusion of TDP-43 was observed even in the WT MNs, this result was not considered as a pathological marker but as consistent with its physiological role (*Fig. 21*).
Additionally, a progressive linearization of the neurites was observed during the development of MNs (*Fig. 22*), suggesting that the initial outgrowth may occur in a random and exploratory manner, but as MNs begin to establish connections with one another, these contacts are stabilized at the expense of non-targeted projections.

However, a high rate of MNs mortality was observed. This could be attributed to an increased susceptibility of the progenitor cells to the transport on ice, as these cells are already partially differentiated and therefore more vulnerable. Therefore, the differentiation was carried out starting from the iPSCs and the resulting MNs were characterized as in previous experiments. The results of the characterization and TDP-43 localization were consistent with the previous. Additionally, the MNs mortality decreased, suggesting that starting from the iPSCs is relevant for the outcome of the differentiation process

Despite the success of the differentiation process, the presence of "flat cells", non-neuronal proliferative cells, was observed, which negatively impacted the MNs survival in longer culture periods (more than 15 days) (*Fig. 23, B panel and 24*). The presence of these proliferative cells suggested that refinements to the protocols were necessary to limit their presence and ensure long-term viability of the MNs cultures. These cells could be a result of inefficient cells management or a problem during the transfection procedure or even in the iPSCs generation. Therefore, different strategies were carried out in this study to overcome the problem and optimize this protocol, to establish a human-based ALS-associated G376D TDP-43 mutation model.

3. From challenges to solutions: optimizing protocols for better outcomes

A key component of this study involved improving the protocols – culture conditions for iPSCs, refining the transfection and differentiation protocols – to ensure high-quality iPSCs, which severely impact the overall experimental outcomes. As described in **Chapter IV, paragraph 3**, high-quality iPSCs should show: compact and well-defined borders, high nucleus-to-cytoplasm ratio, uniform cell morphology, prominent nucleoli, flat colony structure, high refractivity under phase-contrast microscopy and no differentiated cells (*Fig. 25*).

The first improvement was transitioning from manual “scraping” to ReLeSR passage method. The “scraping” method is outdated and may induce spontaneous differentiation, while ReLeSR is a gentle dissociation reagent that selectively detach only undifferentiated cells (*Fig. 27*). This improvement allowed for a more homogeneous population of iPSCs, with less than 20% of differentiated cell, after just 8 passages from thawing (2 passages with “manual picking” and 6 passages with ReLeSR). This is a significant improvement over the initial state, where more than 60% of differentiated cells were present.

Transfection of the NIL plasmid, whether via Lipofectamine or alternative delivery systems, also induces stress to iPSCs. Inadequate selection of transfected colonies may result in the inclusion of differentiated colonies. The presence of already or partially differentiated colonies amidst undifferentiated ones can increase the rate of spontaneous differentiation, thereby increasing the proportion of differentiated cells. Moreover, such colonies may induce differentiation in an undifferentiated colony. Therefore, another optimization of the protocols was the careful selection of post-transfected colonies. This improvement in transfection efficiency is crucial for generating stable NIL-iPSCs lines and subsequently for obtaining good-quality MNs populations.

Despite the first two improvements, “flat cells” persisted during differentiation in MNs. Therefore, another improvement was the addition of Floxuridine, an antimetabolite and pyrimidine analogue, during the differentiation to inhibit the proliferation of these cells. The addition of Floxuridine successfully inhibited their proliferation, allowing to culture MNs for long periods (*Fig. 31*).

CHAPTER VI: CONCLUSIONS AND FUTURE PERSPECTIVES

1. Conclusion

This study aimed to explore the molecular mechanisms underlying the G376D mutation in TARDBP in an Italian familial ALS case. Specifically, the objectives of this project were:

1. Study the expression and sub-cellular localization of TDP-43 in patient-derived fibroblasts under both basal and chronic stress conditions
2. Generate induced pluripotent stem cells (iPSCs) from patient fibroblasts and transfect them with NIL and NIP transposons using PiggyBac system (focusing primarily on NIL-MNs)
3. Differentiate iPSCs into MNs and characterize them through immunocytochemistry
4. Study the expression and sub-cellular localization of TDP-43 in the MNs under both basal and stress conditions (acute and chronic).

To address these aims, a series of experiments were carried out, and the findings are summarized below according to each objective:

1. **Study of the expression and sub-cellular localization of TDP-43 in patient-derived fibroblasts under both basal and chronic stress conditions**

   Patient-derived fibroblasts from symptomatic (s.G376D), asymptomatic (a.G376D) and healthy control (WT) individuals were analysed under basal and chronic stress conditions. Under basal conditions, TDP-43 exhibited its expected nuclear localization, consistent with its physiological role. However, upon chronic stress induction with Sodium Arsenite, subtle but significant differences emerged between the subjects. In particular, the s.G376D fibroblasts showed a reduced ability to form stress granules and a more rapid disassembly of these granules during recovery. This suggests a diminished or altered stress response mechanism in the symptomatic carrier, potentially contributing to disease onset or progression.
2. **Generation of induced pluripotent stem cells (iPSCs) from patient fibroblasts and transfection with NIL and NIP transposons using PiggyBac system (focusing primarily on NIL-MNs)**

   iPSCs were successfully generated from fibroblasts (by Dr. J. Rosati's research group) and transfected with NIL and NIP constructs using PiggyBac system. While early challenges were encountered, particularly due to the presence of numerous differentiated cells, protocols refinements, including improved passaging methods (use of ReLeSR) and a selection of post-transfected colonies, significantly enhanced culture quality and stability. These optimizations allowed me to work with high-quality NIL-iPSCs and provided a foundation for subsequent MNs differentiation.

3. **Differentiate iPSCs into MNs and characterize them through immunocytochemistry**
   iPSCs from all three groups were differentiated into spinal MNs following Garone et al. (2018) differentiation protocol. The resulting MNs showed the typical morphology of MNs and expressed canonical markers such as ChAT, Hb9, βIII- tubulin and others at various stages (days 7, 9, and 12), validating the robustness of the differentiation protocol. However, the emergence of non-neuronal "flat cells" after prolonged culture highlighted a persistent challenge in maintaining pure MN cultures and disrupted their viability. This phenomenon further highlights the complexity of generating stable and mature motor neuronal models for ALS. Nevertheless, the use of Floxuridine to suppress proliferation of these unwanted “flat cells” enabled the extension of MN viability and thus long-term culture.
4. **Study of the expression and sub-cellular localization of TDP-43 in the MNs under both basal and stress conditions (acute and chronic)**
   TDP-43 remained mostly nuclear in MNs, with some diffusion in the neurites, under basal conditions, which aligns with aligns with its physiological roles and suggests that pathological mislocalization may occur at later stages of disease progression, highlighting the need for further investigations in mature MNs.
   However, the inability to culture s.G376D and a.G376D MNs long-term limited the investigation under stress conditions, thereby preventing the full achievement of this objective.

In conclusion, this study provides important insights into the inefficient cellular responses of TDP-43 in symptomatic G376D carriers and offers valuable improvements in iPSC culture and differentiation protocols for ALS modelling. While further refinements are needed to improve the quality of differentiated MNs and reduce the presence of “flat cells,” the results presented here lay the groundwork for using iPSC-derived models to investigate ALS pathogenesis and potential therapeutic interventions targeting G376D TDP-43.

2. Future perspectives

While this study provides important insight in understanding the pathophysiology of ALS in G376D TDP-43 mutation carrier, further analyses and optimization are required.

- **Refinement of ALS models**: the findings of this study highlight the need for further optimization of the differentiation protocol and the development of mature MNs models. Future work will focus on strategies to remove the challenges given by the presence of “flat cells” and to develop models with “mature MNs” to explore the long-term effects of ALS.
- **Acute and chronic stress response on MNs**: future work will aim to complete the final objective of this study by investigating the stress response in iPSCs-derived MNs, and to compare these findings with the previously obtained in fibroblasts.

- **Co-culture systems**: although the study of ALS pathogenesis on MNs is significantly important, to better understand the underlying mechanisms is essential to work on co-culture systems, such as MNs and microglia. Future work will focus on generating microglial cells derived from PBMC (Peripheral Blood Mononuclear Cells) of the same subject used in this study, and culturing them together with the MNs. This system will highlight the role of neuroinflammation in ALS.
- **Therapeutic strategies**: Given that the G376D mutation leads to a particularly aggressive and rapid form of ALS and considering the presence of a large family carrying this mutation in which 1 individual develops symptoms nearly every year, future research will focus on the development of personalized therapeutic strategies. This will include the design and testing of siRNAs [153] (in collaboration with Dr. C. Bucci – University of Salento, LE, Italy) and ASOs (in collaboration with Dr. N. Shneider – Columbia University, NY, USA).
- **Expansion to other ALS-related mutations**: while this study focuses on the G376D mutation, it would be valuable to extend this work to other TDP-43 mutations and other ALS-associated genes. Future works will focus on the comparison of another 2 TDP-43 mutations – A382T and G294V – and another 2 ALS-associated genes – FUS P525L and C9ORF72. Understanding the common and divergent pathological mechanisms in ALS could pave the way for understanding the molecular causes of ALS.

Some of these future directions have already been initiated, and I am currently contributing to their execution.

REFERENCES

1. Hardiman O, Al-Chalabi A, Chio A, Corr EM, Logroscino G, Robberecht W, Shaw PJ, Simmons Z, van den Berg LH. Amyotrophic lateral sclerosis. Nat Rev Dis Primers. 2017 Oct 5;3:17071. doi: 10.1038/nrdp.2017.71. Erratum in: Nat Rev Dis Primers. 2017 Oct 20;3:17085. doi: 10.1038/nrdp.2017.85. PMID: 28980624.

2. Mead RJ, Shan N, Reiser HJ, Marshall F, Shaw PJ. Amyotrophic lateral sclerosis: a neurodegenerative disorder poised for successful therapeutic translation. Nat Rev Drug Discov. 2023 Mar;22(3):185-212. Doi: 10.1038/s41573-022-00612-2. Epub 2022 Dec 21. PMID: 36543887; PMCID: PMC9768794.

3. Masrori P, Van Damme P. Amyotrophic lateral sclerosis: a clinical review. Eur J Neurol. 2020 Oct;27(10):1918-1929. doi: 10.1111/ene.14393. Epub 2020 Jul 7. PMID: 32526057; PMCID: PMC7540334.

4. Longinetti E, Fang F. Epidemiology of amyotrophic lateral sclerosis: an update of recent literature. Curr Opin Neurol. 2019 Oct;32(5):771-776. doi: 10.1097/WCO.0000000000000730. PMID: 31361627; PMCID: PMC6735526.

5. Brown CA, Lally C, Kupelian V, Flanders WD. Estimated Prevalence and Incidence of Amyotrophic Lateral Sclerosis and SOD1 and C9orf72 Genetic Variants. Neuroepidemiology. 2021;55(5):342-353. doi: 10.1159/000516752. Epub 2021 Jul 9. PMID: 34247168.

6. Chiò A, Logroscino G, Traynor BJ, Collins J, Simeone JC, Goldstein LA, White LA. Global epidemiology of amyotrophic lateral sclerosis: a systematic review of the published literature. Neuroepidemiology. 2013;41(2):118-30. doi: 10.1159/000351153. Epub 2013 Jul 11. PMID: 23860588; PMCID: PMC4049265.

7. Brenner D, Weishaupt JH. Update on amyotrophic lateral sclerosis genetics. Curr Opin Neurol. 2019 Oct;32(5):735-739. doi: 10.1097/WCO.0000000000000737. PMID: 31335339.

8. Zarei S, Carr K, Reiley L, Diaz K, Guerra O, Altamirano PF, Pagani W, Lodin D, Orozco G, Chinea A. A comprehensive review of amyotrophic lateral sclerosis. Surg Neurol Int. 2015 Nov 16;6:171. doi: 10.4103/2152-7806.169561. PMID: 26629397; PMCID: PMC4653353.

9. Hardiman O, van den Berg LH, Kiernan MC. Clinical diagnosis and management of amyotrophic lateral sclerosis. Nat Rev Neurol. 2011 Oct 11;7(11):639-49. doi: 10.1038/nrneurol.2011.153. PMID: 21989247.

10. L. Lopiano, A. Mauro, A. Chiò, R. Mutani, "Il Bergamini di Neurologia". (2020)

11. A. Federico, C. Caltagirone, L. Provinciali, G. Tedeschi, "Neurologia Pratica". (2014)

12. Zoccolella S, Giugno A, Logroscino G. Split phenomena in amyotrophic lateral sclerosis: Current evidences, pathogenetic hypotheses and diagnostic implications. Front Neurosci. 2023 Jan 9;16:1100040. doi: 10.3389/fnins.2022.1100040. PMID: 36699516; PMCID: PMC9868395.

13. Pringle CE, Hudson AJ, Munoz DG, Kiernan JA, Brown WF, Ebers GC. Primary lateral sclerosis. Clinical features, neuropathology and diagnostic criteria. Brain. 1992 Apr;115 (Pt 2):495-520. doi: 10.1093/brain/115.2.495. PMID: 1606479.

14. Chiò A, Calvo A, Moglia C, Mazzini L, Mora G; PARALS study group. Phenotypic heterogeneity of amyotrophic lateral sclerosis: a population based study. J Neurol Neurosurg Psychiatry. 2011 Jul;82(7):740-6. doi: 10.1136/jnnp.2010.235952. Epub 2011 Mar 14. PMID: 21402743.

15. Kaufman D, Milstein M. "*Kaufman's Clinical Neurology for Psychiatrists*" (*Chapter 4 - Cranial Nerve Impairments)*, (2013)

16. Finegan E, Chipika RH, Li Hi Shing S, Hardiman O, Bede P. Pathological Crying and Laughing in Motor Neuron Disease: Pathobiology, Screening, Intervention. Front Neurol. 2019 Mar 21;10:260. doi: 10.3389/fneur.2019.00260. PMID: 30949121; PMCID: PMC6438102.

17. Wijesekera LC, Mathers S, Talman P, Galtrey C, Parkinson MH, Ganesalingam J, Willey E, Ampong MA, Ellis CM, Shaw CE, Al-Chalabi A, Leigh PN. Natural history and clinical features of the flail arm and flail leg ALS variants. Neurology. 2009 Mar 24;72(12):1087-94. doi: 10.1212/01.wnl.0000345041.83406.a2. PMID: 19307543; PMCID: PMC2821838.

18. Phukan J, Pender NP, Hardiman O. Cognitive impairment in amyotrophic lateral sclerosis. Lancet Neurol. 2007 Nov;6(11):994-1003. doi: 10.1016/S1474-4422(07)70265-X. PMID: 17945153.

19. Neary D, Snowden JS, Gustafson L, Passant U, Stuss D, Black S, Freedman M, Kertesz A, Robert PH, Albert M, Boone K, Miller BL, Cummings J, Benson DF. Frontotemporal lobar degeneration: a consensus on clinical diagnostic criteria. Neurology. 1998 Dec;51(6):1546-54. doi: 10.1212/wnl.51.6.1546. PMID: 9855500.

20. Brooks BR, Miller RG, Swash M, Munsat TL; World Federation of Neurology Research Group on Motor Neuron Diseases. El Escorial revisited: revised criteria for the diagnosis of amyotrophic lateral sclerosis. Amyotroph Lateral Scler Other Motor Neuron Disord. 2000 Dec;1(5):293-9. doi: 10.1080/146608200300079536. PMID: 11464847.

21. Petrov D, Mansfield C, Moussy A, Hermine O. ALS Clinical Trials Review: 20 Years of Failure. Are We Any Closer to Registering a New Treatment? Front Aging Neurosci. 2017 Mar 22;9:68. doi: 10.3389/fnagi.2017.00068. PMID: 28382000; PMCID: PMC5360725.

22. Andrews JA, Jackson CE, Heiman-Patterson TD, Bettica P, Brooks BR, Pioro EP. Real-world evidence of riluzole effectiveness in treating amyotrophic lateral sclerosis. Amyotroph Lateral Scler Frontotemporal Degener. 2020 Nov;21(7-8):509-518. doi: 10.1080/21678421.2020.1771734. Epub 2020 Jun 23. PMID: 32573277.

23. Armon C. An evidence-based medicine approach to the evaluation of the role of exogenous risk factors in sporadic amyotrophic lateral sclerosis. Neuroepidemiology. 2003 Jul-Aug;22(4):217-28. doi: 10.1159/000070562. PMID: 12792141.

24. Ingre C, Roos PM, Piehl F, Kamel F, Fang F. Risk factors for amyotrophic lateral sclerosis. Clin Epidemiol. 2015 Feb 12;7:181-93. doi: 10.2147/CLEP.S37505. PMID: 25709501; PMCID: PMC4334292.

25. Renton AE, Chiò A, Traynor BJ. State of play in amyotrophic lateral sclerosis genetics. Nat Neurosci. 2014 Jan;17(1):17-23. doi: 10.1038/nn.3584. Epub 2013 Dec 26. PMID: 24369373; PMCID: PMC4544832.

26. Rosen DR, Siddique T, Patterson D, Figlewicz DA, Sapp P, Hentati A, Donaldson D, Goto J, O'Regan JP, Deng HX, et al. Mutations in Cu/Zn superoxide dismutase gene are associated with familial amyotrophic lateral sclerosis. Nature. 1993 Mar 4;362(6415):59-62. doi: 10.1038/362059a0. Erratum in: Nature. 1993 Jul 22;364(6435):362. doi: 10.1038/364362c0. PMID: 8446170.

27. Wang H, Guan L, Deng M. Recent progress of the genetics of amyotrophic lateral sclerosis and challenges of gene therapy. Front Neurosci. 2023 May 12;17:1170996. doi: 10.3389/fnins.2023.1170996. PMID: 37250416; PMCID: PMC10213321.

28. Zou ZY, Zhou ZR, Che CH, Liu CY, He RL, Huang HP. Genetic epidemiology of amyotrophic lateral sclerosis: a systematic review and meta-analysis. J Neurol Neurosurg Psychiatry. 2017 Jul;88(7):540-549. doi: 10.1136/jnnp-2016-315018. Epub 2017 Jan 5. PMID: 28057713.

29. Wang W, Wang L, Lu J, Siedlak SL, Fujioka H, Liang J, Jiang S, Ma X, Jiang Z, da Rocha EL, Sheng M, Choi H, Lerou PH, Li H, Wang X. The inhibition of TDP-43 mitochondrial localization blocks its neuronal toxicity. Nat Med. 2016 Aug;22(8):869-78. doi: 10.1038/nm.4130. Epub 2016 Jun 27. PMID: 27348499; PMCID: PMC4974139.

30. Oda M, Akagawa N, Tabuchi Y, Tanabe H. A sporadic juvenile case of the amyotrophic lateral sclerosis with neuronal intracytoplasmic inclusions. Acta Neuropathol. 1978 Dec 15;44(3):211-6. doi: 10.1007/BF00691069. PMID: 216220.

31. Wang W, Wang L, Lu J, Siedlak SL, Fujioka H, Liang J, Jiang S, Ma X, Jiang Z, da Rocha EL, Sheng M, Choi H, Lerou PH, Li H, Wang X. The inhibition of TDP-43 mitochondrial localization

blocks its neuronal toxicity. Nat Med. 2016 Aug;22(8):869-78. doi: 10.1038/nm.4130. Epub 2016 Jun 27. PMID: 27348499; PMCID: PMC4974139.

32. Laslo P, Lipski J, Nicholson LF, Miles GB, Funk GD. GluR2 AMPA receptor subunit expression in motoneurons at low and high risk for degeneration in amyotrophic lateral sclerosis. Exp Neurol. 2001 Jun;169(2):461-71. doi: 10.1006/exnr.2001.7653. PMID: 11358459.

33. Mejzini R, Flynn LL, Pitout IL, Fletcher S, Wilton SD, Akkari PA. ALS Genetics, Mechanisms, and Therapeutics: Where Are We Now? Front Neurosci. 2019 Dec 6;13:1310. doi: 10.3389/fnins.2019.01310. PMID: 31866818; PMCID: PMC6909825.

34. Pasquali L, Lenzi P, Biagioni F, Siciliano G, Fornai F. Cell to cell spreading of misfolded proteins as a therapeutic target in motor neuron disease. Curr Med Chem. 2014;21(31):3508-34. doi: 10.2174/09298673216661406011615 34. PMID: 24934358.

35. Zhou Y, Liu S, Oztürk A, Hicks GG. FUS-regulated RNA metabolism and DNA damage repair: Implications for amyotrophic lateral sclerosis and frontotemporal dementia pathogenesis. Rare Dis. 2014 Jun 12;2:e29515. doi: 10.4161/rdis.29515. PMID: 25083344; PMCID: PMC4116389.

36. Mackenzie IR, Rademakers R, Neumann M. TDP-43 and FUS in amyotrophic lateral sclerosis and frontotemporal dementia. Lancet Neurol. 2010 Oct;9(10):995-1007. doi: 10.1016/S1474-4422(10)70195-2. PMID: 20864052.

37. Boeynaems S, Bogaert E, Van Damme P, Van Den Bosch L. Inside out: the role of nucleocytoplasmic transport in ALS and FTLD. Acta Neuropathol. 2016 Aug;132(2):159-173. doi: 10.1007/s00401-016-1586-5. Epub 2016 Jun 6. PMID: 27271576; PMCID: PMC4947127.

38. Appel SH, Beers DR, Zhao W. Amyotrophic lateral sclerosis is a systemic disease: peripheral contributions to inflammation-mediated neurodegeneration. Curr Opin Neurol. 2021 Oct 1;34(5):765-772. doi: 10.1097/WCO.0000000000000983. PMID: 34402459.

39. De Vos KJ, Grierson AJ, Ackerley S, Miller CC. Role of axonal transport in neurodegenerative diseases. Annu Rev Neurosci. 2008;31:151-73. doi: 10.1146/annurev.neuro.31.061307.090711. PMID: 18558852.

40. Fischer LR, Culver DG, Tennant P, Davis AA, Wang M, Castellano-Sanchez A, Khan J, Polak MA, Glass JD. Amyotrophic lateral sclerosis is a distal axonopathy: evidence in mice and man. Exp Neurol. 2004 Feb;185(2):232-40. doi: 10.1016/j.expneurol.2003.10.004. PMID: 14736504.

41. Ferraiuolo L, Kirby J, Grierson AJ, Sendtner M, Shaw PJ. Molecular pathways of motor neuron injury in amyotrophic lateral sclerosis. Nat Rev Neurol. 2011 Nov;7(11):616-30. doi: 10.1038/nrneurol.2011.152. PMID: 22051914.

42. Ou SH, Wu F, Harrich D, García-Martínez LF, Gaynor RB. Cloning and characterization of a novel cellular protein, TDP-43, that binds to human immunodeficiency virus type 1 TAR DNA sequence motifs. J Virol. 1995 Jun;69(6):3584-96. doi: 10.1128/JVI.69.6.3584-3596.1995. PMID: 7745706; PMCID: PMC189073.

43. Neumann M, Sampathu DM, Kwong LK, Truax AC, Micsenyi MC, Chou TT, Bruce J, Schuck T, Grossman M, Clark CM, McCluskey LF, Miller BL, Masliah E, Mackenzie IR, Feldman H, Feiden W, Kretzschmar HA, Trojanowski JQ, Lee VM. Ubiquitinated TDP-43 in frontotemporal lobar degeneration and amyotrophic lateral sclerosis. Science. 2006 Oct 6;314(5796):130-3. doi: 10.1126/science.1134108. PMID: 17023659.

44. Geuens T, Bouhy D, Timmerman V. The hnRNP family: insights into their role in health and disease. Hum Genet. 2016 Aug;135(8):851-67. doi: 10.1007/s00439-016-1683-5. Epub 2016 May 23. PMID: 27215579; PMCID: PMC4947485.

45. Prasad A, Bharathi V, Sivalingam V, Girdhar A, Patel BK. Molecular Mechanisms of TDP-43 Misfolding and Pathology in Amyotrophic Lateral Sclerosis. Front Mol Neurosci. 2019 Feb 14;12:25. doi: 10.3389/fnmol.2019.00025. PMID: 30837838; PMCID: PMC6382748.

46. Zhang YJ, Caulfield T, Xu YF, Gendron TF, Hubbard J, Stetler C, Sasaguri H, Whitelaw EC, Cai S, Lee WC, Petrucelli L. The dual functions of the extreme N-terminus of TDP-43 in regulating its biological activity and inclusion formation. Hum Mol Genet. 2013 Aug 1;22(15):3112-22. doi: 10.1093/hmg/ddt166. Epub 2013 Apr 10. PMID: 23575225; PMCID: PMC3699067.

47. Kuo PH, Chiang CH, Wang YT, Doudeva LG, Yuan HS. The crystal structure of TDP-43 RRM1-DNA complex reveals the specific recognition for UG- and TG-rich nucleic acids. Nucleic Acids Res. 2014 Apr;42(7):4712-22. doi: 10.1093/nar/gkt1407. Epub 2014 Jan 23. PMID: 24464995; PMCID: PMC3985631.

48. Ayala YM, De Conti L, Avendaño-Vázquez SE, Dhir A, Romano M, D'Ambrogio A, Tollervey J, Ule J, Baralle M, Buratti E, Baralle FE. TDP-43 regulates its mRNA levels through a negative feedback loop. EMBO J. 2011 Jan 19;30(2):277-88. doi: 10.1038/emboj.2010.310. Epub 2010 Dec 3. PMID: 21131904; PMCID: PMC3025456.

49. Yury O. Chernoff, Anastasia V. Grizel, Aleksandr A. Rubel, Andrew A. Zelinsky, Pavithra Chandramowlishwaran, Tatiana A. Chernova. “Chapter Seven - Application of yeast to studying amyloid and prion diseases”. Advances in Genetics. 2020. https://doi.org/10.1016/bs.adgen.2020.01.002.

50. Tamaki Y, Urushitani M. Molecular Dissection of TDP-43 as a Leading Cause of ALS/FTLD. Int J Mol Sci. 2022 Oct 19;23(20):12508. doi: 10.3390/ijms232012508. PMID: 36293362; PMCID: PMC9604209.

51. de Boer EMJ, Orie VK, Williams T, Baker MR, De Oliveira HM, Polvikoski T, Silsby M, Menon P, van den Bos M, Halliday GM, van den Berg LH, Van Den Bosch L, van Damme P, Kiernan MC, van Es MA, Vucic S. TDP-43 proteinopathies: a new wave of neurodegenerative diseases. J Neurol Neurosurg Psychiatry. 2020 Nov 11;92(1):86–95. doi: 10.1136/jnnp-2020-322983. Epub ahead of print. PMID: 33177049; PMCID: PMC7803890.

52. Kawahara Y, Mieda-Sato A. TDP-43 promotes microRNA biogenesis as a component of the Drosha and Dicer complexes. Proc Natl Acad Sci U S A. 2012 Feb 28;109(9):3347-52. doi: 10.1073/pnas.1112427109. Epub 2012 Feb 9. PMID: 22323604; PMCID: PMC3295278.

53. Arai T, Hasegawa M, Akiyama H, Ikeda K, Nonaka T, Mori H, Mann D, Tsuchiya K, Yoshida M, Hashizume Y, Oda T. TDP-43 is a component of ubiquitin-positive tau-negative inclusions in frontotemporal lobar degeneration and amyotrophic lateral sclerosis. Biochem Biophys Res Commun. 2006 Dec 22;351(3):602-11. doi: 10.1016/j.bbrc.2006.10.093. Epub 2006 Oct 30. PMID: 17084815.

54. Ederle H, Dormann D. TDP-43 and FUS en route from the nucleus to the cytoplasm. FEBS Lett. 2017 Jun;591(11):1489-1507. doi: 10.1002/1873-3468.12646. Epub 2017 Apr 23. PMID: 28380257.

55. Ling SC, Polymenidou M, Cleveland DW. Converging mechanisms in ALS and FTD: disrupted RNA and protein homeostasis. Neuron. 2013 Aug 7;79(3):416-38. doi: 10.1016/j.neuron.2013.07.033. PMID: 23931993; PMCID: PMC4411085.

56. Neumann M, Kwong LK, Lee EB, Kremmer E, Flatley A, Xu Y, Forman MS, Troost D, Kretzschmar HA, Trojanowski JQ, Lee VM. Phosphorylation of S409/410 of TDP-43 is a consistent feature in all sporadic and familial forms of TDP-43 proteinopathies. Acta Neuropathol. 2009 Feb;117(2):137-49. doi: 10.1007/s00401-008-0477-9. Epub 2009 Jan 6. PMID: 19125255; PMCID: PMC2693625.

57. Scotter EL, Vance C, Nishimura AL, Lee YB, Chen HJ, Urwin H, Sardone V, Mitchell JC, Rogelj B, Rubinsztein DC, Shaw CE. Differential roles of the ubiquitin proteasome system and autophagy in the clearance of soluble and aggregated TDP-43 species. J Cell Sci. 2014 Mar 15;127(Pt 6):1263-78. doi: 10.1242/jcs.140087. Epub 2014 Jan 14. PMID: 24424030; PMCID: PMC3953816.

58. Cohen TJ, Hwang AW, Restrepo CR, Yuan CX, Trojanowski JQ, Lee VM. An acetylation switch controls TDP-43 function and aggregation propensity. Nat Commun. 2015 Jan 5;6:5845. doi: 10.1038/ncomms6845. PMID: 25556531; PMCID: PMC4407365.

59. Li Q, Yokoshi M, Okada H, Kawahara Y. The cleavage pattern of TDP-43 determines its rate of clearance and cytotoxicity. Nat Commun. 2015 Jan 29;6:6183. doi: 10.1038/ncomms7183. PMID: 25630387.

60. Duan Y, Du A, Gu J, Duan G, Wang C, Gui X, Ma Z, Qian B, Deng X, Zhang K, Sun L, Tian K, Zhang Y, Jiang H, Liu C, Fang Y. PARylation regulates stress granule dynamics, phase separation, and neurotoxicity of disease-related RNA-binding proteins. Cell Res. 2019 Mar;29(3):233-247. doi: 10.1038/s41422-019-0141-z. Epub 2019 Feb 6. PMID: 30728452; PMCID: PMC6460439.

61. Chang, C. K., Chiang, M. H., Toh, E. K., Chang, C. F., and Huang, T. H. (2013). Molecular mechanism of oxidation-induced TDP-43 RRM1 aggregation and loss of function. FEBS Lett. 587, 575–582. doi: 10.1016/j.febslet.2013.01.038

62. Budini M, Buratti E, Morselli E, Criollo A. Autophagy and Its Impact on Neurodegenerative Diseases: New Roles for TDP-43 and C9orf72. Front Mol Neurosci. 2017 May 30;10:170. doi: 10.3389/fnmol.2017.00170. PMID: 28611593; PMCID: PMC5447761.

63. Dafinca R, Barbagallo P, Talbot K. The Role of Mitochondrial Dysfunction and ER Stress in TDP-43 and C9ORF72 ALS. Front Cell Neurosci. 2021 Apr 1;15:653688. doi: 10.3389/fncel.2021.653688. PMID: 33867942; PMCID: PMC8047135.

64. Iguchi Y, Eid L, Parent M, Soucy G, Bareil C, Riku Y, Kawai K, Takagi S, Yoshida M, Katsuno M, Sobue G, Julien JP. Exosome secretion is a key pathway for clearance of pathological TDP-43. Brain. 2016 Dec;139(Pt 12):3187-3201. doi: 10.1093/brain/aww237. Epub 2016 Sep 27. PMID: 27679482; PMCID: PMC5840881.

65. Nakashima-Yasuda H, Uryu K, Robinson J, Xie SX, Hurtig H, Duda JE, Arnold SE, Siderowf A, Grossman M, Leverenz JB, Woltjer R, Lopez OL, Hamilton R, Tsuang DW, Galasko D, Masliah E, Kaye J, Clark CM, Montine TJ, Lee VM, Trojanowski JQ. Co-morbidity of TDP-43 proteinopathy in Lewy body related diseases. Acta Neuropathol. 2007 Sep;114(3):221-9. doi: 10.1007/s00401-007-0261-2. Epub 2007 Jul 25. PMID: 17653732.

66. Uryu K, Nakashima-Yasuda H, Forman MS, Kwong LK, Clark CM, Grossman M, Miller BL, Kretzschmar HA, Lee VM, Trojanowski JQ, Neumann M. Concomitant TAR-DNA-binding protein 43 pathology is present in Alzheimer disease and corticobasal degeneration but not in other tauopathies. J Neuropathol Exp Neurol. 2008 Jun;67(6):555-64. doi: 10.1097/NEN.0b013e31817713b5. PMID: 18520774; PMCID: PMC3659339.

67. Yokota O, Davidson Y, Bigio EH, Ishizu H, Terada S, Arai T, Hasegawa M, Akiyama H, Sikkink S, Pickering-Brown S, Mann DM. Phosphorylated TDP-43 pathology and hippocampal sclerosis in progressive supranuclear palsy. Acta Neuropathol. 2010 Jul;120(1):55-66. doi: 10.1007/s00401-010-0702-1. Epub 2010 May 30. PMID: 20512649; PMCID: PMC2901929.

68. Hasegawa M, Arai T, Akiyama H, Nonaka T, Mori H, Hashimoto T, Yamazaki M, Oyanagi K. TDP-43 is deposited in the Guam parkinsonism-dementia complex brains. Brain. 2007 May;130(Pt 5):1386-94. doi: 10.1093/brain/awm065. Epub 2007 Apr 17. PMID: 17439983.

69. Freeman SH, Spires-Jones T, Hyman BT, Growdon JH, Frosch MP. TAR-DNA binding protein 43 in Pick disease. J Neuropathol Exp Neurol. 2008 Jan;67(1):62-7. doi: 10.1097/nen.0b013e3181609361. PMID: 18091558.

70. Gao J, Wang L, Huntley ML, Perry G, Wang X. Pathomechanisms of TDP-43 in neurodegeneration. J Neurochem. 2018 Feb 27:10.1111/jnc.14327. doi: 10.1111/jnc.14327. Epub ahead of print. PMID: 29486049; PMCID: PMC6110993.

71. Buratti E. Functional Significance of TDP-43 Mutations in Disease. Adv Genet. 2015;91:1-53. doi: 10.1016/bs.adgen.2015.07.001. Epub 2015 Aug 7. PMID: 26410029.

72. Kabashi E, Valdmanis PN, Dion P, Spiegelman D, McConkey BJ, Vande Velde C, Bouchard JP, Lacomblez L, Pochigaeva K, Salachas F, Pradat PF, Camu W, Meininger V, Dupre N, Rouleau GA. TARDBP mutations in individuals with sporadic and familial amyotrophic lateral sclerosis. Nat Genet. 2008 May;40(5):572-4. doi: 10.1038/ng.132. Epub 2008 Mar 30. PMID: 18372902.

73. Van Deerlin VM, Leverenz JB, Bekris LM, Bird TD, Yuan W, Elman LB, Clay D, Wood EM, Chen-Plotkin AS, Martinez-Lage M, Steinbart E, McCluskey L, Grossman M, Neumann M, Wu IL, Yang WS, Kalb R, Galasko DR, Montine TJ, Trojanowski JQ, Lee VM, Schellenberg GD, Yu CE. TARDBP mutations in amyotrophic lateral sclerosis with TDP-43 neuropathology: a genetic and histopathological analysis. Lancet Neurol. 2008 May;7(5):409-16. doi: 10.1016/S1474-4422(08)70071-1. Epub 2008 Apr 7. PMID: 18396105; PMCID: PMC3546119.

74. Sreedharan J, Blair IP, Tripathi VB, Hu X, Vance C, Rogelj B, Ackerley S, Durnall JC, Williams KL, Buratti E, Baralle F, de Belleroche J, Mitchell JD, Leigh PN, Al-Chalabi A, Miller CC, Nicholson G, Shaw CE. TDP-43 mutations in familial and sporadic amyotrophic lateral sclerosis. Science. 2008 Mar 21;319(5870):1668-72. doi: 10.1126/science.1154584. Epub 2008 Feb 28. PMID: 18309045; PMCID: PMC7116650.

75. Yokoseki A, Shiga A, Tan CF, Tagawa A, Kaneko H, Koyama A, Eguchi H, Tsujino A, Ikeuchi T, Kakita A, Okamoto K, Nishizawa M, Takahashi H, Onodera O. TDP-43 mutation in familial amyotrophic lateral sclerosis. Ann Neurol. 2008 Apr;63(4):538-42. doi: 10.1002/ana.21392. PMID: 18438952.

76. Pesiridis GS, Lee VM, Trojanowski JQ. Mutations in TDP-43 link glycine-rich domain functions to amyotrophic lateral sclerosis. Hum Mol Genet. 2009 Oct 15;18(R2):R156-62. doi: 10.1093/hmg/ddp303. PMID: 19808791; PMCID: PMC2758707.

77. Gendron TF, Josephs KA, Petrucelli L. Review: transactive response DNA-binding protein 43 (TDP-43): mechanisms of neurodegeneration. Neuropathol Appl Neurobiol. 2010 Apr;36(2):97-112. doi: 10.1111/j.1365-2990.2010.01060.x. Epub 2010 Feb 19. PMID: 20202122; PMCID: PMC3052765.

78. Conforti FL, Sproviero W, Simone IL, Mazzei R, Valentino P, Ungaro C, Magariello A, Patitucci A, La Bella V, Sprovieri T, Tedeschi G, Citrigno L, Gabriele AL, Bono F, Monsurrò MR, Muglia M, Gambardella A, Quattrone A. TARDBP gene mutations in south Italian patients with amyotrophic lateral sclerosis. J Neurol Neurosurg Psychiatry. 2011 May;82(5):587-8. doi: 10.1136/jnnp.2009.198309. Epub 2010 Oct 19. PMID: 20959352.

79. Ungaro C, Sprovieri T, Morello G, Perrone B, Spampinato AG, Simone IL, Trojsi F, Monsurrò MR, Spataro R, La Bella V, Andò S, Cavallaro S, Conforti FL. Genetic investigation of amyotrophic lateral sclerosis patients in south Italy: a two-decade analysis. Neurobiol Aging. 2021 Mar;99:99.e7-99.e14. doi: 10.1016/j.neurobiolaging.2020.08.017. Epub 2020 Aug 27. PMID: 32951934.

80. Mitsuzawa S, Akiyama T, Nishiyama A, Suzuki N, Kato M, Warita H, Izumi R, Osana S, Koyama S, Kato T, Suzuki Y, Aoki M. *TARDBP* p.G376D mutation, found in rapid progressive familial ALS, induces mislocalization of TDP-43. eNeurologicalSci. 2018 Apr 12;11:20-22. doi: 10.1016/j.ensci.2018.04.001. PMID: 29928714; PMCID: PMC6006914.

81. Czell D, Andersen PM, Morita M, Neuwirth C, Perren F, Weber M. Phenotypes in Swiss patients with familial ALS carrying TARDBP mutations. Neurodegener Dis. 2013;12(3):150-5. doi: 10.1159/000345835. Epub 2013 Jan 10. PMID: 23327806.

82. Takahashi K, Yamanaka S. Induction of pluripotent stem cells from mouse embryonic and adult fibroblast cultures by defined factors. Cell. 2006 Aug 25;126(4):663-76. doi: 10.1016/j.cell.2006.07.024. Epub 2006 Aug 10. PMID: 16904174.

83. Takahashi K, Tanabe K, Ohnuki M, Narita M, Ichisaka T, Tomoda K, Yamanaka S. Induction of pluripotent stem cells from adult human fibroblasts by defined factors. Cell. 2007 Nov 30;131(5):861-72. doi: 10.1016/j.cell.2007.11.019. PMID: 18035408.

84. Niwa H, Miyazaki J, Smith AG. Quantitative expression of Oct-3/4 defines differentiation, dedifferentiation or self-renewal of ES cells. Nat Genet. 2000 Apr;24(4):372-6. doi: 10.1038/74199. PMID: 10742100.

85. Boyer LA, Lee TI, Cole MF, Johnstone SE, Levine SS, Zucker JP, Guenther MG, Kumar RM, Murray HL, Jenner RG, Gifford DK, Melton DA, Jaenisch R, Young RA. Core transcriptional regulatory circuitry in human embryonic stem cells. Cell. 2005 Sep 23;122(6):947-56. doi: 10.1016/j.cell.2005.08.020. PMID: 16153702; PMCID: PMC3006442.

86. Zhang S, Cui W. Sox2, a key factor in the regulation of pluripotency and neural differentiation. World J Stem Cells. 2014 Jul 26;6(3):305-11. doi: 10.4252/wjsc.v6.i3.305. PMID: 25126380; PMCID: PMC4131272.

87. Cartwright P, McLean C, Sheppard A, Rivett D, Jones K, Dalton S. LIF/STAT3 controls ES cell self-renewal and pluripotency by a Myc-dependent mechanism. Development. 2005 Mar;132(5):885-96. doi: 10.1242/dev.01670. Epub 2005 Jan 26. PMID: 15673569.

88. Park IH, Zhao R, West JA, Yabuuchi A, Huo H, Ince TA, Lerou PH, Lensch MW, Daley GQ. Reprogramming of human somatic cells to pluripotency with defined factors. Nature. 2008 Jan 10;451(7175):141-6. doi: 10.1038/nature06534. Epub 2007 Dec 23. PMID: 18157115.

89. Bourillot PY, Savatier P. Krüppel-like transcription factors and control of pluripotency. BMC Biol. 2010 Sep 27;8:125. doi: 10.1186/1741-7007-8-125. PMID: 20875146; PMCID: PMC2946285.

90. Yi H, Xie B, Liu B, Wang X, Xu L, Liu J, Li M, Zhong X, Peng F. Derivation and Identification of Motor Neurons from Human Urine-Derived Induced Pluripotent Stem Cells. Stem Cells Int. 2018 Jan 24;2018:3628578. doi: 10.1155/2018/3628578. PMID: 29531534; PMCID: PMC5829358.

91. Vlahos K, Sourris K, Mayberry R, McDonald P, Bruveris FF, Schiesser JV, Bozaoglu K, Lockhart PJ, Stanley EG, Elefanty AG. Generation of iPSC lines from peripheral blood mononuclear cells from 5 healthy adults. Stem Cell Res. 2019 Jan;34:101380. doi: 10.1016/j.scr.2018.101380. Epub 2018 Dec 27. PMID: 30605840.

92. Umegaki-Arao N, Pasmooij AM, Itoh M, Cerise JE, Guo Z, Levy B, Gostyński A, Rothman LR, Jonkman MF, Christiano AM. Induced pluripotent stem cells from human revertant keratinocytes for the treatment of epidermolysis bullosa. Sci Transl Med. 2014 Nov 26;6(264):264ra164. doi: 10.1126/scitranslmed.3009342. PMID: 25429057.

93. Yu J, Vodyanik MA, Smuga-Otto K, Antosiewicz-Bourget J, Frane JL, Tian S, Nie J, Jonsdottir GA, Ruotti V, Stewart R, Slukvin II, Thomson JA. Induced pluripotent stem cell lines derived from human somatic cells. Science. 2007 Dec 21;318(5858):1917-20. doi: 10.1126/science.1151526. Epub 2007 Nov 20. PMID: 18029452.

94. Kodo A, Ong S, Wu JC. “Chapter 20 - Transformation to Inducible Pluripotent Stem Cells”. Stem Cell and Gene Therapy for Cardiovascular Disease (2016). https://doi.org/10.1016/B978-0-12-801888-0.00020-5.

95. Gallardo J, Pérez-Illana M, Martín-González N, San Martín C. Adenovirus Structure: What Is New? Int J Mol Sci. 2021 May 15;22(10):5240. doi: 10.3390/ijms22105240. PMID: 34063479; PMCID: PMC8156859.

96. Nakanishi M, Otsu M. Development of Sendai virus vectors and their potential applications in gene therapy and regenerative medicine. Curr Gene Ther. 2012 Oct;12(5):410-6. doi: 10.2174/156652312802762518. PMID: 22920683; PMCID: PMC3504922.

97. Fusaki N, Ban H, Nishiyama A, Saeki K, Hasegawa M. Efficient induction of transgene-free human pluripotent stem cells using a vector based on Sendai virus, an RNA virus that does not integrate into the host genome. Proc Jpn Acad Ser B Phys Biol Sci. 2009;85(8):348-62. doi: 10.2183/pjab.85.348. PMID: 19838014; PMCID: PMC3621571.

98. Malik N, Rao MS. A review of the methods for human iPSC derivation. Methods Mol Biol. 2013;997:23-33. doi: 10.1007/978-1-62703-348-0_3. PMID: 23546745; PMCID: PMC4176696.

99. Okita K, Matsumura Y, Sato Y, Okada A, Morizane A, Okamoto S, Hong H, Nakagawa M, Tanabe K, Tezuka K, Shibata T, Kunisada T, Takahashi M, Takahashi J, Saji H, Yamanaka S. A more efficient method to generate integration-free human iPS cells. Nat Methods. 2011 May;8(5):409-12. doi: 10.1038/nmeth.1591. Epub 2011 Apr 3. PMID: 21460823.

100. Mali P, Chou BK, Yen J, Ye Z, Zou J, Dowey S, Brodsky RA, Ohm JE, Yu W, Baylin SB, Yusa K, Bradley A, Meyers DJ, Mukherjee C, Cole PA, Cheng L. Butyrate greatly enhances derivation of human induced pluripotent stem cells by promoting epigenetic remodeling and the expression of pluripotency-associated genes. Stem Cells. 2010 Apr;28(4):713-20. doi: 10.1002/stem.402. PMID: 20201064; PMCID: PMC3015217.

101. Narsinh KH, Jia F, Robbins RC, Kay MA, Longaker MT, Wu JC. Generation of adult human induced pluripotent stem cells using nonviral minicircle DNA vectors. Nat Protoc. 2011 Jan;6(1):78-88. doi: 10.1038/nprot.2010.173. Epub 2010 Dec 23. PMID: 21212777; PMCID: PMC3657506.

102. Kim D, Kim CH, Moon JI, Chung YG, Chang MY, Han BS, Ko S, Yang E, Cha KY, Lanza R, Kim KS. Generation of human induced pluripotent stem cells by direct delivery of reprogramming proteins. Cell Stem Cell. 2009 Jun 5;4(6):472-6. doi: 10.1016/j.stem.2009.05.005. Epub 2009 May 28. PMID: 19481515; PMCID: PMC2705327.

103. Warren L, Manos PD, Ahfeldt T, Loh YH, Li H, Lau F, Ebina W, Mandal PK, Smith ZD, Meissner A, Daley GQ, Brack AS, Collins JJ, Cowan C, Schlaeger TM, Rossi DJ. Highly efficient reprogramming to pluripotency and directed differentiation of human cells with synthetic modified mRNA. Cell Stem Cell. 2010 Nov 5;7(5):618-30. doi: 10.1016/j.stem.2010.08.012. Epub 2010 Sep 30. PMID: 20888316; PMCID: PMC3656821.

104. Shi Y, Inoue H, Wu JC, Yamanaka S. Induced pluripotent stem cell technology: a decade of progress. Nat Rev Drug Discov. 2017 Feb;16(2):115-130. doi: 10.1038/nrd.2016.245. Epub 2016 Dec 16. PMID: 27980341; PMCID: PMC6416143.

105. Redman M, King A, Watson C, King D. What is CRISPR/Cas9? Arch Dis Child Educ Pract Ed. 2016 Aug;101(4):213-5. doi: 10.1136/archdischild-2016-310459. Epub 2016 Apr 8. PMID: 27059283; PMCID: PMC4975809.

106. Zou J, Maeder ML, Mali P, Pruett-Miller SM, Thibodeau-Beganny S, Chou BK, Chen G, Ye Z, Park IH, Daley GQ, Porteus MH, Joung JK, Cheng L. Gene targeting of a disease-related gene in human induced pluripotent stem and embryonic stem cells. Cell Stem Cell. 2009 Jul 2;5(1):97-110. doi: 10.1016/j.stem.2009.05.023. Epub 2009 Jun 18. PMID: 19540188; PMCID: PMC2720132.

107. Joung JK, Sander JD. TALENs: a widely applicable technology for targeted genome editing. Nat Rev Mol Cell Biol. 2013 Jan;14(1):49-55. doi: 10.1038/nrm3486. Epub 2012 Nov 21. PMID: 23169466; PMCID: PMC3547402.

108. Wakui T, Matsumoto T, Matsubara K, Kawasaki T, Yamaguchi H, Akutsu H. Method for evaluation of human induced pluripotent stem cell quality using image analysis based on the biological morphology of cells. J Med Imaging (Bellingham). 2017 Oct;4(4):044003. doi: 10.1117/1.JMI.4.4.044003. Epub 2017 Nov 2. PMID: 29134187; PMCID: PMC5668125.

109. Doss MX, Sachinidis A. Current Challenges of iPSC-Based Disease Modeling and Therapeutic Implications. Cells. 2019 Apr 30;8(5):403. doi: 10.3390/cells8050403. PMID: 31052294; PMCID: PMC6562607.

110. Fan H, Chu JY. A brief review of short tandem repeat mutation. Genomics Proteomics Bioinformatics. 2007 Feb;5(1):7-14. doi: 10.1016/S1672-0229(07)60009-6. PMID: 17572359; PMCID: PMC5054066.

111. Stifani N. Motor neurons and the generation of spinal motor neuron diversity. Front Cell Neurosci. 2014 Oct 9;8:293. doi: 10.3389/fncel.2014.00293. PMID: 25346659; PMCID: PMC4191298.

112. Wichterle H, Lieberam I, Porter JA, Jessell TM. Directed differentiation of embryonic stem cells into motor neurons. Cell. 2002 Aug 9;110(3):385-97. doi: 10.1016/s0092-8674(02)00835-8. PMID: 12176325.

113. Dimos JT, Rodolfa KT, Niakan KK, Weisenthal LM, Mitsumoto H, Chung W, Croft GF, Saphier G, Leibel R, Goland R, Wichterle H, Henderson CE, Eggan K. Induced pluripotent stem cells generated from patients with ALS can be differentiated into motor neurons. Science. 2008 Aug 29;321(5893):1218-21. doi: 10.1126/science.1158799. Epub 2008 Jul 31. PMID: 18669821.

114. Castillo Bautista CM, Sterneckert J. Progress and challenges in directing the differentiation of human iPSCs into spinal motor neurons. Front Cell Dev Biol. 2023 Jan 5;10:1089970. doi: 10.3389/fcell.2022.1089970. PMID: 36684437; PMCID: PMC9849822.

115. Jessell TM. Neuronal specification in the spinal cord: inductive signals and transcriptional codes. Nat Rev Genet. 2000 Oct;1(1):20-9. doi: 10.1038/35049541. PMID: 11262869.

116. Jessell TM, Sanes JR. Development. The decade of the developing brain. Curr Opin Neurobiol. 2000 Oct;10(5):599-611. doi: 10.1016/s0959-4388(00)00136-7. PMID: 11084323.

117. Hubert KA, Wellik DM. Hox genes in development and beyond. Development. 2023 Jan 1;150(1):dev192476. doi: 10.1242/dev.192476. Epub 2023 Jan 16. Erratum in: Development. 2024 Mar 1;151(5):dev202770. doi: 10.1242/dev.202770. PMID: 36645372; PMCID: PMC10216783.

118. Yang M, Liu M, Sánchez YF, Avazzadeh S, Quinlan LR, Liu G, Lu Y, Yang G, O'Brien T, Henshall DC, Hardiman O, Shen S. A novel protocol to derive cervical motor neurons from induced pluripotent stem cells for amyotrophic lateral sclerosis. Stem Cell Reports. 2023 Sep 12;18(9):1870-1883. doi: 10.1016/j.stemcr.2023.07.004. Epub 2023 Aug 17. PMID: 37595581; PMCID: PMC10545486.

119. Chambers SM, Fasano CA, Papapetrou EP, Tomishima M, Sadelain M, Studer L. Highly efficient neural conversion of human ES and iPS cells by dual inhibition of SMAD signaling. Nat Biotechnol. 2009 Mar;27(3):275-80. doi: 10.1038/nbt.1529. Epub 2009 Mar 1. Erratum in: Nat Biotechnol. 2009 May;27(5):485. PMID: 19252484; PMCID: PMC2756723.

120. Amoroso MW, Croft GF, Williams DJ, O'Keeffe S, Carrasco MA, Davis AR, Roybon L, Oakley DH, Maniatis T, Henderson CE, Wichterle H. Accelerated high-yield generation of limb-innervating motor neurons from human stem cells. J Neurosci. 2013 Jan 9;33(2):574-86. doi: 10.1523/JNEUROSCI.0906-12.2013. PMID: 23303937; PMCID: PMC3711539.

121. Qu Q, Li D, Louis KR, Li X, Yang H, Sun Q, Crandall SR, Tsang S, Zhou J, Cox CL, Cheng J, Wang F. High-efficiency motor neuron differentiation from human pluripotent stem cells and the function of Islet-1. Nat Commun. 2014 Mar 13;5:3449. doi: 10.1038/ncomms4449. PMID: 24622388.

122. Maury Y, Côme J, Piskorowski RA, Salah-Mohellibi N, Chevaleyre V, Peschanski M, Martinat C, Nedelec S. Combinatorial analysis of developmental cues efficiently converts human pluripotent stem cells into multiple neuronal subtypes. Nat Biotechnol. 2015 Jan;33(1):89-96. doi: 10.1038/nbt.3049. Epub 2014 Nov 10. PMID: 25383599.

123. Du ZW, Chen H, Liu H, Lu J, Qian K, Huang CL, Zhong X, Fan F, Zhang SC. Generation and expansion of highly pure motor neuron progenitors from human pluripotent stem cells. Nat Commun. 2015 Mar 25;6:6626. doi: 10.1038/ncomms7626. PMID: 25806427; PMCID: PMC4375778.

124. Ben-Shushan E, Feldman E, Reubinoff BE. Notch signaling regulates motor neuron differentiation of human embryonic stem cells. Stem Cells. 2015 Feb;33(2):403-15. doi: 10.1002/stem.1873. PMID: 25335858.

125. Mazzoni EO, Mahony S, Closser M, Morrison CA, Nedelec S, Williams DJ, An D, Gifford DK, Wichterle H. Synergistic binding of transcription factors to cell-specific enhancers programs motor neuron identity. Nat Neurosci. 2013 Sep;16(9):1219-27. doi: 10.1038/nn.3467. Epub 2013 Jul 21. PMID: 23872598; PMCID: PMC3820498.

126. Hester ME, Murtha MJ, Song S, Rao M, Miranda CJ, Meyer K, Tian J, Boulting G, Schaffer DV, Zhu MX, Pfaff SL, Gage FH, Kaspar BK. Rapid and efficient generation of functional motor neurons from human pluripotent stem cells using gene delivered transcription factor codes. Mol Ther. 2011 Oct;19(10):1905-12. doi: 10.1038/mt.2011.135. Epub 2011 Jul 19. PMID: 21772256; PMCID: PMC3188742.

127. Goto K, Imamura K, Komatsu K, Mitani K, Aiba K, Nakatsuji N, Inoue M, Kawata A, Yamashita H, Takahashi R, Inoue H. Simple Derivation of Spinal Motor Neurons from ESCs/iPSCs Using Sendai Virus Vectors. Mol Ther Methods Clin Dev. 2017 Jan 10;4:115-125. doi: 10.1016/j.omtm.2016.12.007. PMID: 28344997; PMCID: PMC5363292.

128. Goparaju SK, Kohda K, Ibata K, Soma A, Nakatake Y, Akiyama T, Wakabayashi S, Matsushita M, Sakota M, Kimura H, Yuzaki M, Ko SB, Ko MS. Rapid differentiation of human pluripotent stem cells into functional neurons by mRNAs encoding transcription factors. Sci Rep. 2017 Feb 13;7:42367. doi: 10.1038/srep42367. PMID: 28205555; PMCID: PMC5304326.

129. Zhao S, Jiang E, Chen S, Gu Y, Shangguan AJ, Lv T, Luo L, Yu Z. PiggyBac transposon vectors: the tools of the human gene encoding. Transl Lung Cancer Res. 2016 Feb;5(1):120-5. doi: 10.3978/j.issn.2218-6751.2016.01.05. PMID: 26958506; PMCID: PMC4758974.

130. De Santis R, Garone MG, Pagani F, de Turris V, Di Angelantonio S, Rosa A. Direct conversion of human pluripotent stem cells into cranial motor neurons using a piggyBac vector. Stem Cell Res. 2018 May;29:189-196. doi: 10.1016/j.scr.2018.04.012. Epub 2018 Apr 27. Erratum in: Stem Cell Res. 2021 May;53:102296. doi: 10.1016/j.scr.2021.102296. PMID: 29729503.

131. Stoklund Dittlau K, Krasnow EN, Fumagalli L, Vandoorne T, Baatsen P, Kerstens A, Giacomazzi G, Pavie B, Rossaert E, Beckers J, Sampaolesi M, Van Damme P, Van Den Bosch L. Generation of Human Motor Units with Functional Neuromuscular Junctions in Microfluidic Devices. J Vis Exp. 2021 Sep 7;(175). doi: 10.3791/62959. PMID: 34570099.

132. Bellmann J, Goswami RY, Girardo S, Rein N, Hosseinzadeh Z, Hicks MR, Busskamp V, Pyle AD, Werner C, Sterneckert J. A customizable microfluidic platform for medium-throughput modeling of neuromuscular circuits. Biomaterials. 2019 Dec;225:119537. doi: 10.1016/j.biomaterials.2019.119537. Epub 2019 Oct 8. PMID: 31614290; PMCID: PMC7294901.

133. Osaki T, Uzel SGM, Kamm RD. Microphysiological 3D model of amyotrophic lateral sclerosis (ALS) from human iPS-derived muscle cells and optogenetic motor neurons. Sci Adv. 2018 Oct 10;4(10):eaat5847. doi: 10.1126/sciadv.aat5847. PMID: 30324134; PMCID: PMC6179377.

134. Lancaster MA, Renner M, Martin CA, Wenzel D, Bicknell LS, Hurles ME, Homfray T, Penninger JM, Jackson AP, Knoblich JA. Cerebral organoids model human brain development and microcephaly. Nature. 2013 Sep 19;501(7467):373-9. doi: 10.1038/nature12517. Epub 2013 Aug 28. PMID: 23995685; PMCID: PMC3817409.

135. Andersen J, Revah O, Miura Y, Thom N, Amin ND, Kelley KW, Singh M, Chen X, Thete MV, Walczak EM, Vogel H, Fan HC, Paşca SP. Generation of Functional Human 3D Cortico-Motor Assembloids. Cell. 2020 Dec 23;183(7):1913-1929.e26. doi: 10.1016/j.cell.2020.11.017. Epub 2020 Dec 16. PMID: 33333020; PMCID: PMC8711252.

136. Scaffidi P, Misteli T. Reversal of the cellular phenotype in the premature aging disease Hutchinson-Gilford progeria syndrome. Nat Med. 2005 Apr;11(4):440-5. doi: 10.1038/nm1204. Epub 2005 Mar 6. PMID: 15750600; PMCID: PMC1351119.

137. Vera E, Bosco N, Studer L. Generating Late-Onset Human iPSC-Based Disease Models by Inducing Neuronal Age-Related Phenotypes through Telomerase Manipulation. Cell Rep. 2016 Oct 18;17(4):1184-1192. doi: 10.1016/j.celrep.2016.09.062. PMID: 27760320; PMCID: PMC5089807.

138. Martens DS, Van Der Stukken C, Derom C, Thiery E, Bijnens EM, Nawrot TS. Newborn telomere length predicts later life telomere length: Tracking telomere length from birth to child- and adulthood. EBioMedicine. 2021 Jan;63:103164. doi: 10.1016/j.ebiom.2020.103164. Epub 2021 Jan 7. PMID: 33422989; PMCID: PMC7808927.

139. Lu T, Aron L, Zullo J, Pan Y, Kim H, Chen Y, Yang TH, Kim HM, Drake D, Liu XS, Bennett DA, Colaiácovo MP, Yankner BA. REST and stress resistance in ageing and Alzheimer's disease. Nature. 2014 Mar 27;507(7493):448-54. doi: 10.1038/nature13163. Epub 2014 Mar 19. Erratum in: Nature. 2016 Dec 15;540(7633):470. doi: 10.1038/nature20579. PMID: 24670762; PMCID: PMC4110979.

140. Hofmann S, Kedersha N, Anderson P, Ivanov P. Molecular mechanisms of stress granule assembly and disassembly. Biochim Biophys Acta Mol Cell Res. 2021 Jan;1868(1):118876. doi: 10.1016/j.bbamcr.2020.118876. Epub 2020 Sep 29. PMID: 33007331; PMCID: PMC7769147.

141. Millar SR, Huang JQ, Schreiber KJ, Tsai YC, Won J, Zhang J, Moses AM, Youn JY. A New Phase of Networking: The Molecular Composition and Regulatory Dynamics of Mammalian Stress Granules. Chem Rev. 2023 Jul 26;123(14):9036-9064. doi: 10.1021/acs.chemrev.2c00608. Epub 2023 Jan 20. PMID: 36662637; PMCID: PMC10375481.

142. Buchan JR, Parker R. Eukaryotic stress granules: the ins and outs of translation. Mol Cell. 2009 Dec 25;36(6):932-41. doi: 10.1016/j.molcel.2009.11.020. PMID: 20064460; PMCID: PMC2813218.

143. Fernandes N, Nero L, Lyons SM, Ivanov P, Mittelmeier TM, Bolger TA, Buchan JR. Stress Granule Assembly Can Facilitate but Is Not Required for TDP-43 Cytoplasmic Aggregation. Biomolecules. 2020 Sep 25;10(10):1367. doi: 10.3390/biom10101367. Erratum in: Biomolecules. 2021 Dec 17;11(12):1895. doi: 10.3390/biom11121895. PMID: 32992901; PMCID: PMC7650667.

144. Colombrita C, Zennaro E, Fallini C, Weber M, Sommacal A, Buratti E, Silani V, Ratti A. TDP-43 is recruited to stress granules in conditions of oxidative insult. J Neurochem. 2009 Nov;111(4):1051-61. doi: 10.1111/j.1471-4159.2009.06383.x. Epub 2009 Sep 16. PMID: 19765185.

145. Fernandes N, Eshleman N, Buchan JR. Stress Granules and ALS: A Case of Causation or Correlation? Adv Neurobiol. 2018;20:173-212. doi: 10.1007/978-3-319-89689-2_7. PMID: 29916020.

146. Ratti A, Gumina V, Lenzi P, Bossolasco P, Fulceri F, Volpe C, Bardelli D, Pregnolato F, Maraschi A, Fornai F, Silani V, Colombrita C. Chronic stress induces formation of stress granules and pathological TDP-43 aggregates in human ALS fibroblasts and iPSC-motoneurons. Neurobiol Dis. 2020 Nov;145:105051. doi: 10.1016/j.nbd.2020.105051. Epub 2020 Aug 20. PMID: 32827688.

147. La Bella V, Cisterni C, Salaün D, Pettmann B. Survival motor neuron (SMN) protein in rat is expressed as different molecular forms and is developmentally regulated. Eur J Neurosci. 1998 Sep;10(9):2913-23. doi: 10.1111/j.1460-9568.1998.00298.x. PMID: 9758161.

148. La Bella V, Kallenbach S, Pettmann B. Expression and subcellular localization of two isoforms of the survival motor neuron protein in different cell types. J Neurosci Res. 2000 Nov 1;62(3):346-56. doi: 10.1002/1097-4547(20001101)62:3<346::AID-JNR4>3.0.CO;2-D. PMID: 11054803.

149. D'Anzi A, Perciballi E, Ruotolo G, Ferrari D, Notaro A, Lombardi I, Gelati M, Frezza K, Bernardini L, Torrente I, De Luca A, La Bella V, Luigi Vescovi A, Rosati J. Production of CSSi013-A (9360) iPSC line from an asymptomatic subject carrying an heterozygous mutation in TDP-43 protein. Stem Cell Res. 2022 Aug;63:102835. doi: 10.1016/j.scr.2022.102835. Epub 2022 Jun 6. PMID: 35714448.

150. Bidollari E, Rotundo G, Altieri F, Amicucci M, Wiquel D, Ferrari D, Goldoni M, Bernardini L, Consoli F, De Luca A, Fanelli S, Lamorte G, D'Agruma L, Vescovi AL, Squitieri F, Rosati J. Generation of induced pluripotent stem cell line CSSi008-A (4698) from a patient affected by

advanced stage of Dentato-Rubral-Pallidoluysian atrophy (DRPLA). Stem Cell Res. 2019 Oct;40:101551. doi: 10.1016/j.scr.2019.101551. Epub 2019 Aug 27. PMID: 31493762.

151. Rosa A, Papaioannou MD, Krzyspiak JE, Brivanlou AH. miR-373 is regulated by TGFβ signaling and promotes mesendoderm differentiation in human Embryonic Stem Cells. Dev Biol. 2014 Jul 1;391(1):81-8. doi: 10.1016/j.ydbio.2014.03.020. Epub 2014 Apr 4. PMID: 24709321; PMCID: PMC4081558.

152. Garone MG, de Turris V, Soloperto A, Brighi C, De Santis R, Pagani F, Di Angelantonio S, Rosa A. Conversion of Human Induced Pluripotent Stem Cells (iPSCs) into Functional Spinal and Cranial Motor Neurons Using PiggyBac Vectors. J Vis Exp. 2019 May 1;(147). doi: 10.3791/59321. PMID: 31107442.

153. Romano R, De Luca M, Del Fiore VS, Pecoraro M, Lattante S, Sabatelli M, La Bella V, Bucci C. Allele-specific silencing as therapy for familial amyotrophic lateral sclerosis caused by the p.G376D *TARDBP* mutation. Brain Commun. 2022 Dec 16;4(6):fcac315. doi: 10.1093/braincomms/fcac315. PMID: 36751500; PMCID: PMC9897181.

TRACEABLE ACHIEVEMENTS

Peer-reviewed publications:

- Romano R, De Luca M, Del Fiore VS, **Pecoraro M**, Lattante S, Sabatelli M, La Bella V, Bucci C. Allele-specific silencing as therapy for familial amyotrophic lateral sclerosis caused by the p.G376D *TARDBP* mutation. Brain Commun. 2022 Dec 16;4(6):fcac315. doi: 10.1093/braincomms/fcac315. PMID: 36751500; PMCID: PMC9897181.
- Wasielewska JM, Chaves JCS, Cabral-da-Silva MC, **Pecoraro M**, Viljoen SJ, Nguyen TH, Bella V, Oikari LE, Ooi L, White AR. A patient-derived amyotrophic lateral sclerosis blood-brain barrier model for focused ultrasound-mediated anti-TDP-43 antibody delivery. Fluids Barriers CNS. 2024 Aug 13;21(1):65. doi: 10.1186/s12987-024-00565-1. PMID: 39138578; PMCID: PMC11323367.
- Perciballi E, Bovio F, Ferro S, Forcella M, Rosati J, Carletti RM, D'Anzi A, Gelati M, La Bella V, Innocenti M, Spataro R, **Pecoraro M**, Lombardi I, Vulcano E, Ruotolo G, Mercurio S, Sabatelli M, Lattante S, Malm T, Ohtonen S, Vescovi AL, Fusi P, Ferrari D. Mitochondrial and energy metabolism dysfunctions are hallmarks of TDP-43^{G376D} fibroblasts from members of an Amyotrophic Lateral Sclerosis family. Cell Death Dis. 2025 Apr 10;16(1):272. doi: 10.1038/s41419-025-07584-2. PMID: 40210682; PMCID: PMC11986161.

Conference posters:

- **Pecoraro M**, Notaro A, Conigliaro A, Spataro R, Conforti F.L, Alessandro R, La Bella V. *Role of the chronic stress on the TDP-43 subcellular localization in fibroblasts of the three different ALS-related TARDBP mutations*. FENS Forum. 2022 Jul.
- Conforti F.L., **Pecoraro M**, Perrone B., Mosca V., Ruffo P., La Bella V. *Do ATXN-1 intermediate poly-CAG expansions play a prognostic role in Amyotrophic Lateral Sclerosis?*. Human Genome Meeting. 2024 Apr
- Conforti F.L., **Pecoraro M,** Perrone B., Mosca V., Ruffo P., La Bella V. *ATXN1 intermediate repeats and clinical progression in ALS patients*. European Human Genetics Conference. 2024 Jun
- Perrone B., De Amicis F., **Pecoraro M.,** Ruffo P., Spataro R., Conforti F.L. *When genotype is not predictive of phenotype in a large ALS family*. XXVII CONGRESSO NAZIONALE SIGU. 2024 Oct

Conference Speaker:

- **Pecoraro M**. *Role of the ALS-related G376D TARDBP mutation in the pathophysiology of motor neuron degeneration*. Workshop ScintilLA. 2025 Jan

ACKNOWLEDGEMENT

First and foremost, I want to dedicate this thesis to the late Professor Vincenzo La Bella, my tutor throughout this journey. His premature departure has left a profound void in me – and in all who had the privilege of knowing him. I am deeply grateful for the opportunity he gave me to work on this challenging project. I will always remember his advice, the countless things he thought me, and the lab meeting brimming with ideas, which he shared with enthusiasm. Thank you, professor.

I would also like to sincerely thank my current tutor, Dr. Fabio Bucchieri, for his guidance and for helping me complete this journey.

I wish to thank the past and current members of the ALS Center. Thank you, Dr. Rossella Spataro, for your support during my PhD. Thank you, Dr. Antonietta Notaro, for have been a great and kind teacher. Thank you, Dr. Tiziana Colletti, for your unwavering support with everything, for being our "Wikipedia" and for never saying no to a dose of caffein accompanied by my endless rants. Thank you, Dr Lavinia Guccione, for never letting a day go by without suggesting our sacred coffee breaks. Thank you, Viviana Mosca, for helping me with everything, for being a listening ear of my monologues when I got overwhelmed, for all the sacrificed Saturdays, for helping me with this thesis and for so much more.

I am also grateful to all the collaborators who took part on this project: Dr Jessica Rosati, Dr Alessandro Rosa, Dr Riccardo Alessandro, Dr Alice Conigliaro. I extend my gratitude to the co-authors listed in the publications. A special thank you to Dr. Jared Sterneckert and his group – Tanya, Elly e Ram – for supporting me in the most difficult time. I want also to thank Dr Giuseppe Salemi e Dr. Paolo Aridon. A heartfelt thanks to Dr. Francesca Luisa Conforti for all the support over the past year and her help with the final touches of the thesis.

Lastly, I want to thank all my friends and family for all the support and encouragement. With all my heart, I want to thank my parents that have always encouraged me since the first day of university, my brother and sister, who made me laugh when I needed the most, my grandmother to always encourage me to follow my dream.

To my partner. Tiziano – thank you for listening to every boring detail and problem, for keeping me grounded when I felt overwhelmed. And I want to thank my son, Leonardo, who always was ready to welcome home with open arms and a big smile, effortlessly making all the stress and workload melt away. I love you.

Last but not least